MARTIN MARIETTA ENERGY SYSTEMS LIBRARIES
3 4456 0360682 7

CENTRAL RESEARCH LIBRARY
DOCUMENT COLLECTION

AEC RESEARCH AND DEVELOPMENT REPORT

ORNL 1611
Special

DECLASSIFIED
CLASSIFICATION CHANGED TO:
BY AUTHORITY OF: AEC 11-1-61
BY: Lockheed 8-6-68

THE SKYSHINE EXPERIMENTS AT THE BULK SHIELDING FACILITY

H. E. Hungerford

CENTRAL RESEARCH LIBRARY
DOCUMENT COLLECTION
LIBRARY LOAN COPY
DO NOT TRANSFER TO ANOTHER PERSON
If you wish someone else to see this document, send in name with document and the library will arrange a loan.

OAK RIDGE NATIONAL LABORATORY
OPERATED BY
CARBIDE AND CARBON CHEMICALS COMPANY
A DIVISION OF UNION CARBIDE AND CARBON CORPORATION
UCC
POST OFFICE BOX P
OAK RIDGE, TENNESSEE

[redacted]

ORNL-1611

This document consists of 115 pages.
Copy 39 of 149, Series A.

Contract No. W-7405-Eng-6

Shielding Section
Physics Division

THE SKYSHINE EXPERIMENTS AT THE BULK SHIELDING FACILITY

H. E. Hungerford

[redacted]

Date Issued:

JUL 2 1954

OAK RIDGE NATIONAL LABORATORY
Operated by
CARBIDE AND CARBON CHEMICALS COMPANY
A Division of Union Carbide and Carbon Corporation
Post Office Box P
Oak Ridge, Tennessee

[redacted]

MARTIN MARIETTA ENERGY SYSTEMS LIBRARIES

3 4456 0360682 7

[redacted]

ORNL 1611
Special

INTERNAL DISTRIBUTION

1. H. Bethe (consultant)
2. E. P. Blizard
3. C. E. Center
4. R. A. Charpie
5. C. E. Clifford
6. G. T. Chapman
7. R. G. Cochran
8. Sylvan Cromer
9. J. B. Dee
10. L. B. Emlet (K-25)
11. W. K. Ergen
12. A. P. Fraas
13. H. E. Hungerford
14. W. H. Jordan
15. J. A. Lane
16. C. E. Larson
17. F. C. Maienschein
18. J. L. Meem
19. K. Z. Morgan
20. F. H. Murray
21. R. H. Ritchie
22. A. Simon
23. A. H. Snell
24. H. E. Stern
25. C. L. Storrs
26. A. M. Weinberg
27. T. A. Welton
28. H. P. Yockey
29. Biology Library
30. Health Physics Library
31-36. ANP Library
37. Metallurgy Library
38. Reactor Experimental Engineering Library
39-43. Central Research Library
44. Laboratory Records, ORNL R.C.
45-50. Laboratory Records Department

EXTERNAL DISTRIBUTION

51. Air Force Engineering Office, Oak Ridge
52. Air Force Plant Representative, Burbank
53. Air Force Plant Representative, Seattle
54. Air Force Plant Representative, Wood-Ridge
55. ANP Project Office, Fort Worth
56-58. Argonne National Laboratory (Permit Anderson, J. W. Butler, and J. R. Dietrich)
59. Armed Forces Special Weapons Project (Sandia)
60. Armed Forces Special Weapons Project, Washington (E. C. LaVier)
61-69. Atomic Energy Commission, Washington (1 copy to Col. M. J. Nielsen, Col. T. A. Redfield, [illegible] R. Horner, and A. F. Thompson)
70. Battelle Memorial Institute
71. Boeing Airplane Company (C. J. Leisy)
72. Brookhaven National Laboratory (M. Fox)
73. Bureau of Aeronautics (R. Zirkind)
74. Bureau of Ships (T. Rockwell)
75. Carbide and Carbon Chemicals Company (Y-12 Plant)
76. Chief of Naval Research
77. Commonwealth Edison Company
78-79. Convair, Fort Worth (J. C. Flack)
80. Convair, San Diego (C. H. Helms)
81-82. Curtiss-Wright Corporation, Wright Aeronautical Division (K. Campbell and H. Reese)
83. Department of the Navy - OP-362

[redacted]

[redacted]

84. Detroit Edison Company
85. duPont Company, Augusta
86. duPont Company, Wilmington
87. Foster Wheeler Corporation
88. General Dynamics Corp., Electric Boat Division (E. L. Czapek)
89-91. General Electric Company, ANPD (C. Thornton)
92. General Electric Company, Richland
93. Glen L. Martin Company (T. F. Magey)
94-95. Knolls Atomic Power Laboratory (H. E. Stone and L. H. Weinberg)
96. Lockheed Aircraft Company (E. A. Cleveland)
97. Lockland Area Office
98. Los Alamos Scientific Laboratory
99. Materials Laboratory (WADC) (Col. P. L. Hill)
100. Monsanto Chemical Company
101. National Advisory Committee for Aeronautics, Cleveland (A. Silverstein)
102. National Advisory Committee for Aeronautics, Washington
103. Naval Research Laboratory (W. R. Faust)
104. North American Aviation, Inc.
105-108. Nuclear Development Associates, Inc. (H. Goldstein)
109-113. Nuclear Powered Aircraft Branch, Weapon Systems Division (WADC) (Col. C. D. Gaffer)
114. Oak Ridge Operations (K. Kasschau)
115. Patent Branch, Washington
116. Phillips Petroleum Company
117-120. Powerplant Laboratory (WADC) (A. M. Nelson and F. M. Westfall)
121-122. Pratt and Whitney Aircraft Division (Fox Project) (C. F. deGanahl)
123. Rand Corporation
124. San Francisco Operations Office
125. USAF Headquarters
126. U.S. Naval Radiological Defense Laboratory
127. University of California Radiation Laboratory, Berkeley
128. University of California Radiation Laboratory, Livermore
129. Walter Kidde Nuclear Laboratories, Inc.
130-131. Westinghouse Electric Corporation (J. J. Taylor)
132-149. Technical Information Service, Oak Ridge

[redacted]

Table of Contents

	Abstract	xii
	Introduction	1
I.	Repeat of the Air Scattering Experiments	3
	Experimental Arrangement	3
	Experimental Procedure and Results	6
	Shield Weight Calculations Based on Data from Repeat Experiments	13
	Neutron shield weight calculations	16
	Gamma-ray shield weight calculations	17
	Conclusions	18
II.	Some General Experiments on Air Scattering and Related Phenomena	20
	Vertical Traverses above the Reactor	21
	Scan of a Quadrant of Water Surface above the Reactor	25
	Radiation Pattern along the Pool Centerline	27
	Characteristics of the Water Surface as a Secondary Radiation Source	30
	Scattering from Reactor and Instrument Bridges	34
	Effect of Lead at Crew Position on Radiation Received	40
	Effect of Interposing a Lead Slab at Various Positions Between Reactor and Detector	40
	Radiation Distribution in Air over Crew Position	47
	Effect of Pool Walls on Radiation at Crew Position	49
	Shield Weight Calculations Based on New Data	55
III.	Summary and Conclusions	59
App. A.	Tables of Data	61
App. B.	Predictions of Scattering Effects by Pool Walls	102

List of Figures

1. Standard Divided Shield 4

2. Arrangement for Skyshine Experiments 4

3. Fast Neutron Dose at Crew Position as a Function of Detector Height above Water Surface for Various Water Thicknesses (y) above Reactor 7

4. Gamma-Ray Dose at Crew Position as a Function of Detector Height above Water Surface for Various Thickesses (y) above Reactor 8

5. Fast Neutron Dose at Surface of Crew Position as a Function of Reactor Shield Thickness 10

6. Gamma-Ray Dose at Surface of Crew Position as a Function of Reactor Shield Thickness (Without Lead Around Detector) 11

7. Skyshine Experiments: Lead-Lined Cylindrical Container for Anthracene Crystal and Phototube; Simulating a Crew Box 12

8. Attenuation of Gamma Rays by Lead Crew Shield 14

9. Comparison of Gamma-Ray Doses at Crew Position -- With and Without Lead Shadow Shield in Place 15

10. Illustration Showing Positions of Detectors for Vertical Traverse and Horizontal Scan Measurements 22

11. Thermal Neutron Flux Measurements Directly above BSR for Various Water Thicknesses (y) above Reactor 23

12. Gamma-Ray Dose Measurements Directly above BSR for Various Water Thicknesses (y) above Reactor 24

13. Thermal Neutron Flux Pattern over Quadrant of Water Surface Directly above Reactor 26

14. Thermal Neutron Flux along Vertical Traverses Made at Various Points on 1 m^2 Quadrant above BSR 28

15. Gamma Radiation Pattern over Quadrant of Water Surface Directly above Reactor 29

List of Figures, Cont.

16. Thermal Neutron Flux Pattern at Water Surface along Pool Centerline 31

17. Gamma-Ray Dose Patterns near Water Surface along Pool Centerline 32

18. Radiation Received at Crew Position for Various Locations of Instrument Bridge 36

19. Gamma-Ray Dose Measurements along Vertical Traverse Line near BSR, with Reactor Mounted First on Its Bridge, then on H-Beam 37

20. Gamma-Ray Dose Measurements along Water Surface Traverse West of Pool Centerline, with Reactor Mounted First on Its Bridge, then on H-Beam 38

21. Effect of Lead at Crew Position on Gamma-Ray Dose Received 41

22. Illustration Showing Positions of Lead Slab along Vertical Traverse Lines A, B, and C 43

23. Variation of Gamma-Ray Dose at Crew Position When a Lead Slab is Moved along Vertical Paths Between Reactor and Detector 44

24. Variation of Thermal Neutron Flux at Crew Position When a Lead Slab Is Moved along Vertical Paths Between Reactor and Detector 45

25. Radiation Distribution in Air above Crew Position 48

26. Effect of Wall Scattering on Fast Neutron Dose Received at Crew Position for Various Water Thicknesses (y) above Reactor (Vertical Traverse Measurements) 50

27. Effect of Wall Scattering on Thermal Neutron Flux Received at Crew Position for Various Water Thicknesses (y) above Reactor (Vertical Traverse Measurements) 51

28. Effect of Wall Scattering on Gamma-Ray Dose Received at Crew Position for Various Water Thicknesses (y) above Reactor (Vertical Traverse Measurements) 52

List of Figures, Cont.

29. Neutron Dose at Crew Position as a Function of Reactor-Detector Distance from Pool Centerline for Various Water Thicknesses (y) above Reactor 53

30. Gamma-Ray Dose at Crew Position as a Function of Reactor-Detector Distance from Pool Centerline for Various Water Thicknesses (y) above Reactor 54

A-1. Correlation Chart of Figures and Tables 101

List of Tables

A-1. Neutron and Gamma-Ray Doses at Crew Position - 30-cm Water Thickness above Reactor 62

A-2. Neutron and Gamma-Ray Doses at Crew Position - 60-cm Water Thickness above Reactor 63

A-3. Neutron and Gamma-Ray Doses at Crew Position - 90-cm Water Thickness above Reactor 64

A-4. Neutron and Gamma-Ray Doses at Crew Position - 116-cm Water Thickness above Reactor 65

A-5. Neutron and Gamma-Ray Doses at Crew Position - 142-cm Water Thickness above Reactor 66

A-6. Neutron and Gamma-Ray Doses at Surface of Crew Position as a Function of Reactor Shield Thickness 67

A-7. Attenuation of Gamma Rays by Lead Crew Shield 68

A-8. Comparison of Gamma-Ray Doses at Crew Position - With and Without Lead Shadow Shields in Place 69

A-9. Thermal Neutron Flux Measurements on a Vertical Line Directly above BSR 70

A-10. Thermal Neutron Flux Measurements near Water Surface Directly above BSR 71

A-11. Gamma-Ray Dose Measurements on a Vertical Line Directly above BSR 72

A-12. Gamma-Ray Dose Measurements near Water Surface Directly above BSR 73

A-13. Thermal Neutron Flux Measurements near Water Surface over 1 m^2 Quadrant above BSR 74

A-14. Gamma-Ray Dose Measurements at Water Surface over 1 m^2 Quadrant above BSR 75

A-15. Thermal Neutron Flux Measurements at Water Surface along Pool Centerline 76

List of Tables, Cont.

A-16. Gamma-Ray Dose Vertical Traverse Measurements near Water Surface at Various Points along Pool Centerline 77

A-17. Gamma-Ray Measurements near Water Surface along Pool Centerline 79

A-18. Comparison of Experimental Gamma-Ray Dose D_L at Point Q with Interpolated Dose D_L' at Point Q' 80

A-19. Effect of Moving Instrument Bridge to Various Positions over Pool on Radiation Received at Crew Position 81

A-20. Gamma-Ray Vertical Traverse Measurements under Reactor Bridge and under H-Beam 82

A-21. Gamma-Ray Horizontal Traverse Measurements on Water Surface under Reactor Bridge and under H-Beam 83

A-22. Effect of Lead at the Crew Position on the Gamma-Ray Dose Received 84

A-23. Vertical Traverse Lines of Lead Slab Interposed Between Reactor and Detector 85

A-24. Positions of Lead Slab along Vertical Traverse Lines 85

A-25. Effect on Radiation of Interposing Lead Slab between BSR and Detector at Crew Position 86

A-26. Radiation Distribution in Air above Crew Position 87

A-27. Effect of Wall Scattering on Fast Neutron Dose Received at Crew Position for Various Water Thicknesses above Reactor 88

A-28. Effect of Wall Scattering on Thermal Neutron Flux Received at Crew Position for Various Water Thicknesses above Reactor 92

A-29. Effect of Wall Scattering on Gamma-Ray Dose Received at Crew Position for Various Water Thicknesses above Reactor 96

A-30. Effect of Rotating Crew Position Around Reactor Toward Pool Centerline from Original Reactor-Detector Position 5 ft from Pool Wall 100

Acknowledgements

The author wishes to express his sincere appreciation to those without whose help this report could not have been written: to Earl W. Hessee, of Convair, for his welcome and able assistance in the setting up and performing of the experiments; to E. P. Blizard for his valuable suggestions and guidance as consultant to the project; to F. H. Murray and to R. Aronson of Nuclear Development Associates for their review of all or part of the manuscript; to Mrs. Lorraine Abbott for her painstaking and untiring work in editing and preparing of the manuscript for publication; to R. M. Freestone of Reproduction Division for the excellent job done on the preparation of the figures; and to all those others not specifically mentioned who aided either in the performance of the experiments or in the preparation of the manuscript.

Abstract

The measurements and calculations of the previously reported air scattering or "skyshine" experiments (CF-52-7-37) have been repeated with many of the uncertainties removed. In addition, several experiments of a more general nature are reported.

Part I of this report describes the repeat experiments. Shield weight calculations based upon the new data indicate that the plastic side-shield of the crew compartment need be only 9.5 cm thick, instead of 17.8 cm as in the original design. This reduction of 8.3 cm in crew-shield thickness means a weight saving of about 5100 lb. Calculations based on the present gamma-ray data indicate that the lead side-shield thickness of 1.54 cm originally specified is approximately correct.

The experiments presented in Part II were performed to gain more basic information on several aspects of air scattering. Such phenomena were investigated as the radiation patterns existing about the reactor and at various parts of the pool, and scattering effects from the pool walls and bridges. Calculations made using some of this additional data show that if excess neutron shielding is removed from the reactor shield rather than from the crew shield, there is a weight saving of about 8400 lb.

THE SKYSHINE EXPERIMENTS AT THE BULK SHIELDING FACILITY

H. E. Hungerford

Introduction

In the spring of 1952 during the formulation of plans for construction of the ORNL Tower Shielding Facility a group of experiments were performed at the Bulk Shielding Facility on air scattering from reactor to crew position of a divided shield. The purpose of the experiments was to obtain measurements which could be compared with the estimates of dose within the crew shield of the Standard Divided Shield which were made by the ANP Shielding Board of 1950.(1) The results of these experiments have been published.(2)

Since a full-scale mockup of the divided shield, with its 15-m reactor-crew separation, could not be put into the 40-ft BSF pool, a group of tests were devised which could be performed readily and cheaply and which would yield some desired information on the air-scattered dose received at the crew position. One side of the reactor shield was simulated by lowering the water in

(1) Report of the ANP Shielding Board, ANP-53 (Oct. 16, 1950).

(2) J. L. Meem and H. E. Hungerford, Air Scattering Experiments at the Bulk Shielding Facility (Preliminary Issue), CF-52-7-37 (July 8, 1952).

the pool to various levels above the reactor. Some of the radiation emerging from the water surface was scattered back through the air to a point on the surface 5 m away which represented the crew position. Detectors lowered into the water at this point measured the dose at various depths that represented various thicknesses of crew-shield side walls. A correction factor was then applied to the data to convert back to a 15 m separation. Lead slabs located near the reactor simulated the gamma-ray shadow shield in the reactor component of the divided shield.

The shielding characteristics of lead at the crew position was observed by encasing a gamma-ray detector in a lead-lined container and varying the amount of lead on the top of the container through which radiation reaching the detector had to pass. Because the primary direction of the radiation escaping from the pool water was upward, the experiments were popularly dubbed the "skyshine" experiments.

It was emphasized in the preliminary report[2] that the experiments were crude and preliminary in nature. Although the experimental neutron data in these first experiments seemed to check well with the Shielding Board calculations, the gamma-ray data differed by a factor of 27. This was attributed to the many uncertainties involved, some of which were:

(1) The low intensities encountered using a reactor power of only 10 kw may have caused errors in the experimental data.

(2) The exact amount of water above the reactor was not known.

(3) The results of the necessary extrapolations of the experimental data were in doubt.

(4) The scale-up factor was only approximate.

(5) The amount of scattering from pool walls, bridges, and other obstacles were undetermined.

(6) The radiation distribution at the water surface above the reactor was not known.

In view of all the uncertainties it was decided to repeat the experiments more carefully, checking the results of the preliminary work and collecting new data of a more basic nature. By the time the experiments were resumed permission had been granted to operate the Bulk Shielding Reactor at a power of 100 kw.

I. Repeat of the Air Scattering Experiments

Experimental Arrangement

A schematic view of the aircraft divided shield as designed by the Shielding Board is shown in Fig. 1,[3] and the general arrangement

(3) For details see ANP-53, op. cit., pp 66-68.

DWG. 14667

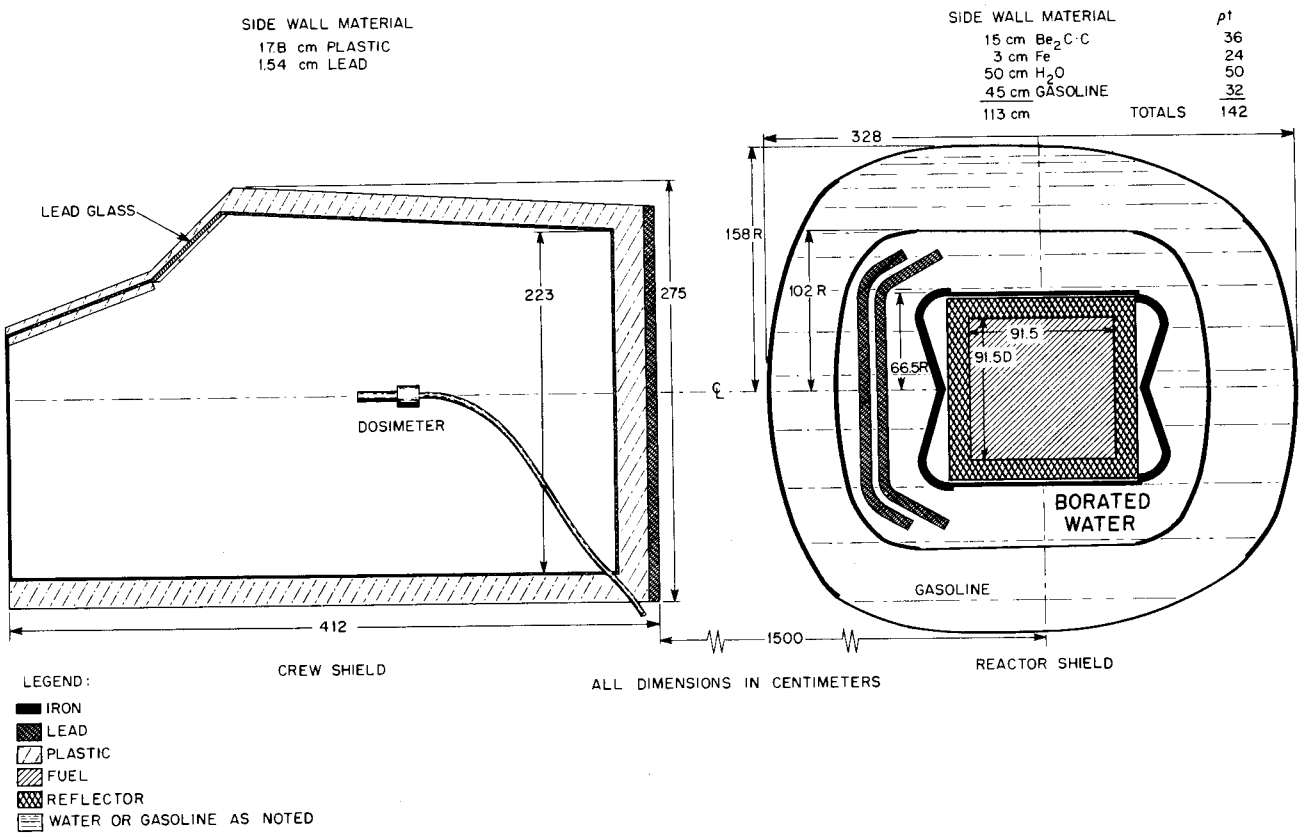

Fig. 1. Standard Divided Shield.

DWG. 14666

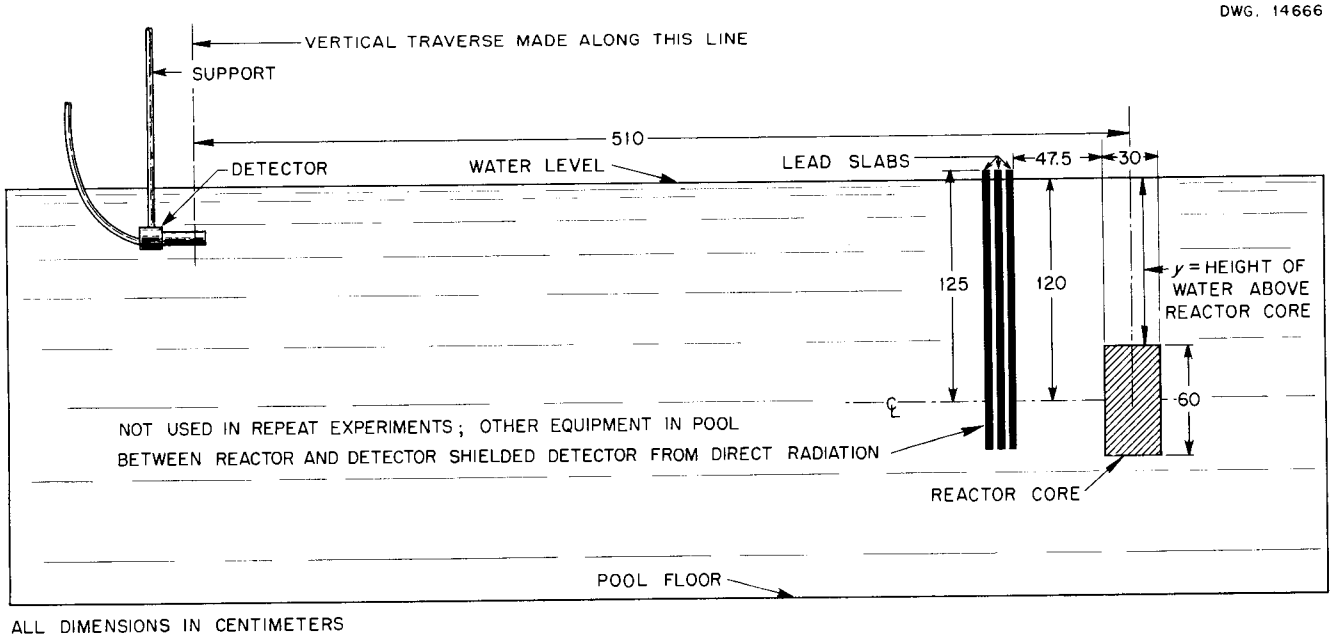

Fig. 2. Experimental Arrangement for Skyshine Experiments at the BSF.

for these tests is shown in Fig. 2. At the time of the repeat tests other equipment in the pool prevented the use of the lead slabs as a shadow shield. However, a mockup of the reactor portion of the divided shield (used in another experiment) served to shield the detectors at the crew position from direct radiation and did not interfere with the air scattering tests. The effect of the lead shadow shield had previously been determined in the earlier tests.

Among the improvements introduced in the experimental arrangements of the new tests were:

(1) A water level control which measured the water level and kept it constant to 0.2 cm.

(2) An improved apparatus for mounting the detectors at the crew position.

(3) A more accurate method of determining the reactor-detector separation.

The new detector mount was designed to hold the nose of each detector up, since the scattered radiation was presumably incident upon the water from a primarily downward direction. For some of the measurements a large, bottomless aluminum tank was installed in the pool at the crew position, within which the detectors were lowered. In this way the reactor-induced water activity was kept from circulating to the detectors and interfering with the measurements.

Experimental Procedure and Results

With the higher reactor power available the results of the preliminary experiments were checked at water thicknesses of 30, 60, and 90 cm above the reactor, and then measurements were extended to include thicknesses of 116 cm and 142 cm. The last two water thicknesses were chosen because 116 cm represents the water-equivalent design shield thickness of the reactor component of the divided shield for neutrons, and likewise, 142 cm represents the water-equivalent design thickness for gamma radiation.(4) The data obtained at these levels obviated the extrapolation of the measurements to these thicknesses, as was done in the preliminary calculations.

At each level vertical traverses were taken at the crew position, measuring the radiation above and below the water surface. The results of these traverses are shown in Figs. 3 and 4.(5) Even with the increase in power the fast neutron intensity at the 116- and 142-cm levels was too low to obtain reliable fast neutron dosimeter measurements. For these levels data from a 12-in. BF_3 thermal neutron counter was normalized to the dosimeter. Sufficient fast neutron data was taken to insure a correct normalizing factor.

---

(4) See CF-52-7-37, op. cit., p. 10; also ANP-53, op. cit., p 77.

(5) Except where noted all data presented in this report is given in terms of the new reactor power calibration reported by J. L. Meem, E. B. Johnson and H. E. Hungerford, Energy per Fission and Power of the BSR, CF-53-5-21 (May 12, 1953).

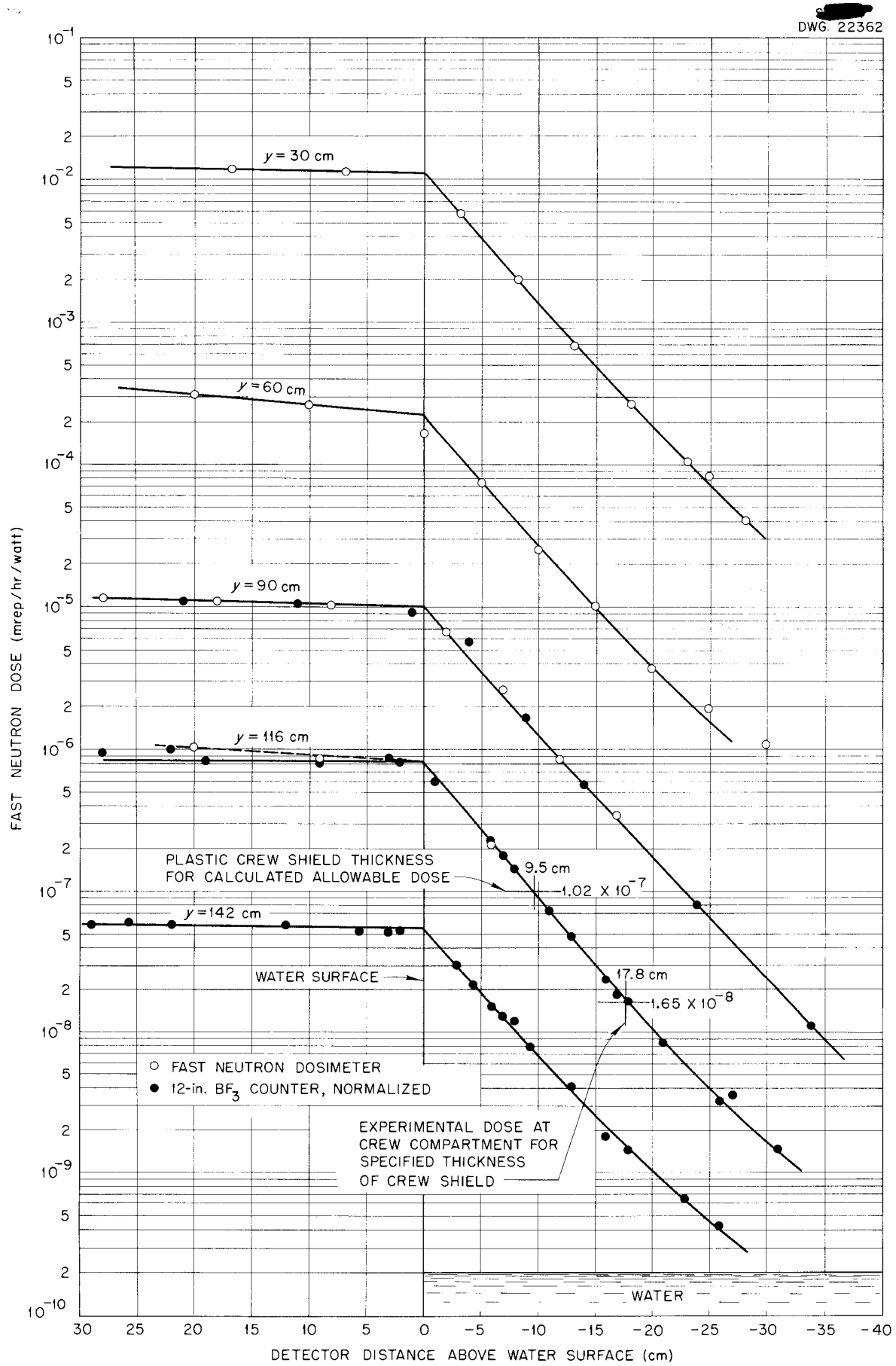

Fig. 3. Fast Neutron Dose at Crew Position as a Function of Detector Height above Water Surface for Various Water Thicknesses (y) above Reactor.

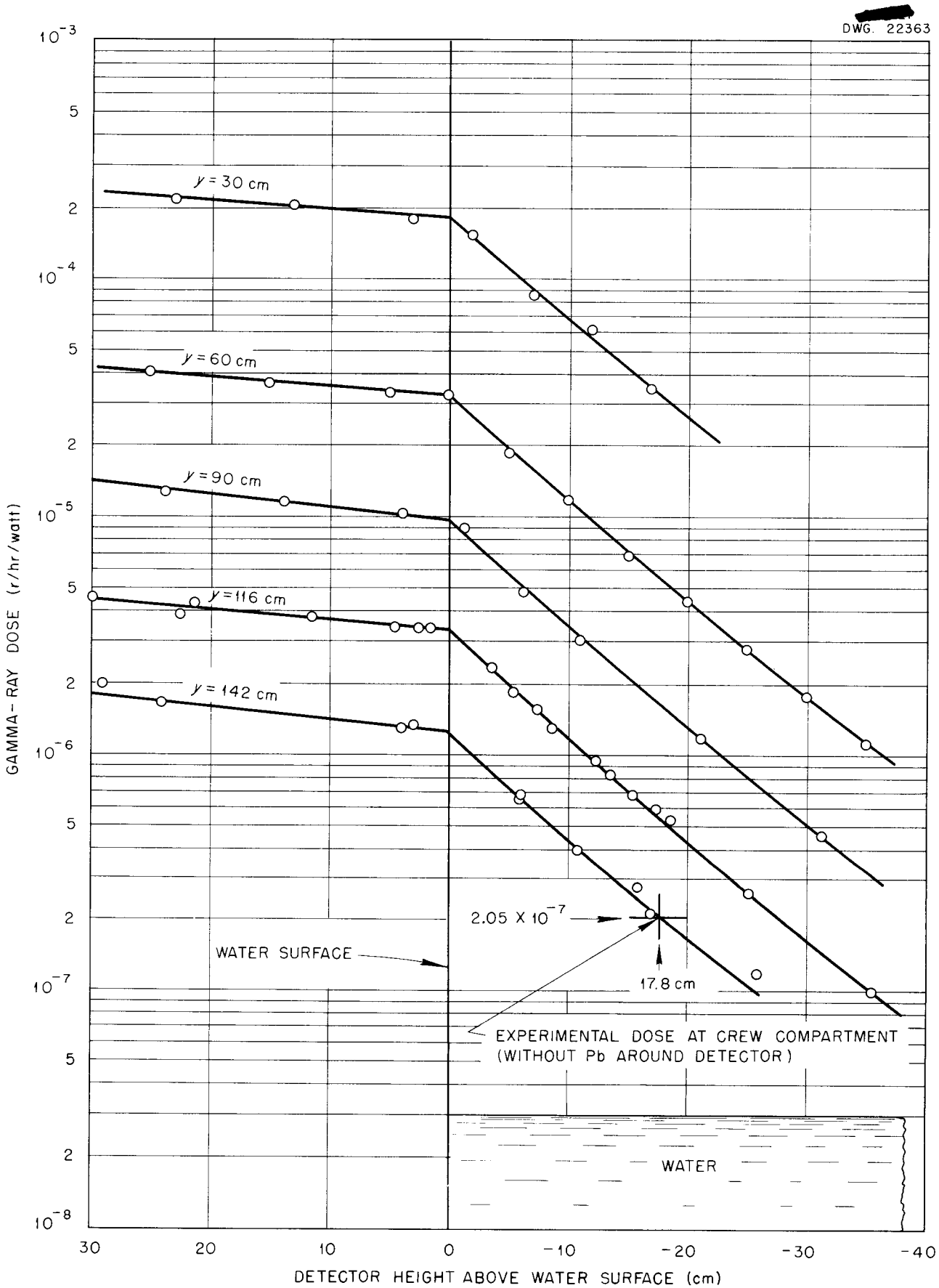

Fig. 4. Gamma-Ray Dose at Crew Position as a Function of Detector Height above Water Surface for Various Water Thicknesses (y) above Reactor Core.

Both Figs. 3 and 4 show the experimentally determined crew-shield doses for a plastic-equivalent crew shield thickness of 17.8 cm. The measurements for Figs. 3 and 4 are given in Tables A-1 through A-5 of Appendix A*

Figures 5 and 6 show the experimental doses at the surface of the crew position (i.e., at the water surface) as a function of the reactor shield thickness (water thickness above the reactor). In each figure the solid line represents the present data, and the dashed line shows the preliminary data. A study of the figures shows that the extrapolation of the preliminary data was far from accurate. These curves were drawn from the data in Table A-6.

In order to test the effect of lead on the gamma-ray dose at the crew position, a phototube and anthracene crystal were mounted in a lead-lined container (shown in Fig. 7) as in the preliminary tests. The sides and bottom of the container were lined with 3 in. of lead. The crystal detector was mounted directly underneath the thin aluminum cover. Various thicknesses of lead were placed on the cover and measurements were made under water at a plastic crew shield thickness of 17.8 cm. The current from the phototube was measured, rather than the pulses as was done in the preliminary experiments.

---

* All tables will be found in Appendix A.

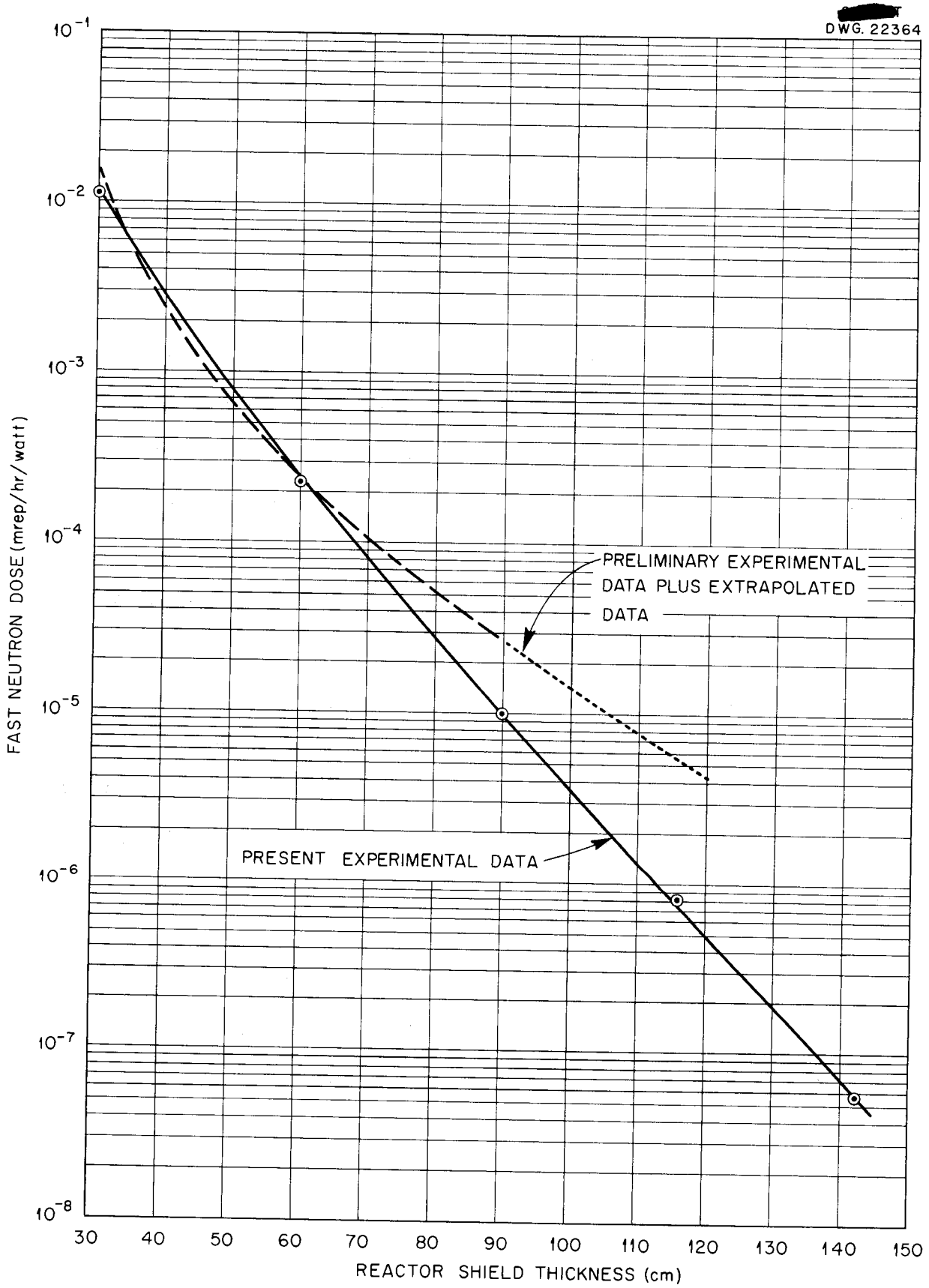

Fig. 5. Fast Neutron Dose at Surface of Crew Position as a Function of Reactor Shield Thickness.

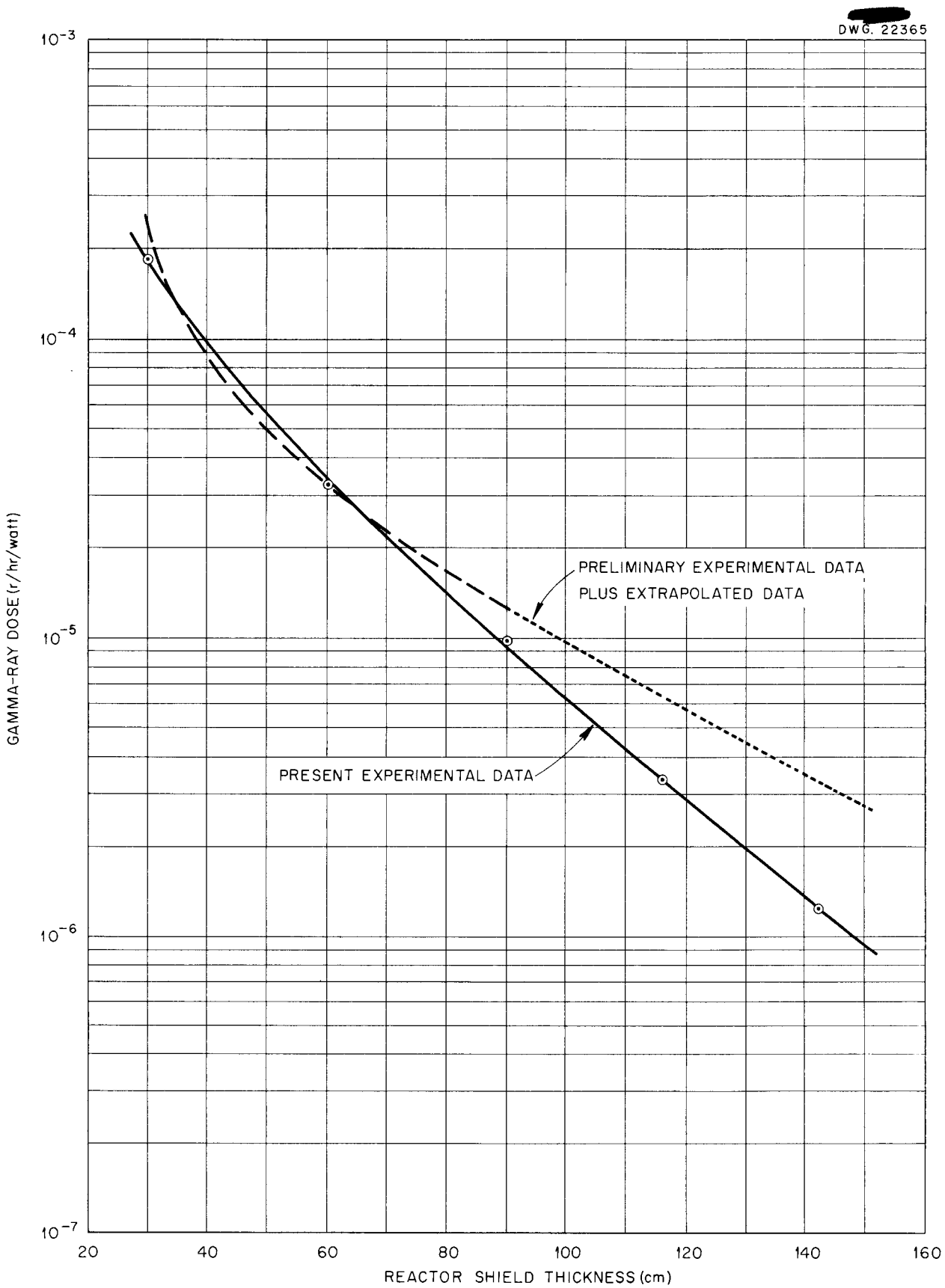

Fig. 6. Gamma-Ray Dose at Surface of Crew Position as a Function of Reactor Shield Thickness (Without Lead Around Detector).

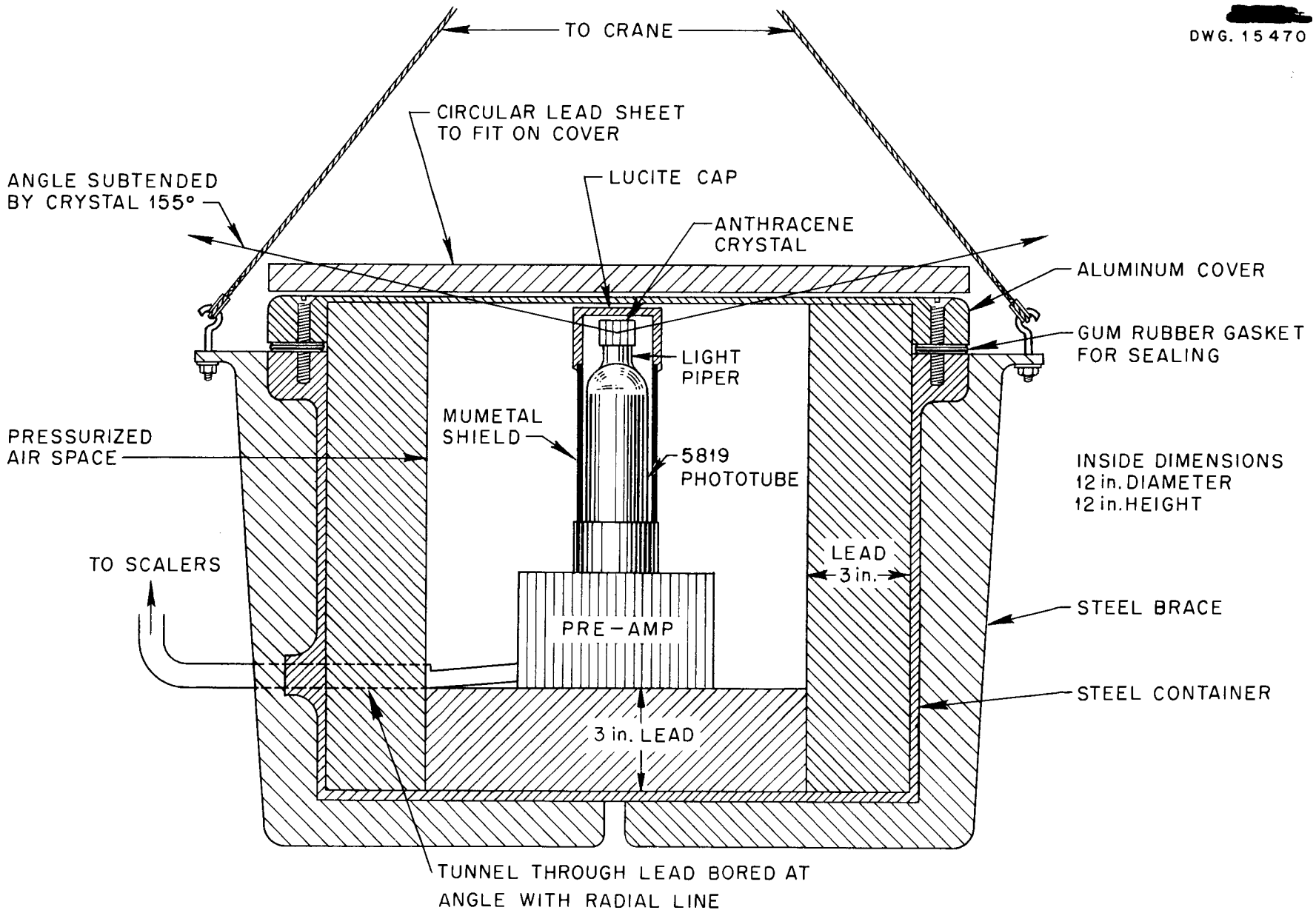

Fig. 7. Skyshine Experiments: Lead-Lined Cylindrical Container for Anthracene Crystal and Phototube, Simulating a Crew Box.

The current is a better criterion of dose than the count rate since it represents the integrated ionization rate. The data obtained is plotted in Fig. 8 from the summary given in Table A-7.

In addition to the present measurements, a determination of the effect of the lead shadow shield on the radiation at the crew position is reported here from results of the earlier tests not previously presented. For this test the water above the reactor was 90 cm, and vertical traverses were made with a gamma-ray detector at the crew position with and without the lead slabs forming the shadow shields in place (See Fig. 9 and Table A-8). The presence of the shadow shield reduced the gamma radiation at the crew by a factor of 0.52. The fast neutron dose was not affected.

Shield Weight Calculations Based on Data from Repeat Experiments

In the following calculations the scale-up factor is the same as that used in the preliminary report. Unfortunately there is no way of verifying this factor experimentally, so a region of uncertainty still remains in the calculations. As used in the preliminary report the scale-up factor S consisted of the following parts:

$$S = (A_a/A_b)(L_a/L_b)(\sqrt{r_s/r_a})(d_b/d_a)(P_a)$$

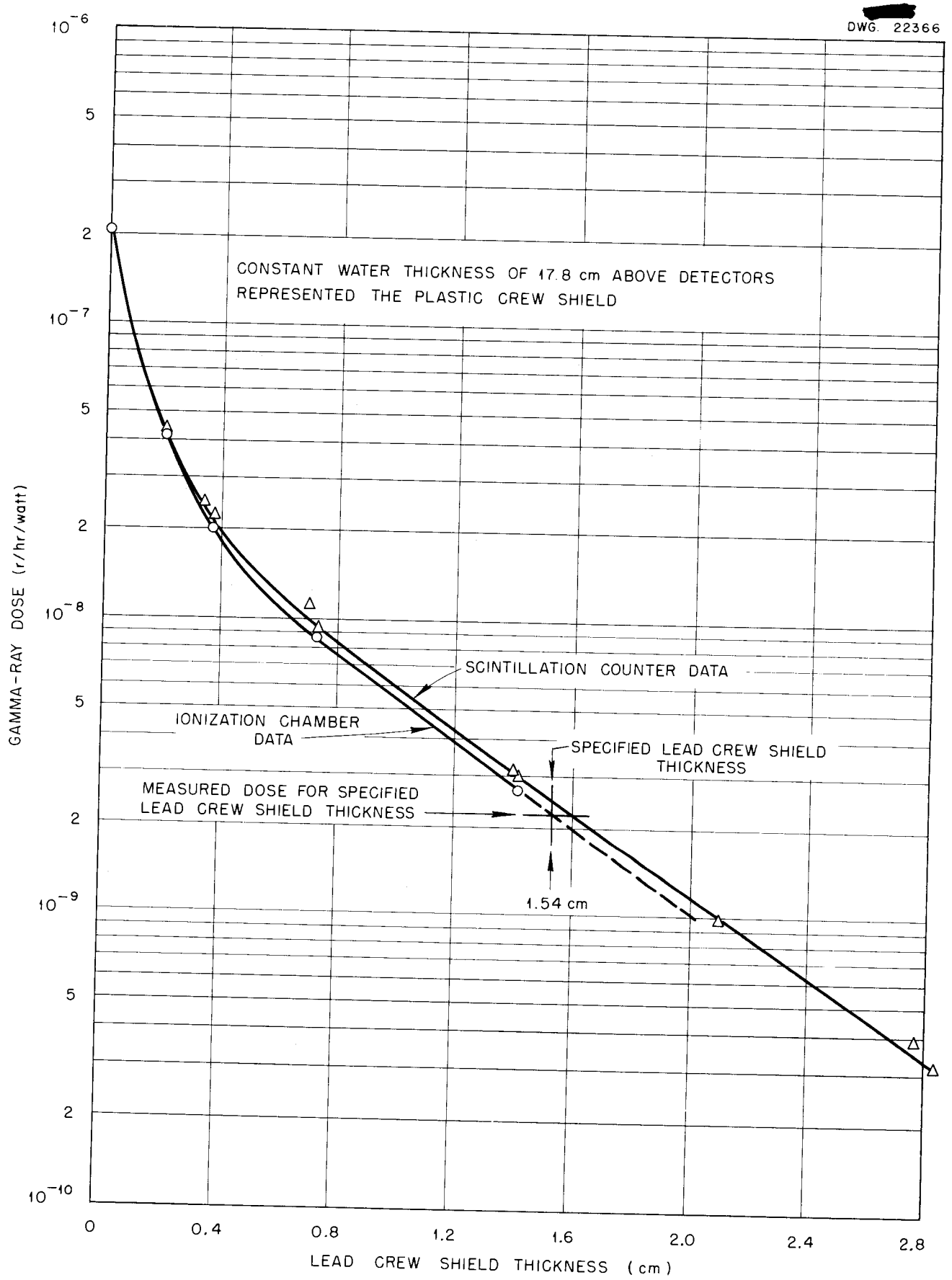

Fig. 8. Attenuation of Gamma Rays by Lead Crew Shield.

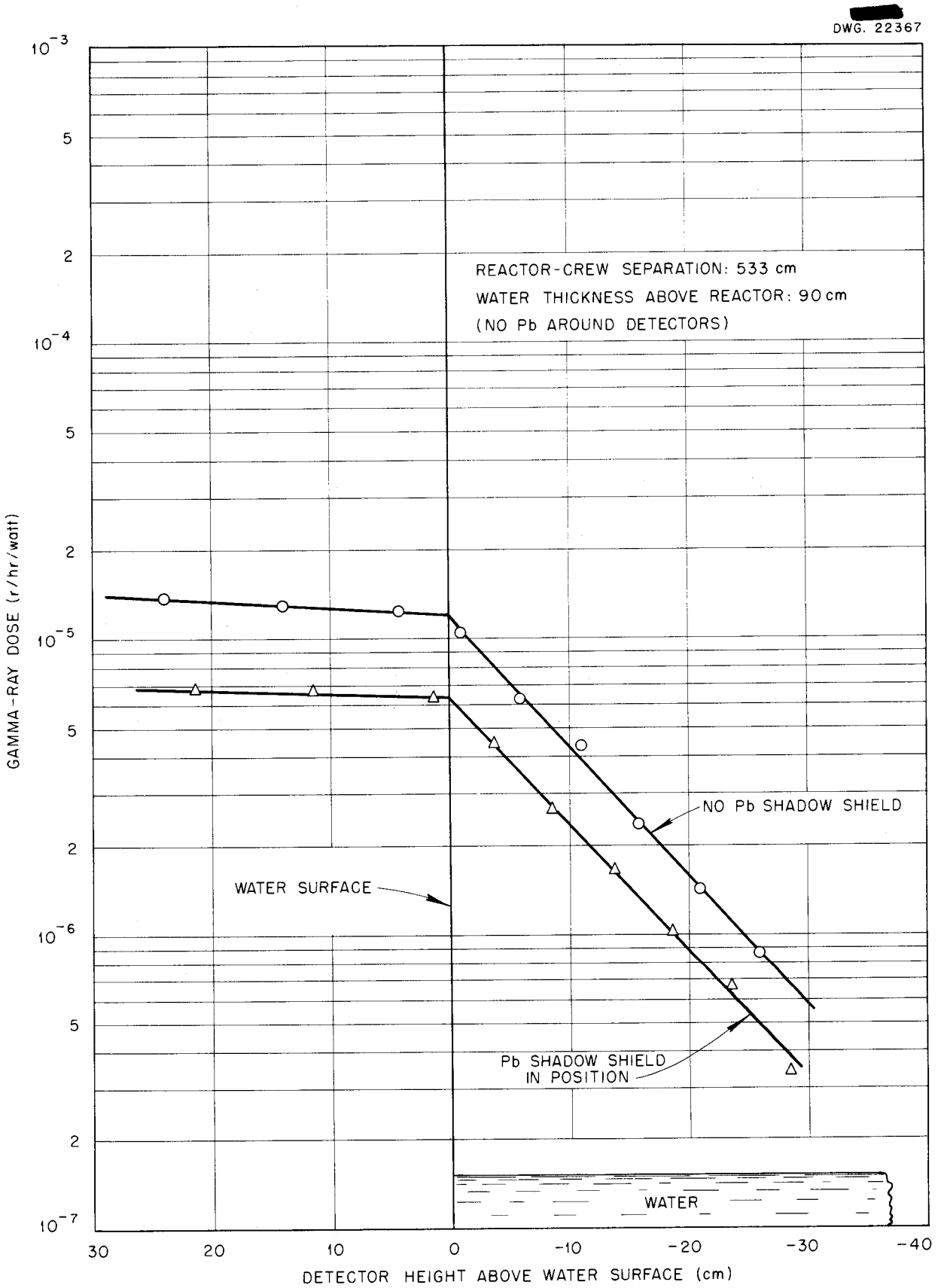

Fig. 9. Comparison of Gamma-Ray Doses at Crew Position — With and Without Lead Shadow Shield in Place.

where subscript a refers to the aircraft reactor and subscript b refers to the BSR, and

A_a/A_b = ratio of areas exposed = 16,

L_a/L_b = ratio of leakages per watt = 0.2 (quite low since there is a much lower concentration of uranium in the aircraft reactor),

$\sqrt{r_s/r_a}$ = correction for leakage from a cylindrical shield instead of a plane surface = 1.8,

d_b/d_a = correction for reactor-crew separation distance = 1/3,

P_a = power of the aircraft reactor = 2×10^8 watts (data on the BSR is normalized to 1 watt).

When all the above corrections were applied, an upper limit of $S = 3.8 \times 10^8$ was found. Since the best estimates at the time of the preliminary tests* indicated that the wall-scattered radiation was two or three times the air-scattered radiation for both neutrons and gamma rays, a lower limit on S of 1.3×10^8 was determined with the most probable value being

$$S = 2.1 \times 10^8$$

The latter value is used for these calculations.

Neutron Shield Weight Calculations. In order to determine the minimum thickness of the neutron shield, it was first necessary to calculate the dose reaching the crew compartment in the airplane from the experimental data:

$$D_n = S\phi_n(e)$$

---

* It is shown later in this report that scattering from the pool walls and bridges contribute less to the dose at the detector than had been first estimated (see, for instance, pages 34 and 49 in Part II). A theoretical discussion is presented in Appendix B.

where

D_n = neutron dose reaching crew compartment of airplane,

$\phi_n(e)$ = experimental neutron dose at crew position (see Fig. 3)

$= 1.65 \times 10^{-8}$ mrep/hr/watt.

Thus,

$$D_n = (2.1 \times 10^8)(1.65 \times 10^{-8}) = 3.46 \text{ mrep/hr}$$

The Shielding Board specified a neutron dose within the crew compartment of 21.5 mrep/hr. Since the experimental dose as measured is only 16% of the specified dose, some plastic may be removed from the airplane crew shield, effecting a saving in weight. The experimental dose corresponding to the specified crew dose is just

$$\frac{1.65 \times 10^{-8}}{0.16} = 1.02 \times 10^{-7} \text{ mrep/hr/watt}$$

Referring to the experimental data in Fig. 3, it is found that the crew shield thickness corresponding to the above dose with 116 cm water above the reactor is 9.5 cm or 8.3 cm less than the thickness specified in the standard design. If it is assumed that the plastic crew shield weighs 610 lb per centimeter thickness, the weight saved by removing the 8.3 cm plastic is 5100 lb.

Gamma-Ray Shield Weight Calculations. The gamma-ray dose penetrating crew compartment in the airplane as indicated by this

experiment was calculated as follows:

$$D_\gamma = S\,\Gamma(e)R$$

where

D_γ = gamma-ray dose reaching the interior of the crew compartment of airplane,

$\Gamma(e)$ = experimental gamma-ray dose at crew position through specified wall thickness of 17.8 cm plastic plus 1.54 cm lead (see Fig. 8) = 2.2×10^{-9} r/hr/watt,

R = ratio of experimental gamma dose with lead shadow shields to dose without shadow shields = 0.52.

Thus,

$$D_\gamma = (2.1 \times 10^{8})(2.2 \times 10^{-9})(0.52) = 0.24 \text{ r/hr}$$

The Shielding Board calculated a gamma-ray dose of 0.25 r/hr. The experimental measurements thus agree well with the original calculations, indicating that the gamma shield is correctly designed for the crew compartment.

Conclusions

The experiments were made as clean as possible so that uncertainties in the measurements were kept to a minimum. Elimination of the extrapolation procedure used in the preliminary tests removed a large source of error. Many of the uncertainties which existed at the beginning of

the present set of tests were minimized by the collection of new data which is presented in section II.*

Agreement between experiment and calculation for the gamma-ray dose at crew position is better than one would expect because of the uncertainties still remaining. The fact that the experimental neutron results are much better than the Shielding Board calculations bespeaks the conservatism of those calculations.

---

* See also summary section III.

II. Some General Experiments on Air Scattering and Related Phenomena

The experiments described in section I of this report were all designed and performed under a definite set of conditions which required that the reactor, the detectors, the lead slabs, and the water level of the pool be in such a configuration as to mock up a portion of a divided shield. Using the data obtained from the experiments one was able to calculate (with the aid of certain scale-up factors) the dose to be expected under operating conditions in the crew compartment of a nuclear aircraft.

The results of the experiments and calculations cannot be considered to be completely trustworthy within themselves without further investigation into the limitations and bias of the experiments. There must be taken into account such considerations as the behavior of radiations under the conditions imposed by the experiment, the spatial distribution and directions of radiations near the reactor and detector, the magnitude of the source area of the water above the reactor which may contribute to the dose at the detector, the effect of scattering from pool walls and bridges on the dose at the detector, and many others.

A considerable amount of time was spent gathering data of a more basic nature which were designed to help clarify some of the uncertainties inherent in the experiments of part I, with the hope of gaining a fuller understanding of the experiments. Some of the general experiments performed are described in the following pages.

Vertical Traverses above the Reactor

Some of the most important data collected during these experiments showed the attenuation of radiation directly over the reactor as a function of distance from the reactor. These measurements were made both with the pool completely filled and with water levels that corresponded to the reactor shield thicknesses used in the tests in Part I. It was physically impossible to make vertical "centerline" measurements because the reactor control mechanism prevented the detectors from being placed any nearer than 7.5 cm from the vertical centerline of the reactor.

The vertical line along which the measurements were made is shown in Fig. 10. These traverses were at a z position 15.5 cm south of the north face of the reactor or 7.5 cm from the center of the reactor. The thermal neutron and gamma measurements at the various pool levels are shown in Figs. 11 and 12, respectively. Large gamma-ray background from the reactor prevented use of the fast neutron dosimeter here.

It is to be noted that at any given distance above the reactor a measurement made with the counter surrounded by water is higher than the same measurements made with the detector at or just above the water surface. The difference for thermal neutrons is a factor of between 2.5 and 3 (compare solid and dashed curves of Fig.11); for gamma rays the difference is approximately 20% at distances greater than 1 m (Fig. 12). This is explainable on the basis that there is more radiation scattered into the

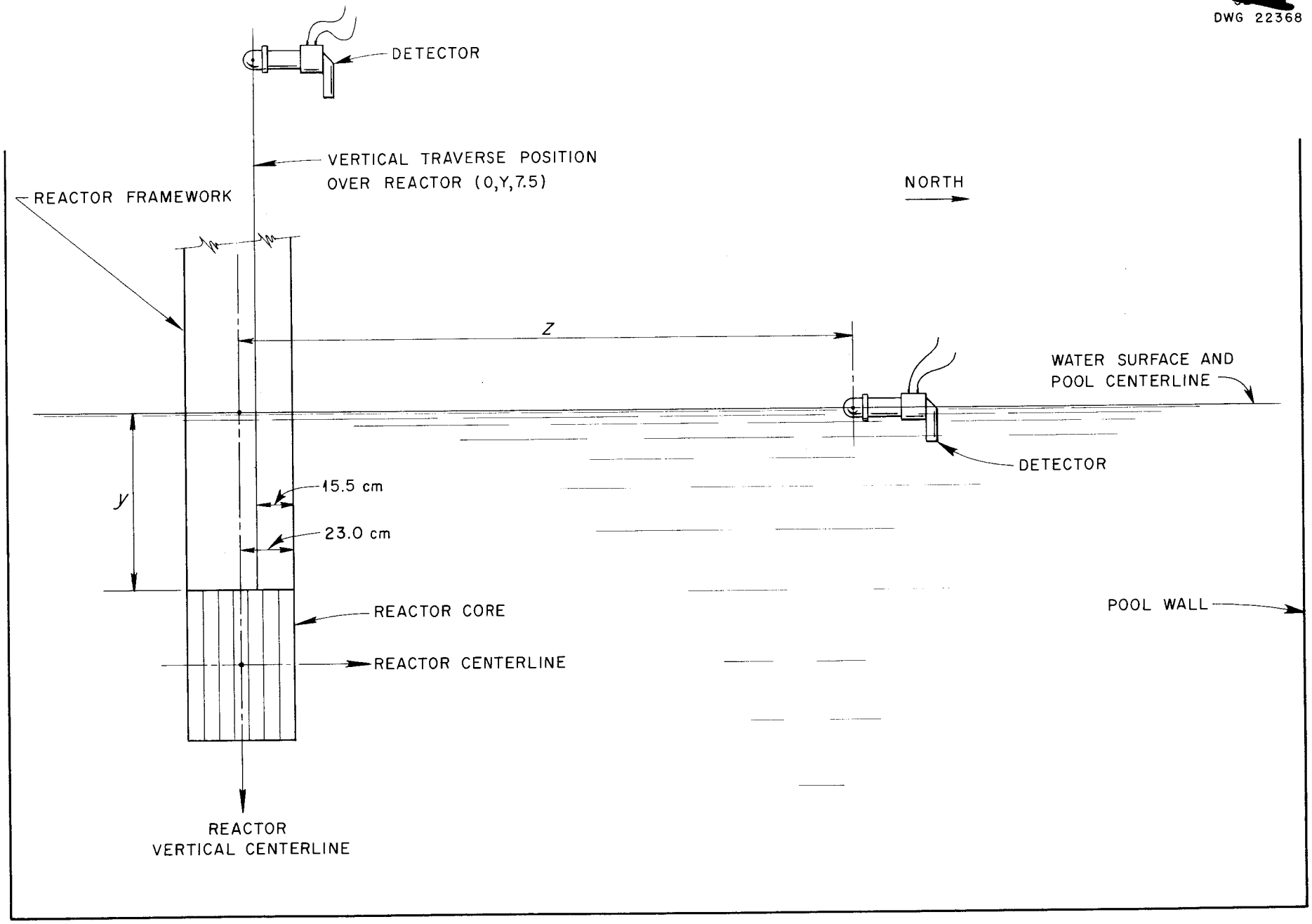

Fig. 10. Illustration Showing Positions of Detectors for Vertical Traverse and Horizontal Scan Measurements.

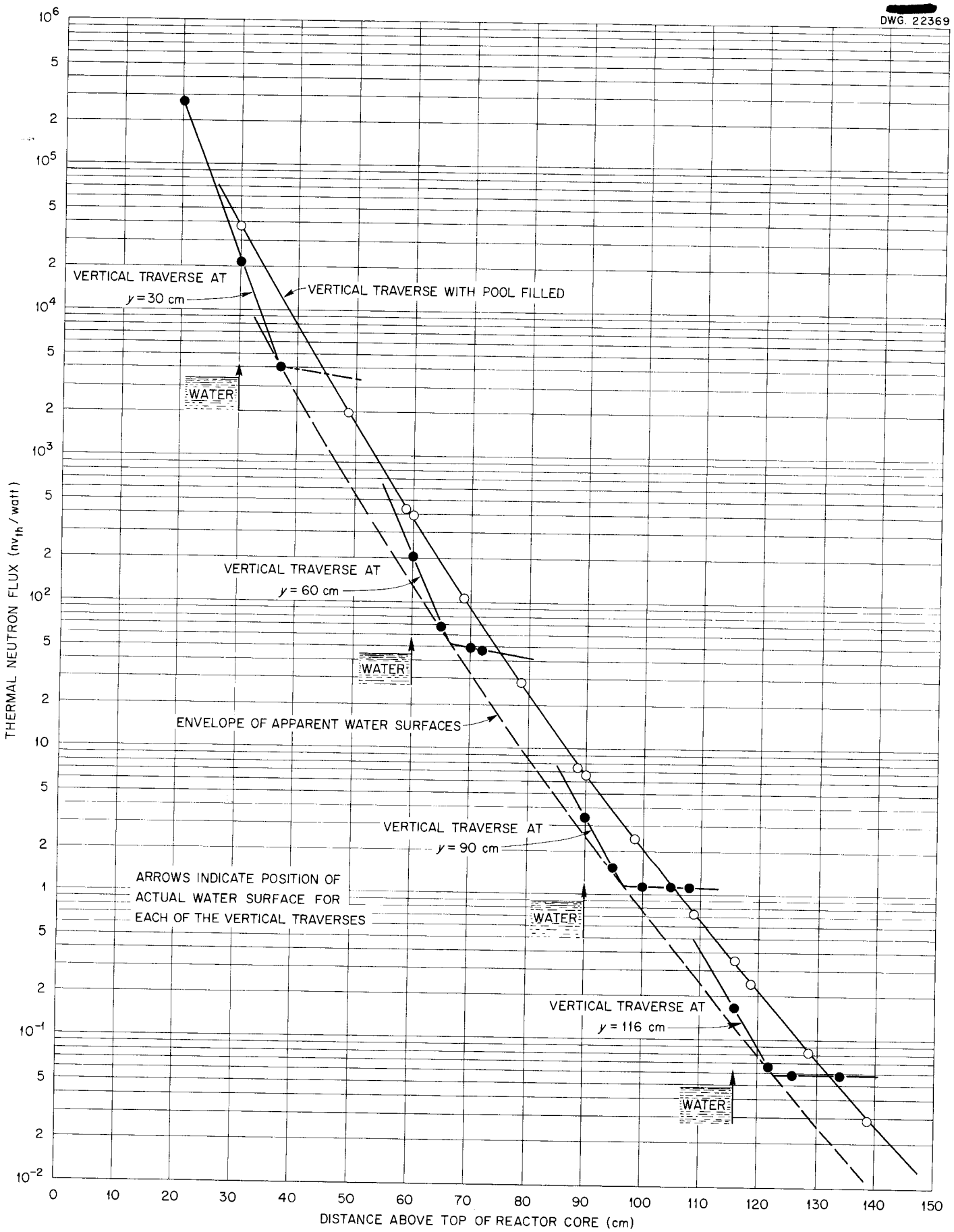

Fig. 11. Thermal Neutron Flux Measurements Directly above BSR for Various Water Thicknesses (y) above Reactor.

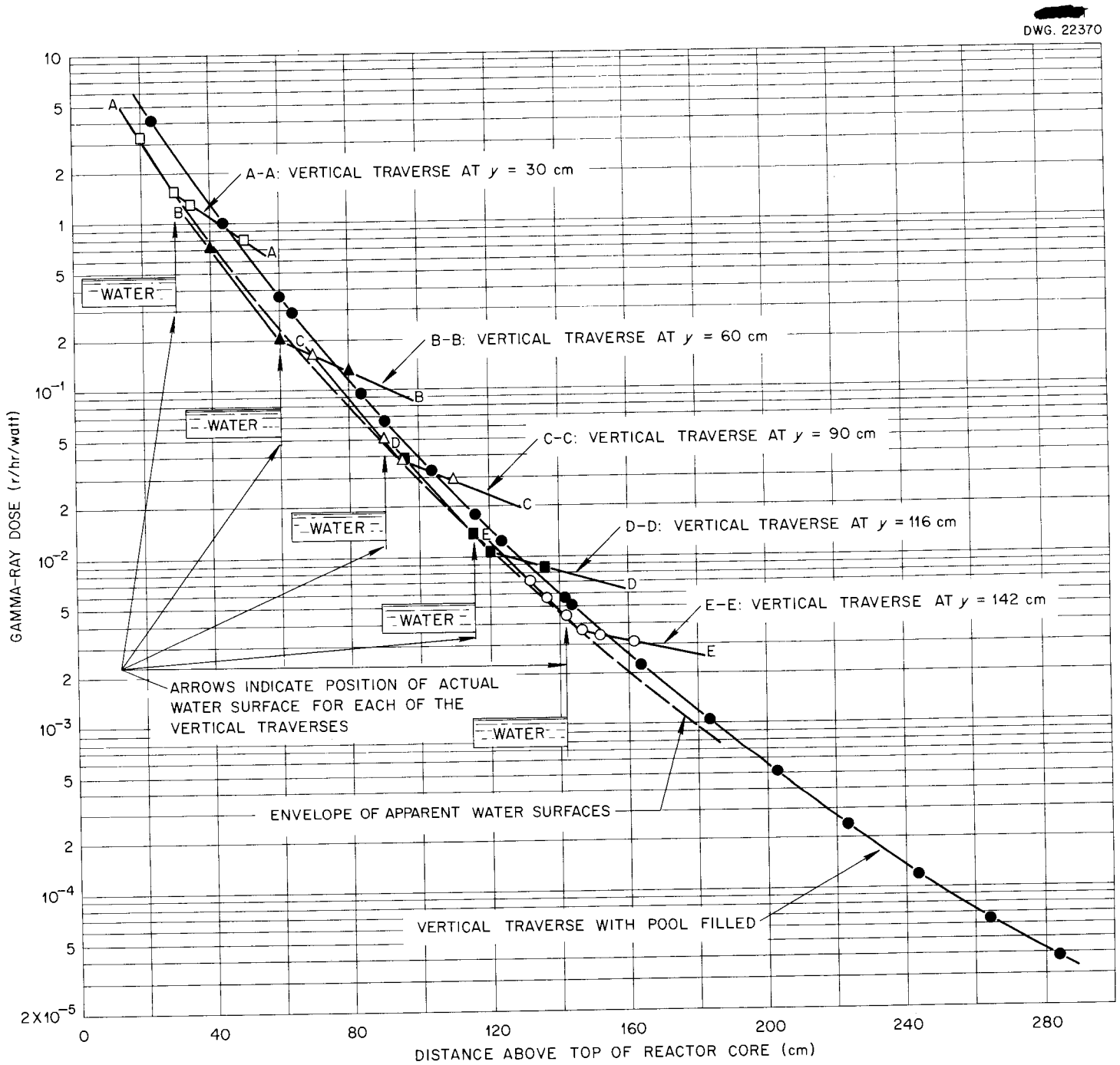

Fig. 12. Gamma-Ray Dose Measurements Directly Above BSR for Various Water Thicknesses (y) Above Reactor.

detector when it is in the denser material because of the increased number of scattering centers surrounding the counter.

The depression of flux in the proximity of the boundary of the attenuating medium (the water surface) may be described in terms of an apparent displacement of the surface. In Figs. 11 and 12 the discrepancies between the actual and apparent water surfaces are shown. It is clear that when the detector is in air its position should be described according to its distance from the apparent water surface. All other figures are corrected to the apparent water surfaces where necessary. It is to be noted that the slopes of the thermal neutron curves in water are steeper close to the water surface than the attenuation in water at the same level. This is attributable to the diffusion properties of thermal neutrons near the boundary of a diffusive medium. The experimental data is tabulated in Tables A-9 through A-12 in Appendix A.

Scan of a Quadrant of Water Surface above the Reactor

Radiation received at the crew must emerge from the water surface near the reactor, so that as far as the detector is concerned the water surface is the radiation source. In order to study the patterns of the emerging radiation, a scan of the water surface directly above the reactor was made with both a thermal neutron detector and a gamma-ray detector. The thermal neutron flux existing over a square meter of water surface above the reactor at a water level of 116 cm is shown in Fig. 13. The neutron intensity falls away rapidly from the origin of the scan. At

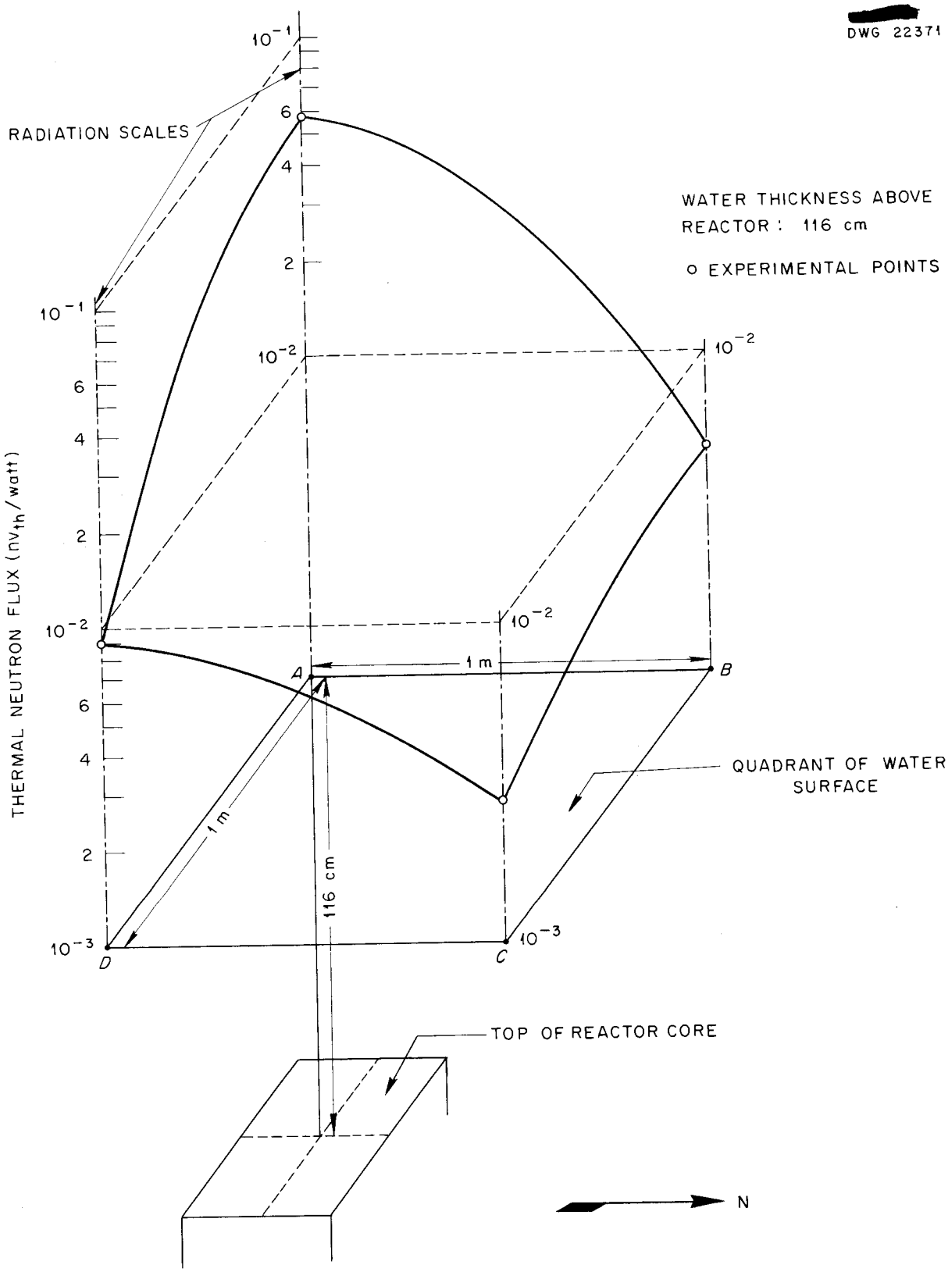

Fig. 13. Thermal Neutron Flux Pattern over Quadrant of Water Surface Directly Above Reactor.

each of the points A, B, C, and D shown in Fig. 13 vertical traverses were made with the thermal neutron detector from about 20 cm above the water surface to 20 cm below the water surface. These measurements are plotted in Fig. 14.

The gamma-ray scan shown in Fig. 15 was made with a water level of 142 cm. A complete scan was made of a square 25 cm on a side and additional points were taken along the line AB. The results of these measurements were used to extrapolate the data to points C and D, which then gave the flux over a square meter*. The gamma-ray flux over a square meter of water surface above the reactor is much more uniform than the neutron flux.

The data from which Figs. 13, 14, and 15 were drawn are presented in Tables A-13 and A-14.

Radiation Pattern along the Pool Centerline

At some point on the water surface of the pool the intensity of radiation arriving at the detector through the air equalled that arriving through the water. The place where this happened marked the edge or boundary of the water surface as a source of radiation to the detector. In order to determine the size of this surface source, a

* At the time of these measurements other equipment in the pool prevented the positioning of the detector at points C and D.

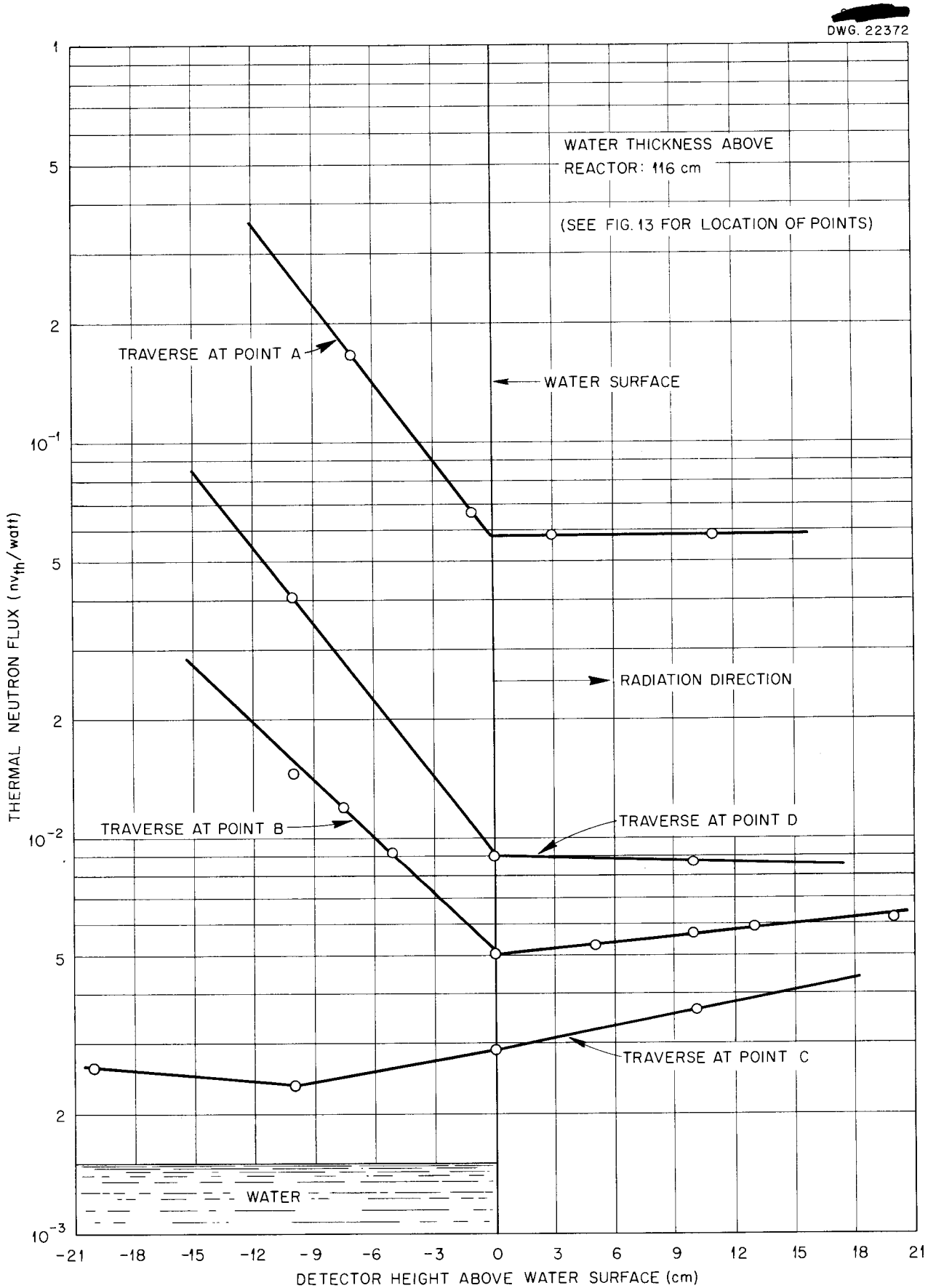

Fig. 14. Thermal Neutron Flux Along Vertical Traverses Made at Various Points on 1 m^2 Quadrant above BSR.

[redacted]

DWG 22373

WATER THICKNESS ABOVE REACTOR: 142 cm

○ EXPERIMENTAL AND INTERPOLATED POINTS

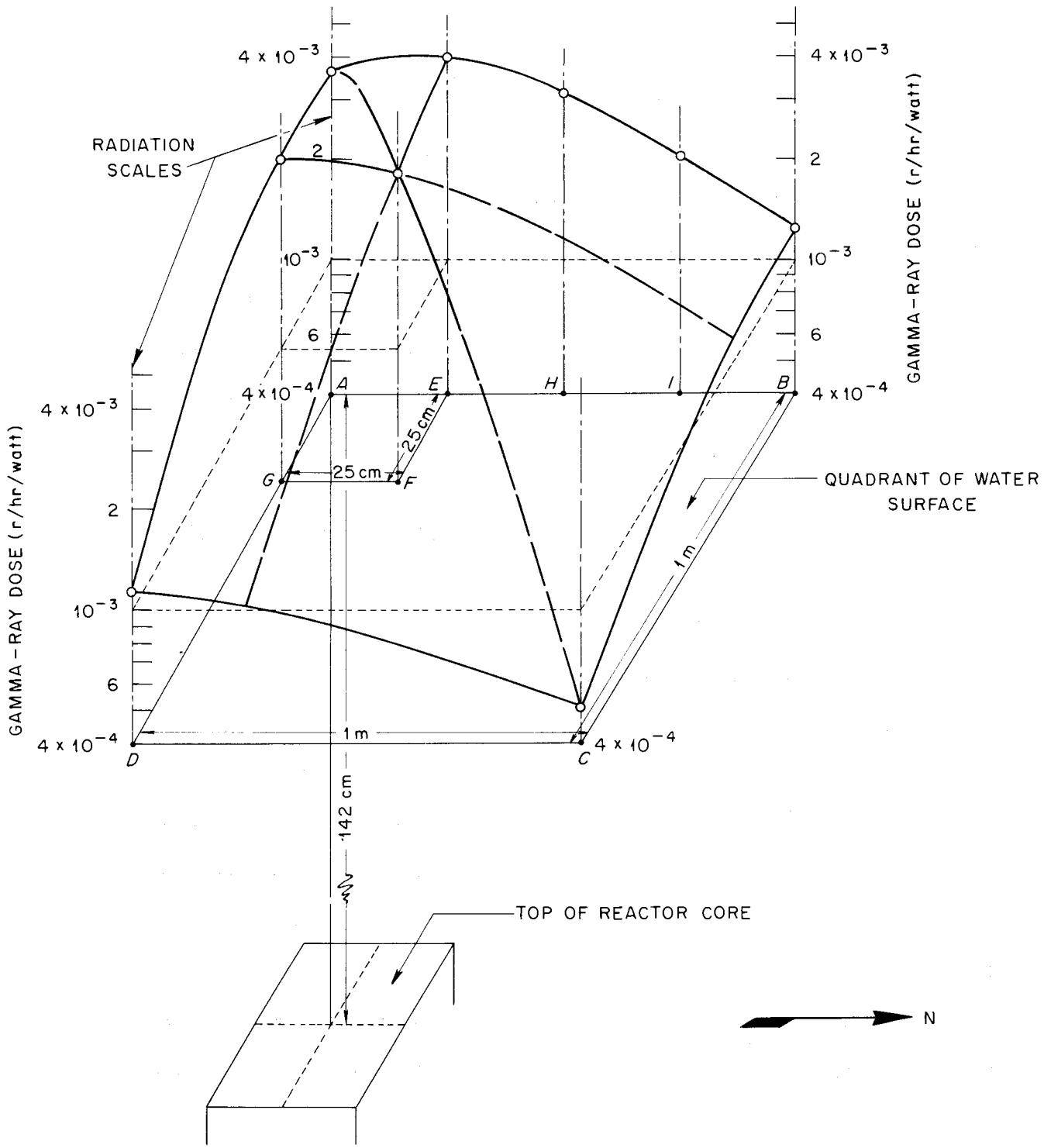

Fig. 15. Gamma Radiation Pattern over Quadrant of Water Surface Directly Above Reactor.

scan of the water surface along the pool centerline from reactor position to crew position was made both for gamma rays and for thermal neutrons. The neutron traverse, made at a water level of 116 cm is shown in Fig. 16, and the gamma-ray scan, made at a water level of 142 cm, is shown in Fig. 17. At most of the points of the gamma-ray scan vertical traverses near the water surface were made, the results of which are shown in the insets of Fig. 17. The sharp drop in the data of Fig. 17 at 400 cm is due to the presence in the pool of the Divided Shield Mockup which shielded the detector at crew position from direct radiation. The data is presented in Tables A-15 to A-17.

Characteristics of the Water Surface as a Secondary Radiation Source

From a study of Figs. 13 through 17, it is apparent that the neutrons emerging from the water surface above the reactor were much more highly collimated than the gamma rays. As shown in Fig. 16, the neutron intensity dropped a factor of e in 55 cm and a factor of e^2 in about 77 cm. This means that the main cone of radiation for neutrons was limited to an angle of about 21° from the vertical, covering a solid angle of about 0.4 steradian. The neutron intensity dropped sharply from the origin to about a 125-cm distance from the reactor center and then flattened out at larger distances, fairly well following the 1/R attenuation law for scattered radiation, as is shown in Fig. 16. This indicates that the neutron radiation existing above the water outside

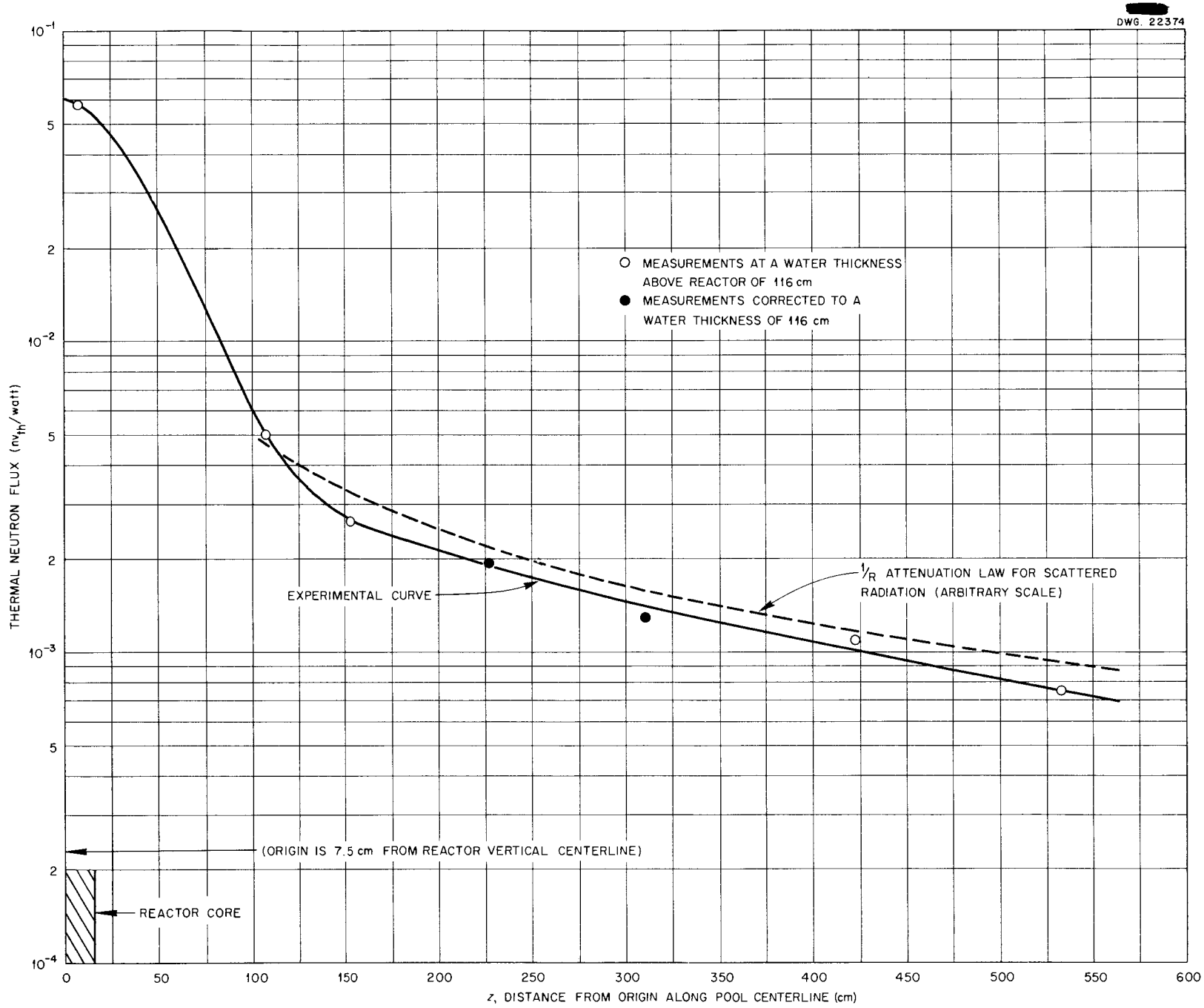

Fig. 16. Thermal Neutron Flux Pattern at Water Surface Along Pool Centerline.

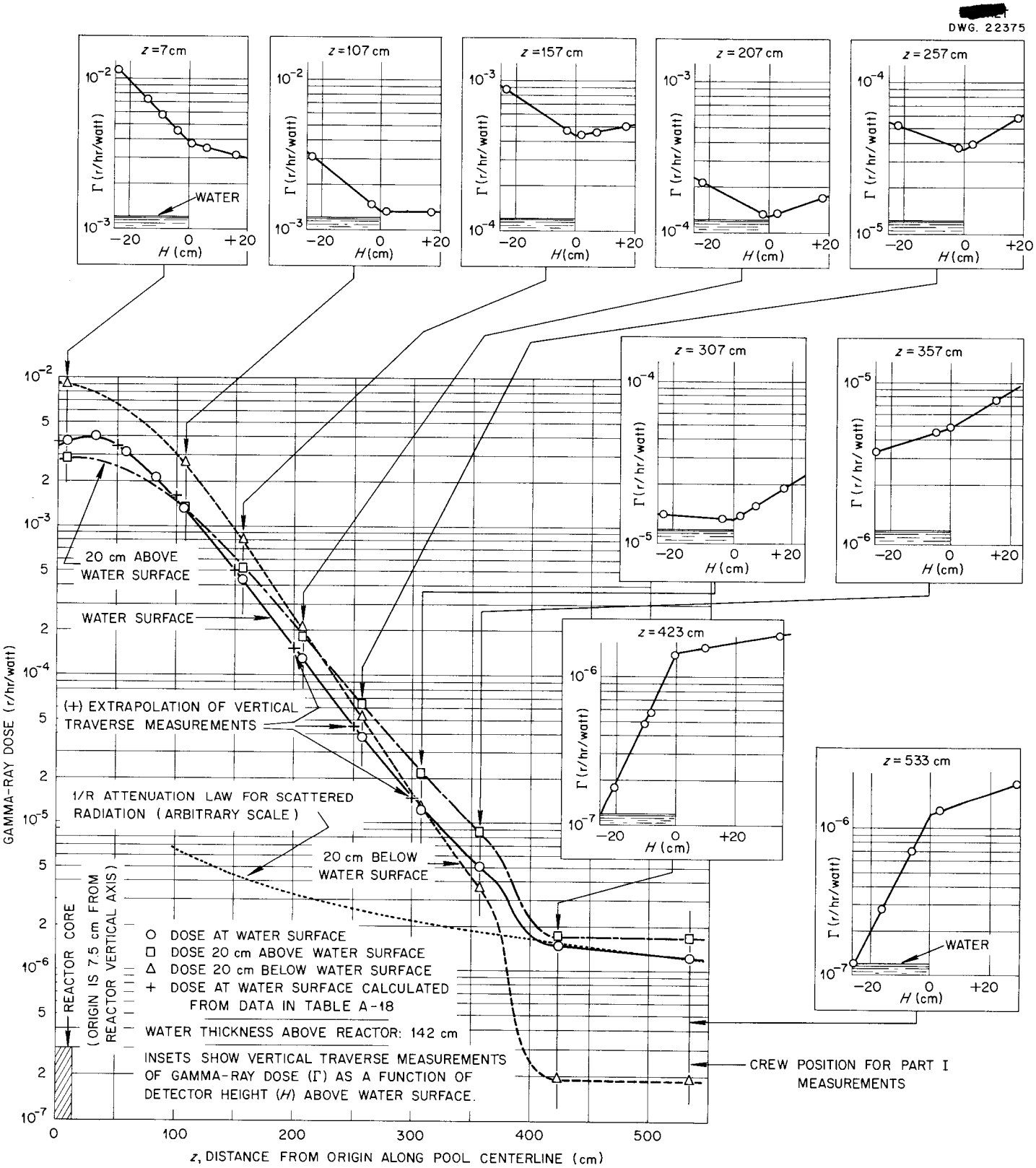

Fig. 17. Gamma-Ray Dose Patterns Near Water Surface Along Pool Centerline.

of a radius of 125 cm from the reactor was mainly scattered radiation.

On the other hand the picture for the gamma rays was quite different. They were not as highly collimated. In fact they were still emerging from the water surface at distances as far away as 300 cm from the reactor, as can be clearly seen from the insets of Fig. 17. The gamma intensity dropped a factor of e in about 95 cm and a factor of e^2 in 155 cm. This means the main radiative cone lies within about 30° from the vertical, covering a solid angle of about 0.7 steradian, but there were significant source contributions out to 300 cm covering a solid angle of 3.1 steradians. The 1/R attenuation law was not followed except beyond about 400 cm, as indicated in Fig. 17.

The gamma radiation emerging from the water surface above the reactor appears to have travelled largely along straight lines to the surface. This is evidenced by the fact that the dose appears to be attenuated according to the thickness of water interposed between the reactor and the detector. Seven calculations were made of straight-line path lengths L, from the center of the reactor to points on the surface at distances of from 0 to 300 cm from the reactor vertical centerline. Gamma-ray doses D_L' corresponding to water thicknesses L were then

read from Fig. 12. These values of D_L' are given in Table A-18, Appendix A. The D_L' values are plotted as large "+" symbols in Fig. 17. The agreement between the experimental points and the points obtained by this graphical analysis is surprisingly good.

Referring to the dip in the curves of the gamma-ray scan of Fig. 17, it is to be noted that if the lead shadow slabs shown in Fig. 2 had been put in the pool, the drop in the radiation pattern would have occurred between 50 to 75 cm z distance and would have been even greater.

The effectiveness of the extended water surface as a source may be deduced from this phenomenon. It is quite possible that the 1/R attenuation law may hold for gamma rays in as near as 1 m from the reactor position with the shadow shield in place. At any rate, the effect of the extended radiation source (without the shadow shield) at the crew position is to multiply the gamma radiation received at the crew position by a factor of 2. This points up the fact that the shadow shield factor R used in the calculations of gamma dose at the crew (Part I, page 13) must be used, since only with the shadow shield present does the experiment adequately mock up the reactor side shield.

Scattering from Reactor and Instrument Bridges

Preliminary theoretical calculations indicated that the

scattering from the instrument and reactor bridges would make up a significant percentage of the scattered beam measured by the detector. Accordingly, a great deal of time was spent trying to determine the effect these bridges had upon the radiation at the detectors.

One series of tests was performed as follows: Detectors were placed at the crew position and measurements were taken with the instrument bridge rolled into various positions above the detectors. As shown in Fig. 18 the results of the measurements were not startling. In fact, the maximum difference noted for the various detectors with the instrument bridge in best and worst positions for scattering to the detector was of the order of 12%. The reactor was then moved off its bridge and suspended from a single H-Beam straddling the pool, and the measurements were repeated. The difference between these measurements (not shown) was only about 3%. It was concluded that scattering from the bridges did not contribute significantly to the radiation at the detector. The data is tabulated in Table A-19.

In order to test the effect of scattering from just the reactor bridge at points near the bridge, another series of tests was run with the reactor first on its bridge, then on the H-Beam. Vertical and horizontal gamma-ray traverses were made under the reactor bridge or H-Beam on the west side of the reactor. The location and results of the traverses are shown in Figs. 19 and 20. It should be noted here that

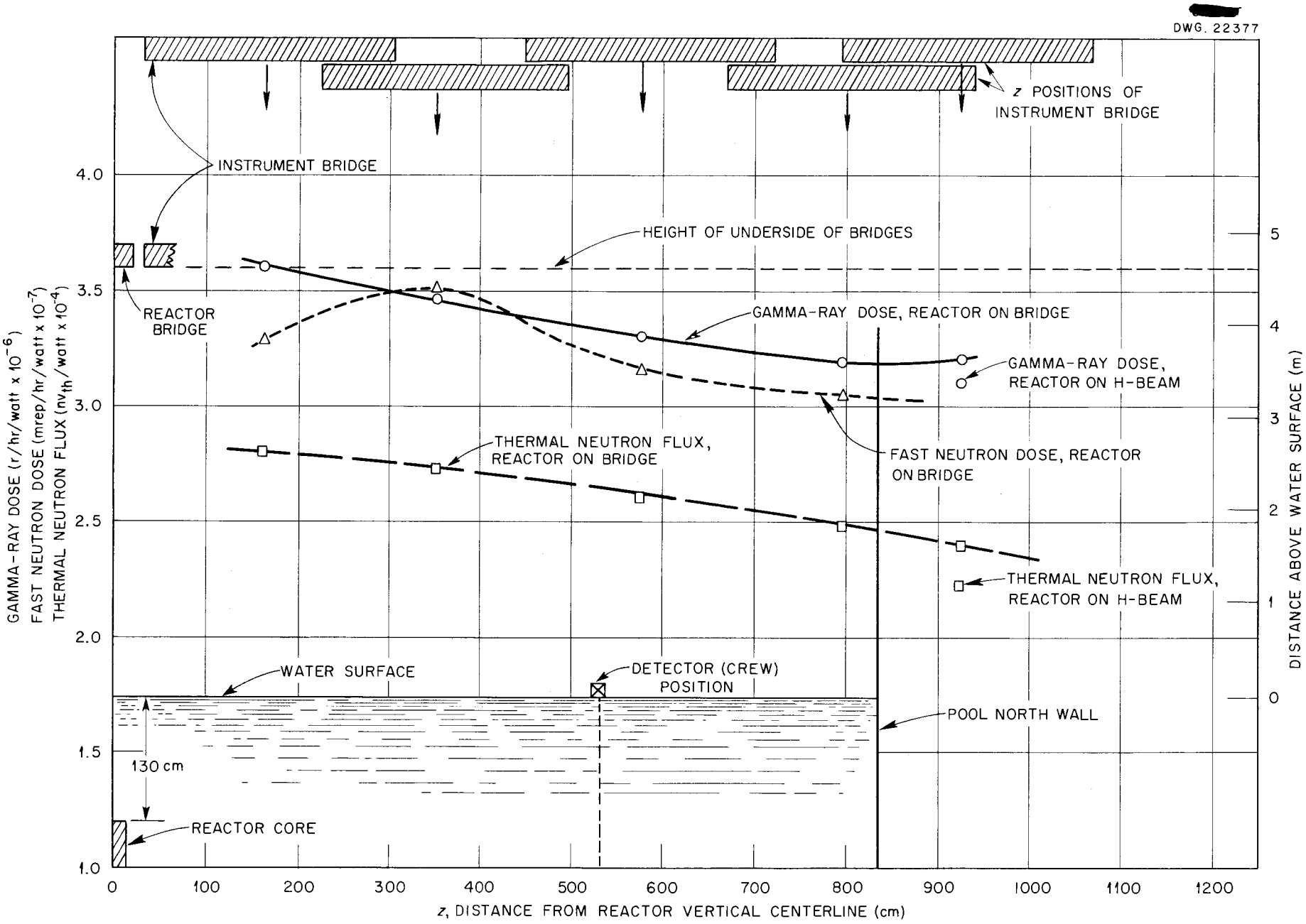

Fig. 18. Radiation Received at Crew Position for Various Locations of Instrument Bridge.

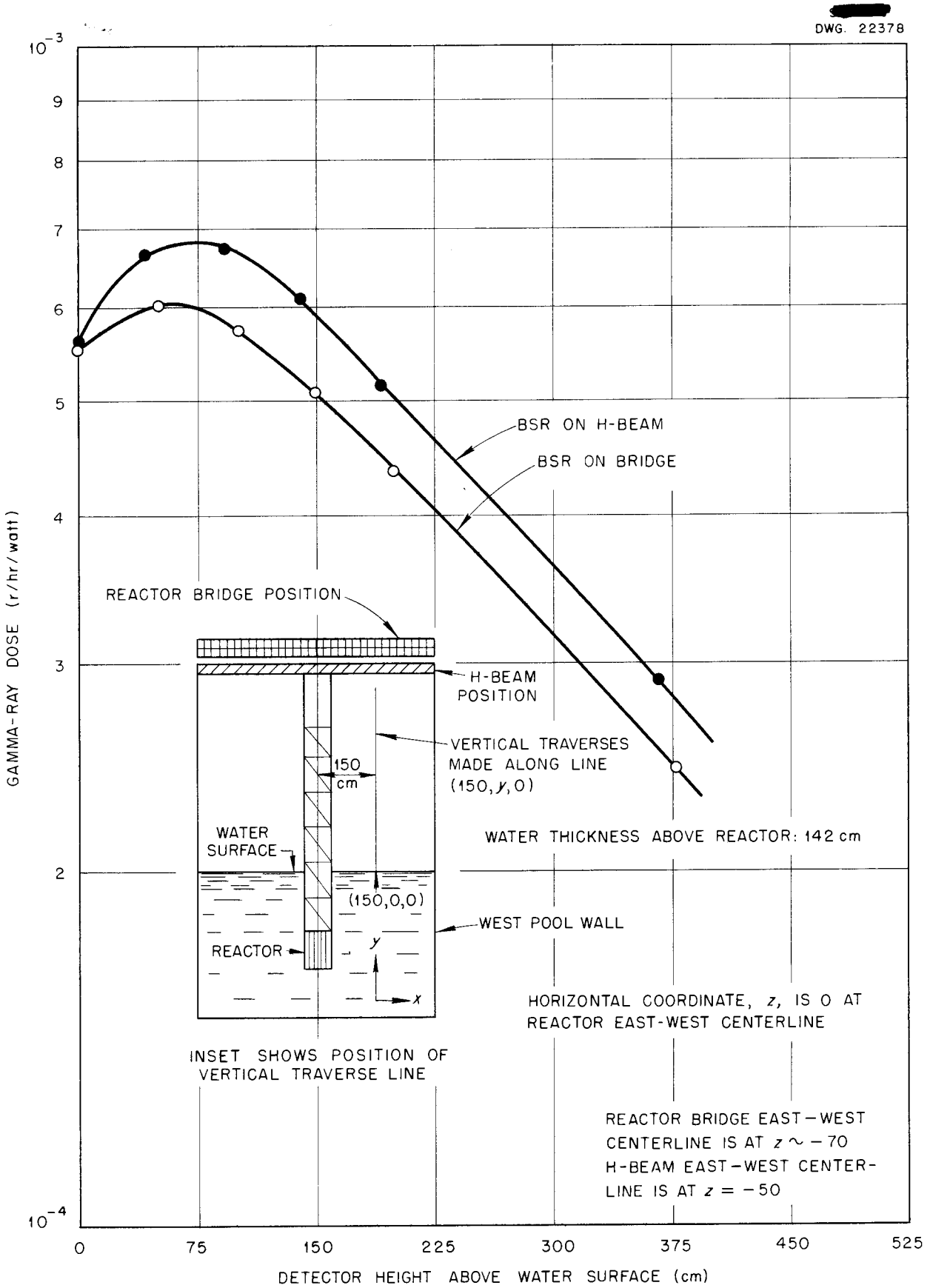

Fig. 19. Gamma-Ray Dose Measurements along Vertical Traverse Line Near BSR, with Reactor Mounted First on Its Bridge, Then on H-Beam.

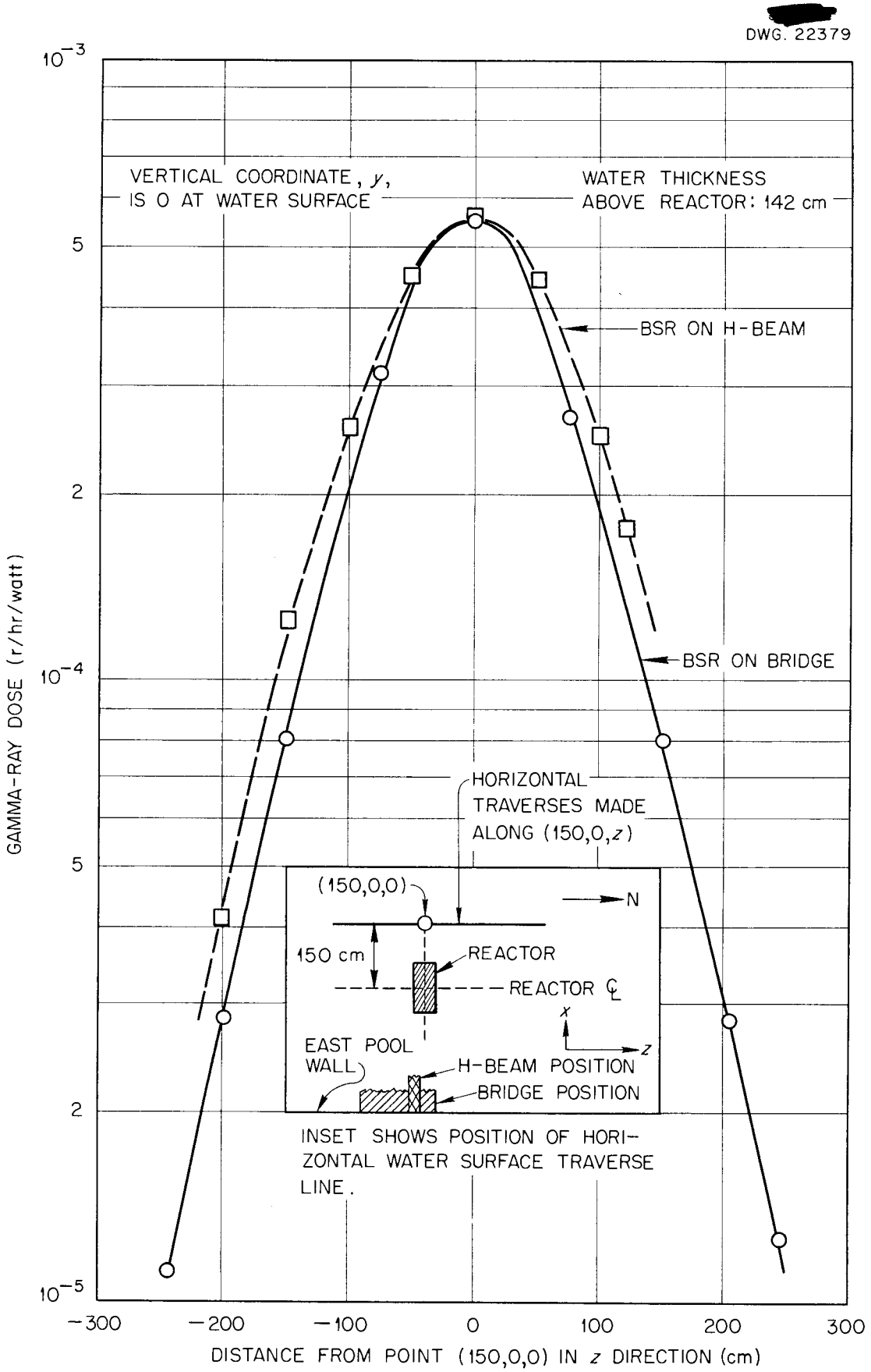

Fig. 20. Gamma-Ray Dose Measurements Along Water Surface Traverse West of Pool Centerline, With Reactor Mounted First on Its Bridge, Then on H-Beam.

the reactor is suspended from one side of its bridge, so that its east-west centerline is about 70 cm south of the reactor center. When the reactor was suspended on the H-beam, for reasons of balance the axis of the H-beam was 50 cm south of the reactor center. The above traverses were run using the reactor east-west centerline as a reference, rather than the bridge and H-beam east-west axis. The measurements with the reactor located on the H-beam are 15 to 20% higher than the corresponding measurements under the bridge. Offhand, higher readings would have been expected with the reactor on its bridge. Apparently the intensity of radiation scattered back from the air above the bridge to the detector was greater than that scattered from bridge to detector and was partially blocked out by the presence of the bridge. In this case, the scattering from the bridge had a negative effect.

The following test, offered as a confirmation of the above results, was run. At the time the vertical traverse under the H-Beam was made, the gamma-ray detector was placed first directly under the H-Beam, 367 cm above the water surface, and a reading was taken; then at the same height above the water another reading was taken 50 cm from the beam (Table A-20). The reading obtained under the beam was 2.80×10^{-4} r/hr/watt, and the reading at the same height away from the beam was 2.91×10^{-4}, some 4% higher. (Data for the curves of Figs. 19 and 20 are shown in Tables A-20 and A-21.)

Effect of Lead at Crew Position on Radiation Received

In addition to the lead tests reported in Part I, vertical traverses at the crew position were made with a gamma-ray detector in the lead-lined container (Fig. 7). One traverse was made with no lead covering on the container and another was made with a 5/64-in. lead cover. A plot of the results (Fig. 21) shows that the shapes of the two traverses are approximately the same. The 5/64 in. of lead decreased the dose by about a factor of 5. Examination of the energies* involved show that for an assumed angle of penetration of 45° the energy of gammas absorbed by 5/64 in. of lead was around 0.3 Mev, whereas the slope of the traverse curve in water shows that the energy of the typical scattered gamma photon entering the detector was nearer 1.0 Mev. This would indicate that although a great deal of low-energy radiation reaches the crew, the shielding must be designed for the higher gamma-ray energies. The data is reported in Table A-22.

Effect of Interposing a Lead Slab at Various Positions Between the Reactor and Detector

In order to find out something about the directions of the primary and scattered radiation which contributed to the dose at the crew, the following experiment was performed. A gamma detector and thermal neutron counter were located at the crew position (in this case 4.6 m from the midpoint of the reactor for convenience in the setup).

---

* For assumed 20° angle of penetration, the energies were calculated to be 0.4 and 2 Mev, respectively.

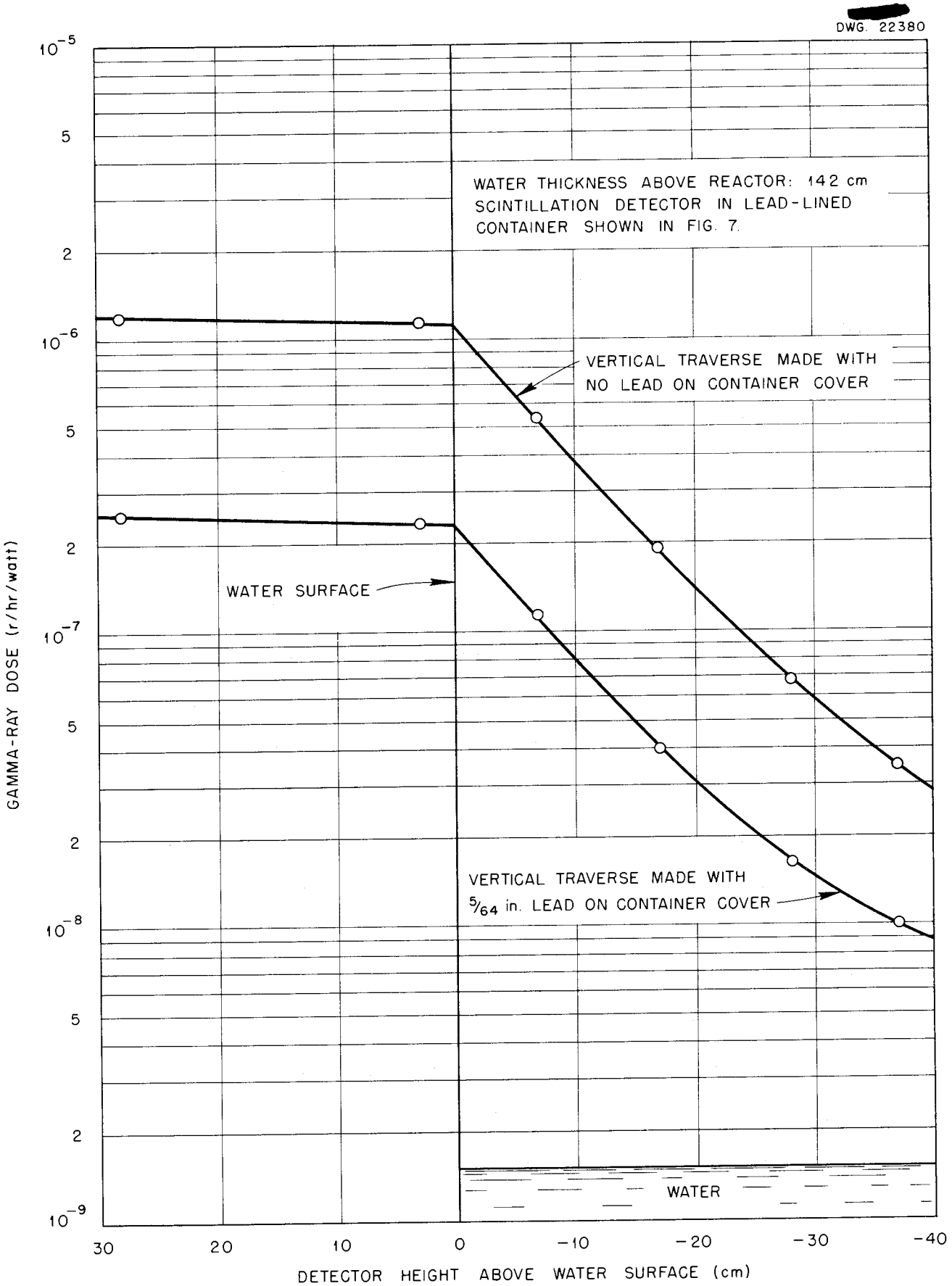

Fig. 21. Effect of Lead at Crew Position on Gamma-Ray Dose Received.

A lead slab was hung from the crane and placed at various positions in the water and air between reactor and detector, as given in Tables A-23 and A-24. A set-up of the experiment is shown in Fig. 22. Essentially the slab was moved into six positions along each of three vertical lines (A, B, and C) which were located at approximately 1.2, 2.4, and 3.8 m from the reactor, respectively. The results of measurements taken at each position are shown in Figs. 23 and 24 from the data of Table A-25.

As was expected, the lead slab cut out a considerable amount of gamma radiation when it was located near the water surface (Fig. 23). This information supports the theory that the greater part of gamma radiation reaching the detector at the crew position is scattered through small angles. This data also indicates that the gamma radiation emerging from the water surface is not highly collimated. If it were, the higher positions of the lead would have greater effect upon the radiation at the crew, since with larger scattering angles the detector would receive radiation from scattering centers located fairly high above the water surface.

This experiment also yields more evidence for the validity of the factor of 0.52 used as a lead shadow shield correction for the shield calculation of Part I. Position 1A of the lead slab in this test is fairly close to the position of the shadow shield slabs in

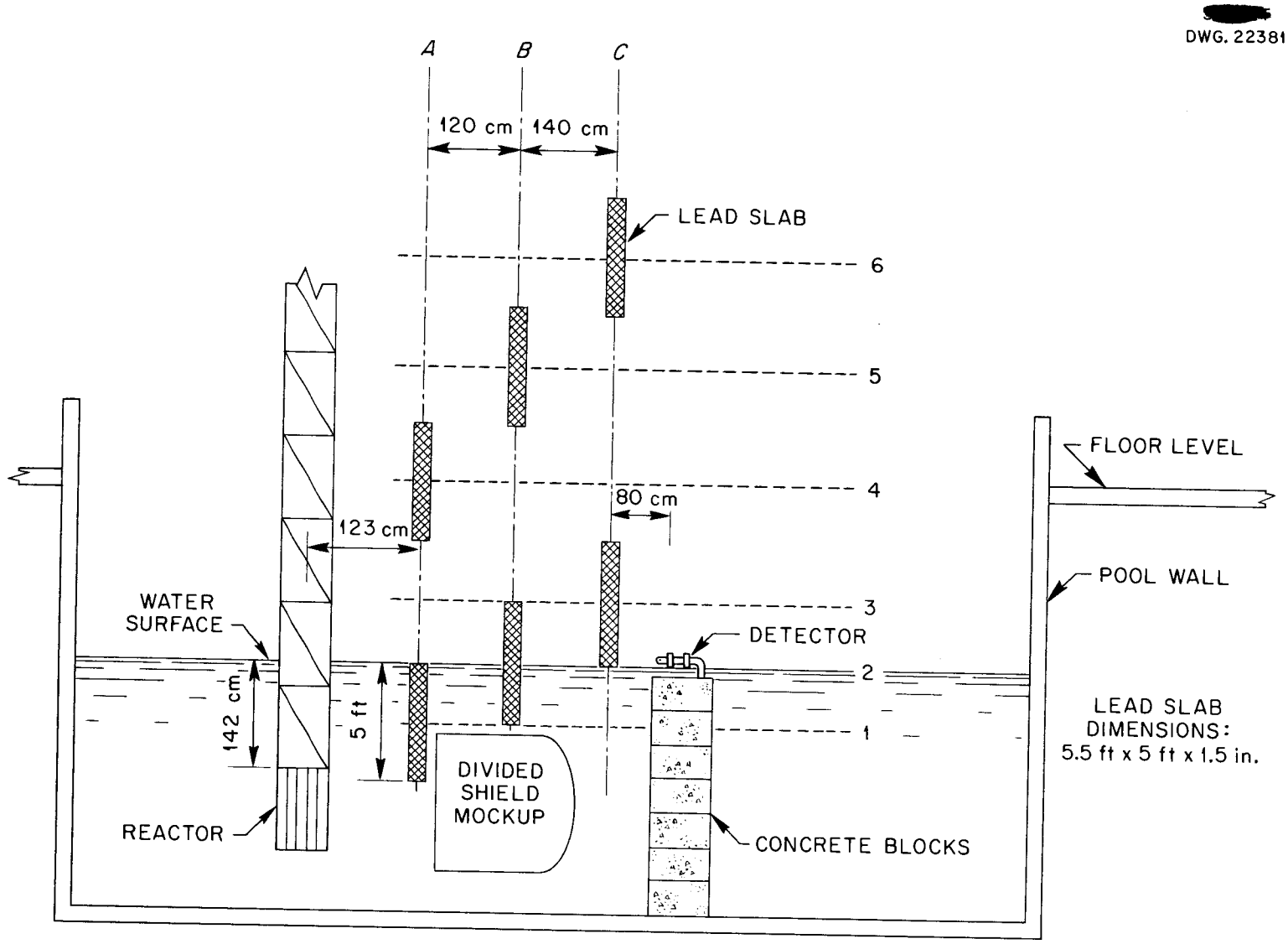

Fig. 22. Illustration Showing Positions of Lead Slab Along Vertical Traverse Lines *A*, *B*, and *C*.

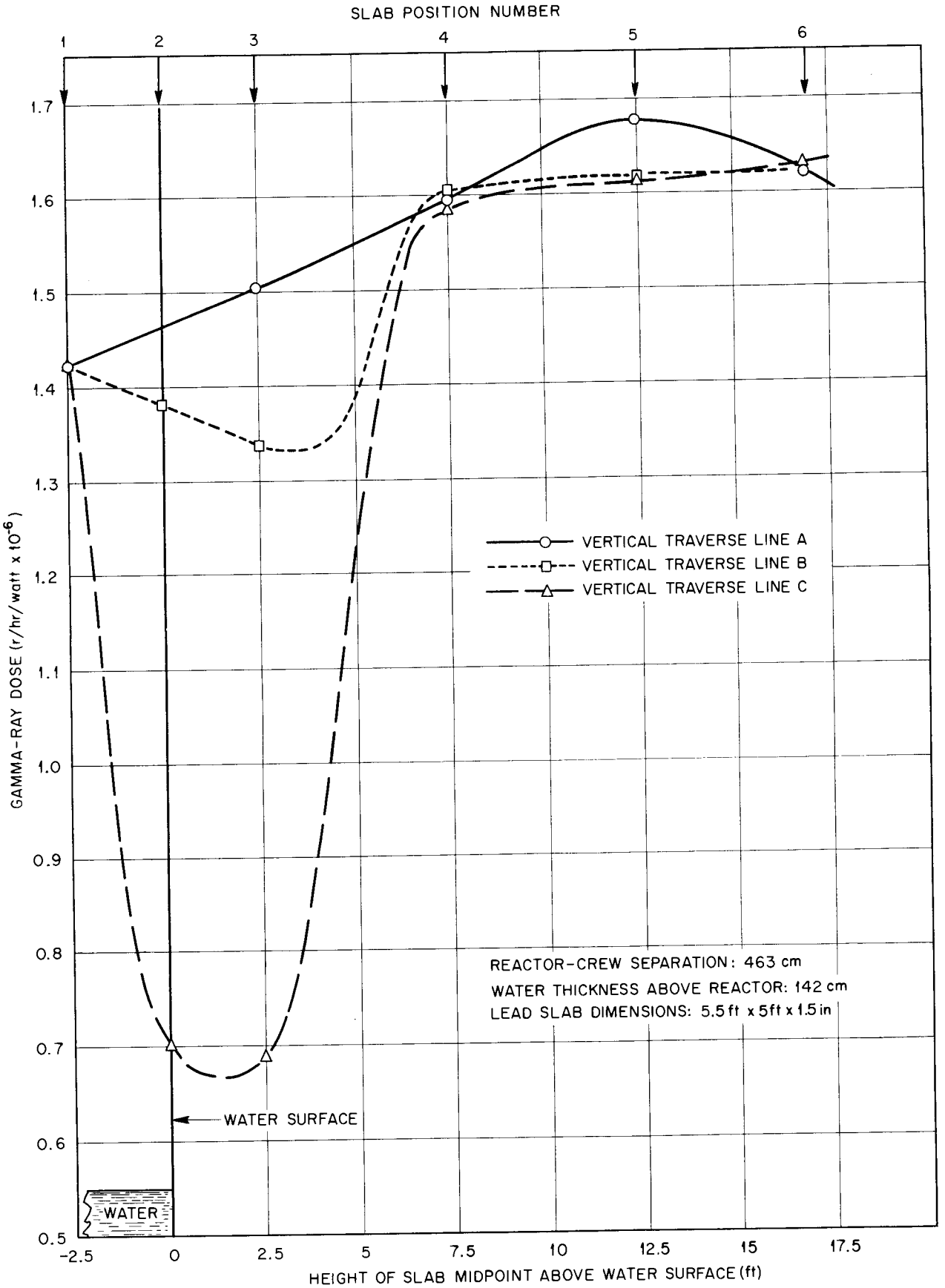

Fig. 23. Variation of the Gamma-Ray Dose at Crew Position when a Lead Slab Is Moved along Vertical Paths between Reactor and Detector.

[redacted]
DWG. 22383

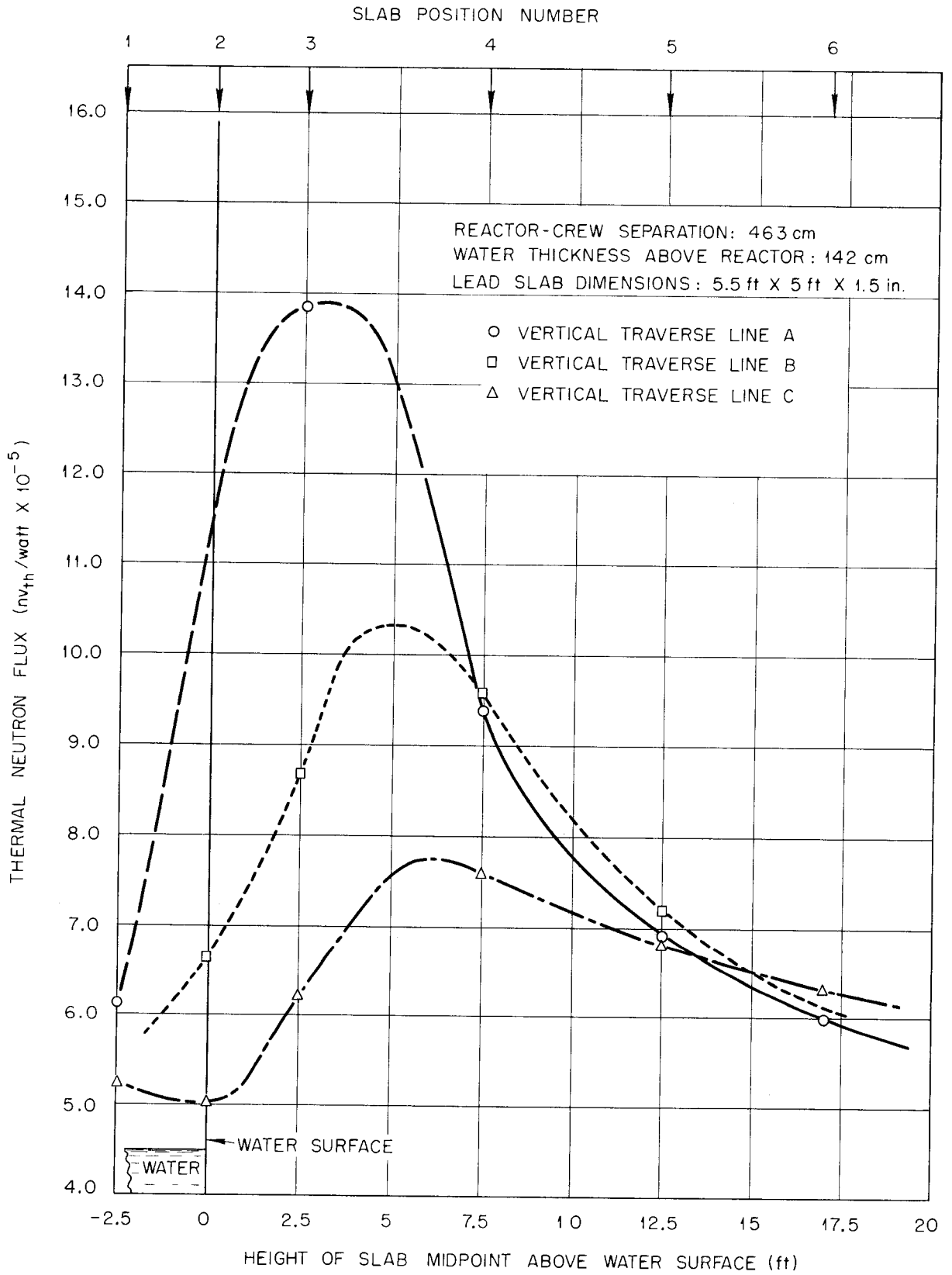

Fig. 24. Variation of Thermal Neutron Flux at Crew Position when a Lead Slab Is Moved along Vertical Paths Between Reactor and Detector.

Fig. 1. The ratio of the radiation reaching the detector with the lead in position 1A to that in position 6A is 0.8. If it is assumed that the lead in position 6A does not block any radiation to the detector and that each of the three shadow shield slabs in Fig. 1 would have approximately the same attenuation effect as the one slab in position 1A, then $(0.8)^3 = 0.51$.* The original measurements with the shadow shield were made at a water thickness of 90 cm above the reactor. The present observations were made at a thickness of 60 cm. The difference in water levels apparently did not affect greatly the shadow shield factor at the crew position. This appears to be confirmation that the radiation from reactor to detector is reduced by a factor of 0.52 when the lead shadow shield is present.

In Fig. 24, it is noted that the lead slab had an opposite effect on thermal neutrons. Here the presence of the lead near the surface of the water increased the radiation at the detector considerably. Apparently, the lead scattered some neutrons which were traveling in a predominantly upward direction away from the water surface into a predominantly downward direction, thus increasing the thermal flux at the detector. Thermal neutrons emerging from the water surface would not be expected to be highly collimated and thus would be subject to scattering by the lead slab.

---

* For this statement to apply, it must be true that most of the radiation reaching the detector travels along paths which are intercepted by the shadow shield on its insertion.

Radiation Distribution in Air over Crew Position

Measurements were taken in the air on a vertical line directly above the crew position to determine the neutron and gamma-ray distribution at various heights above the water surface. Results are plotted in Fig. 25 from the data of Table A-26. The fast neutron dose increased at an approximate rate of 3.7×10^{-4} mrep/hr/watt per meter height above the water surface, and the gamma dose increased at an approximate rate of 4.8×10^{-5} r/hr/watt per meter height above the surface. There was a slight leveling off of the gamma dose at about 1.5 m, and beyond the top of the pool walls the gamma dose curve broke; on the other hand, as high as the fast neutrons could be measured the dose continued to rise. Again this is evidence that the neutrons emerging from the water surface were highly collimated, while the gamma rays were not. The break in the gamma curve at the top of the pool (3 m above the water) indicated that just below this level there is abundant wall scattering by the gammas.

The thermal neutrons on the other hand showed only a 13% increase in intensity from the water surface to a height of 2-1/2 m, at which height the thermal neutron flux was at its maximum. Above this point it slowly declined. The space in the pool above the water surface may be visualized as having been filled by a cloud of thermal neutrons which was more or less of constant density within the confines of the

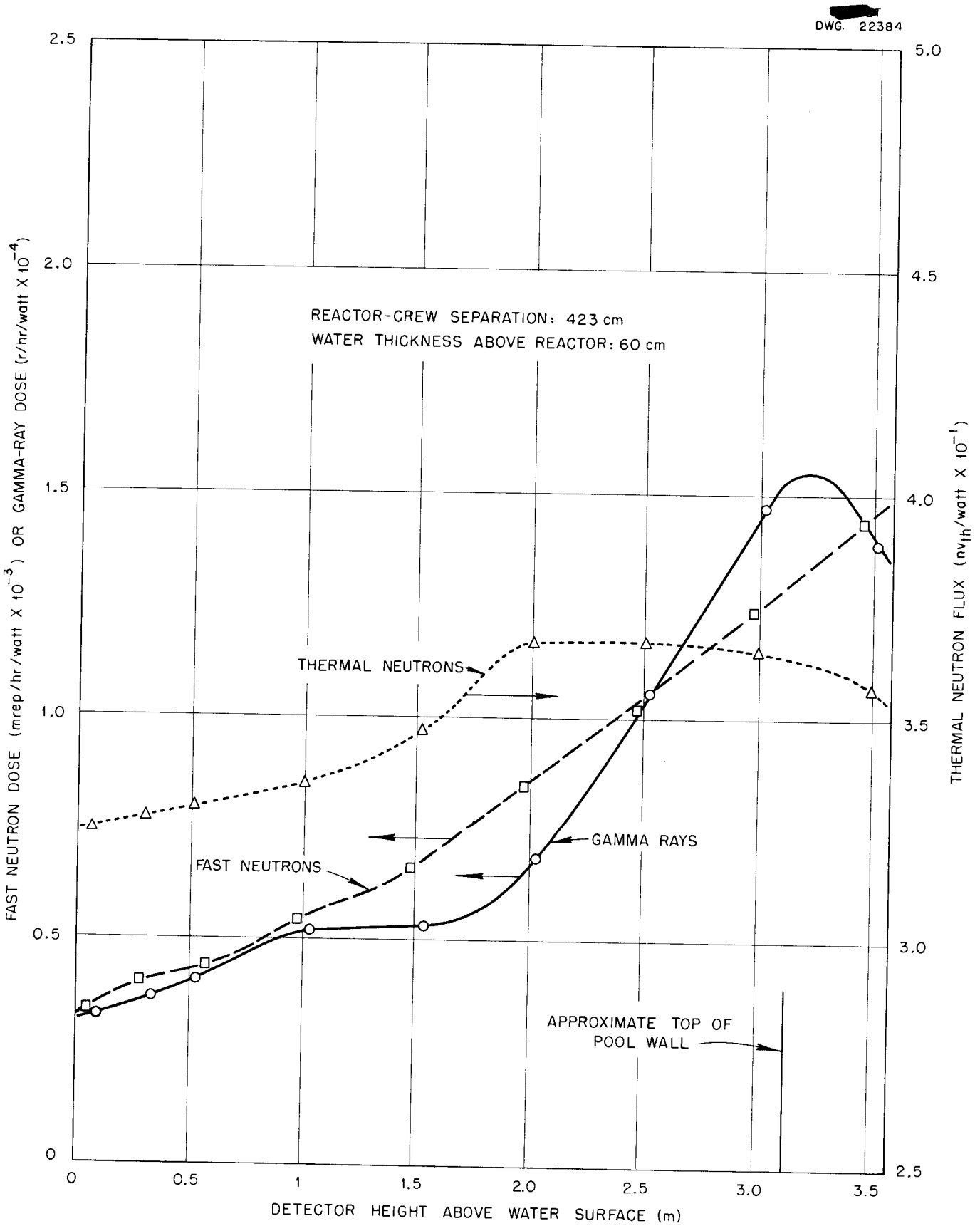

Fig. 25. Radiation Distribution in Air above Crew Position.

pool walls. The air nuclei plus the pool walls acted as scattering centers to keep the flux random and therefore nearly constant.

Effect of Pool Walls on Radiation at Crew Position

In order to estimate how much of the radiation at the crew position was scattered by the pool walls, the following series of experiments were performed.

The reactor was mounted on the H-Beam described previously and detectors were placed at a crew position 4.2 m from the reactor; this separation had to be used in order to perform the experiment without other apparatus in the pool interfering with the position of the detectors. Vertical traverse measurements were made at the crew position at various water thicknesses (y) above the reactor. This arrangement was the same as described in Part I, except that the reactor and the crew position were moved to various locations with respect to the pool walls as follows:

(1) On pool centerline, 10 ft from either wall.

(2) 5 ft from centerline, 5 ft from west wall.

(3) 7-1/2 ft from centerline, 2-1/2 ft from west wall.

The results of these traverses are shown in Figs. 26 through 28. The shapes of the curves are about the same as those of Figs. 3 and 4. The magnitudes are slightly higher because the crew is nearer the reactor. The effect of the walls is graphically depicted in Figs.29 and 30,

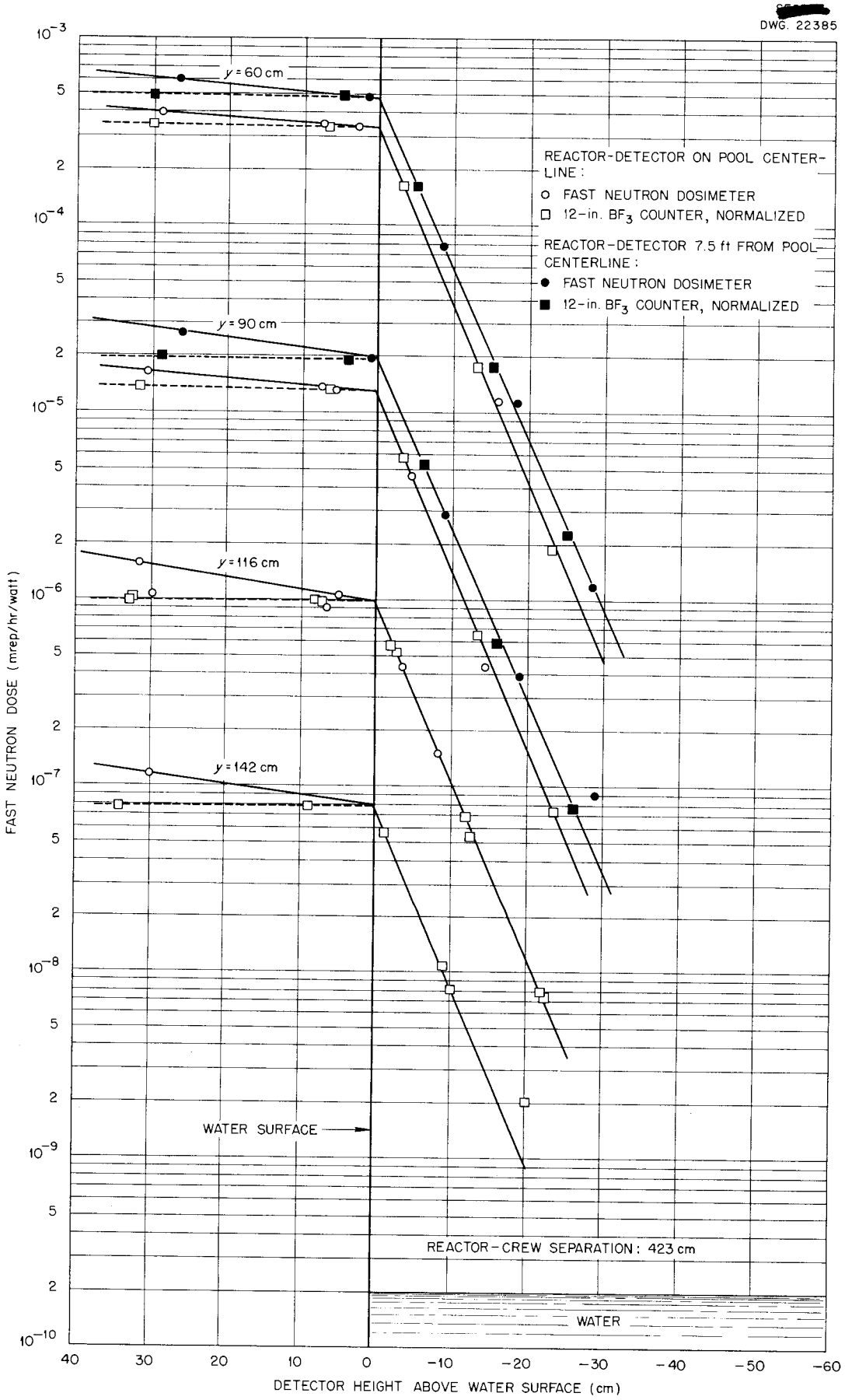

Fig. 26. Effect of Wall Scattering on Fast Neutron Dose Received at Crew Position for Various Water Thicknesses (y) Above Reactor (Vertical Traverse Measurements).

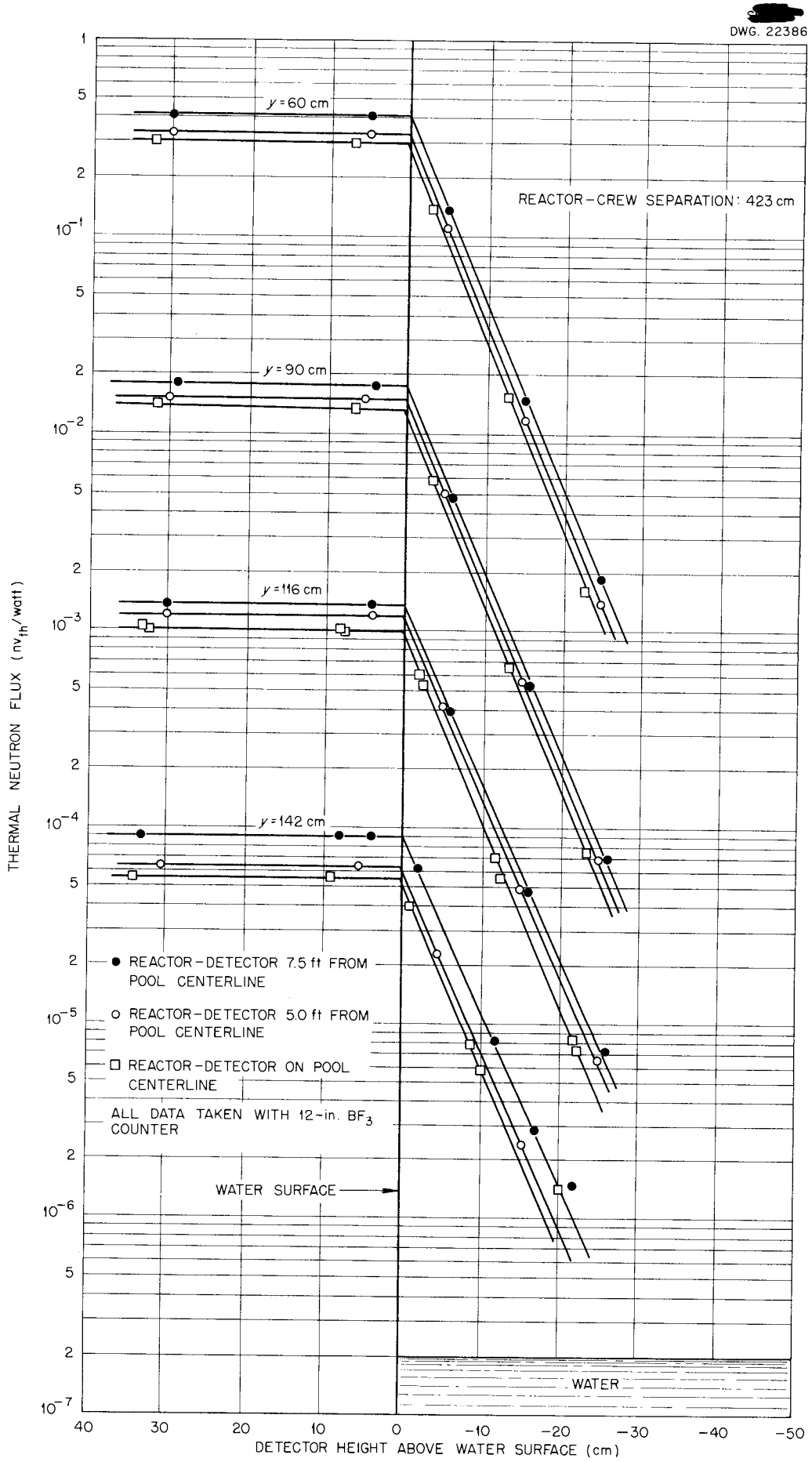

Fig. 27. Effect of Wall Scattering on Thermal Neutron Flux Received at Crew Position for Various Water Thicknesses (y) Above Reactor (Vertical Traverse Measurements).

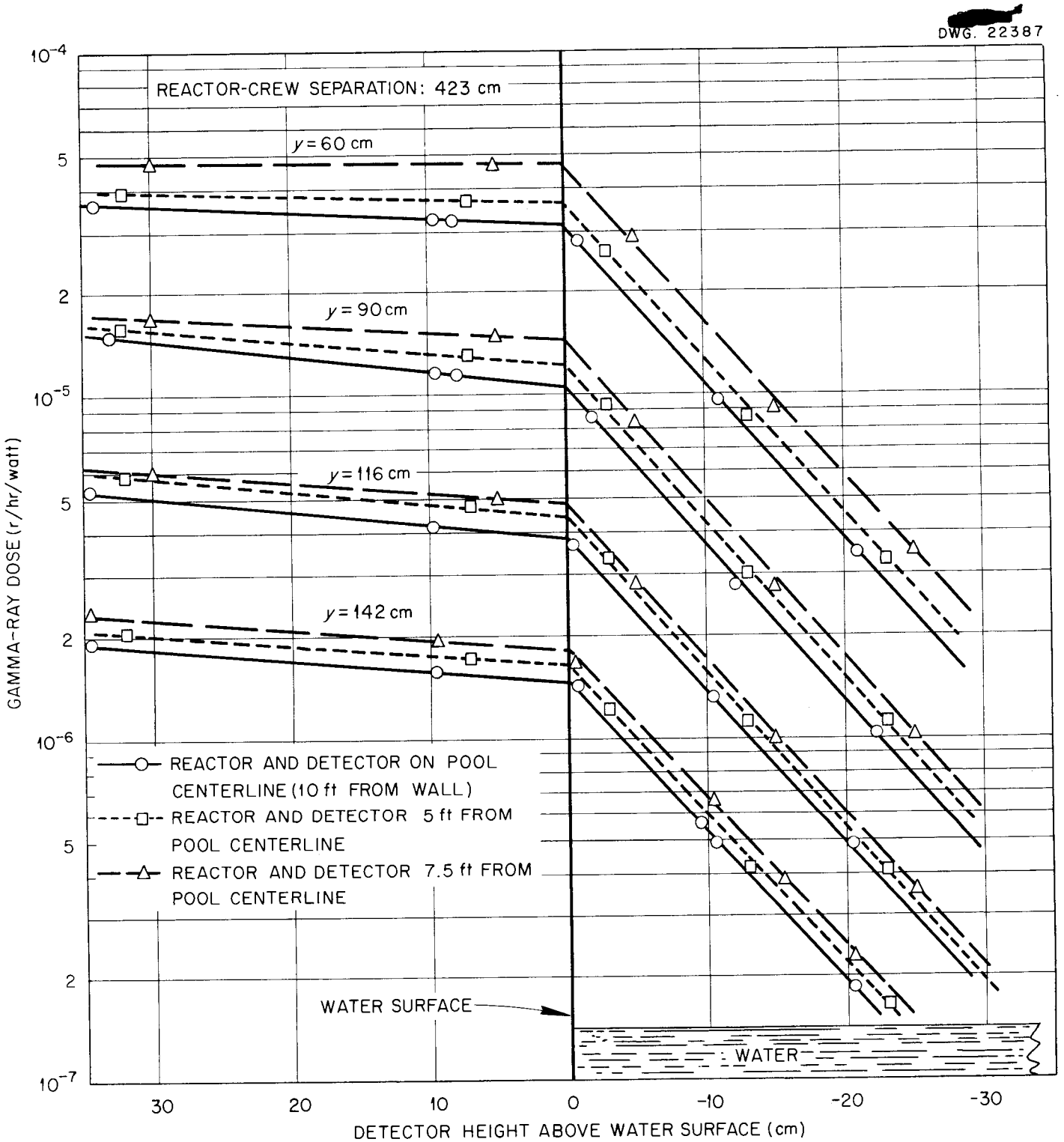

Fig. 28. Effect of Wall Scattering on Gamma-Ray Dose Received at Crew Position for Various Water Thicknesses (y) above Reactor (Vertical Traverse Measurements).

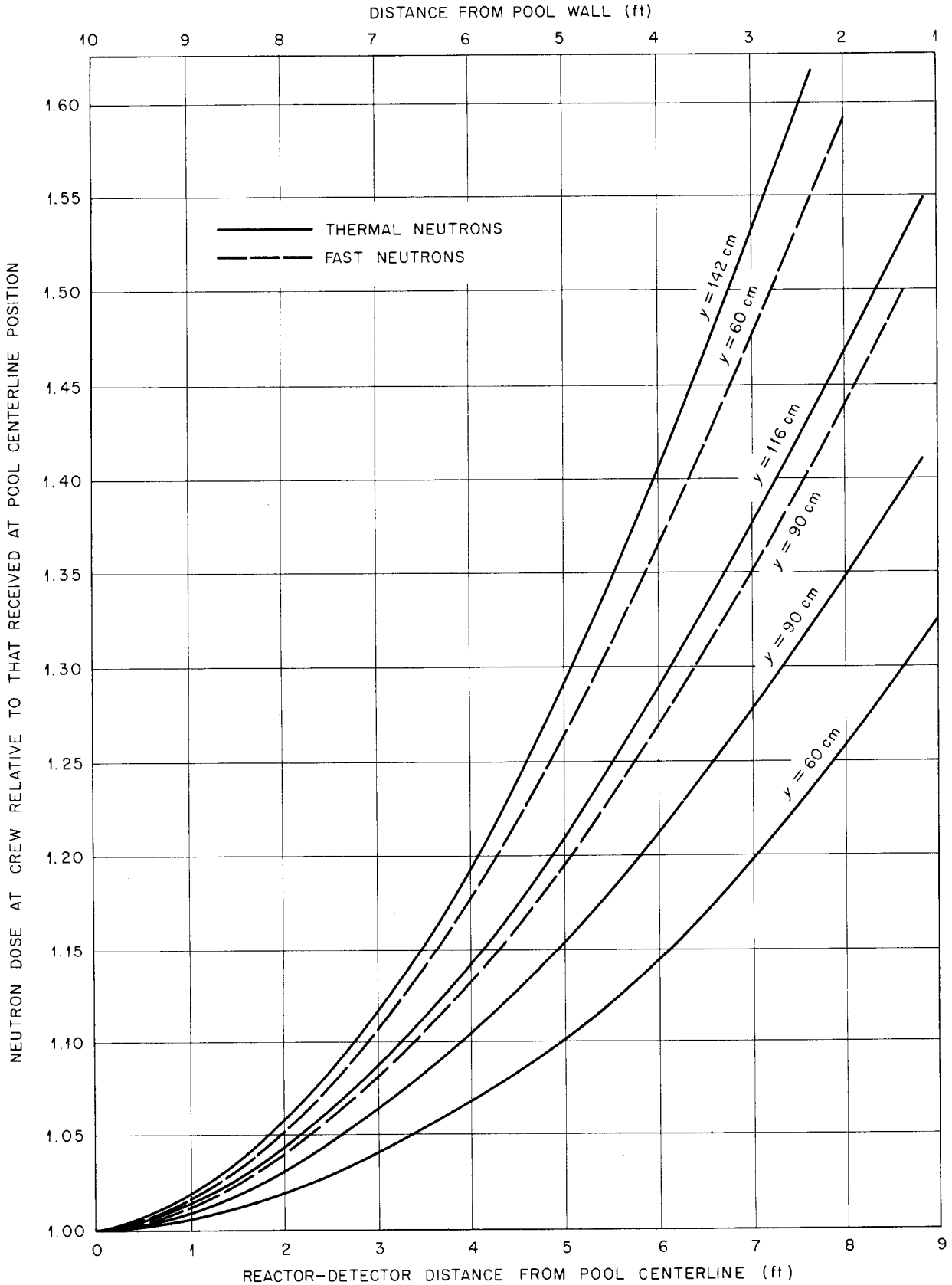

Fig. 29. Neutron Dose at Crew Position as a Function of Reactor-Detector Distance From Pool Centerline for Various Water Thicknesses (y) above Reactor.

[redacted]
DWG. 22389

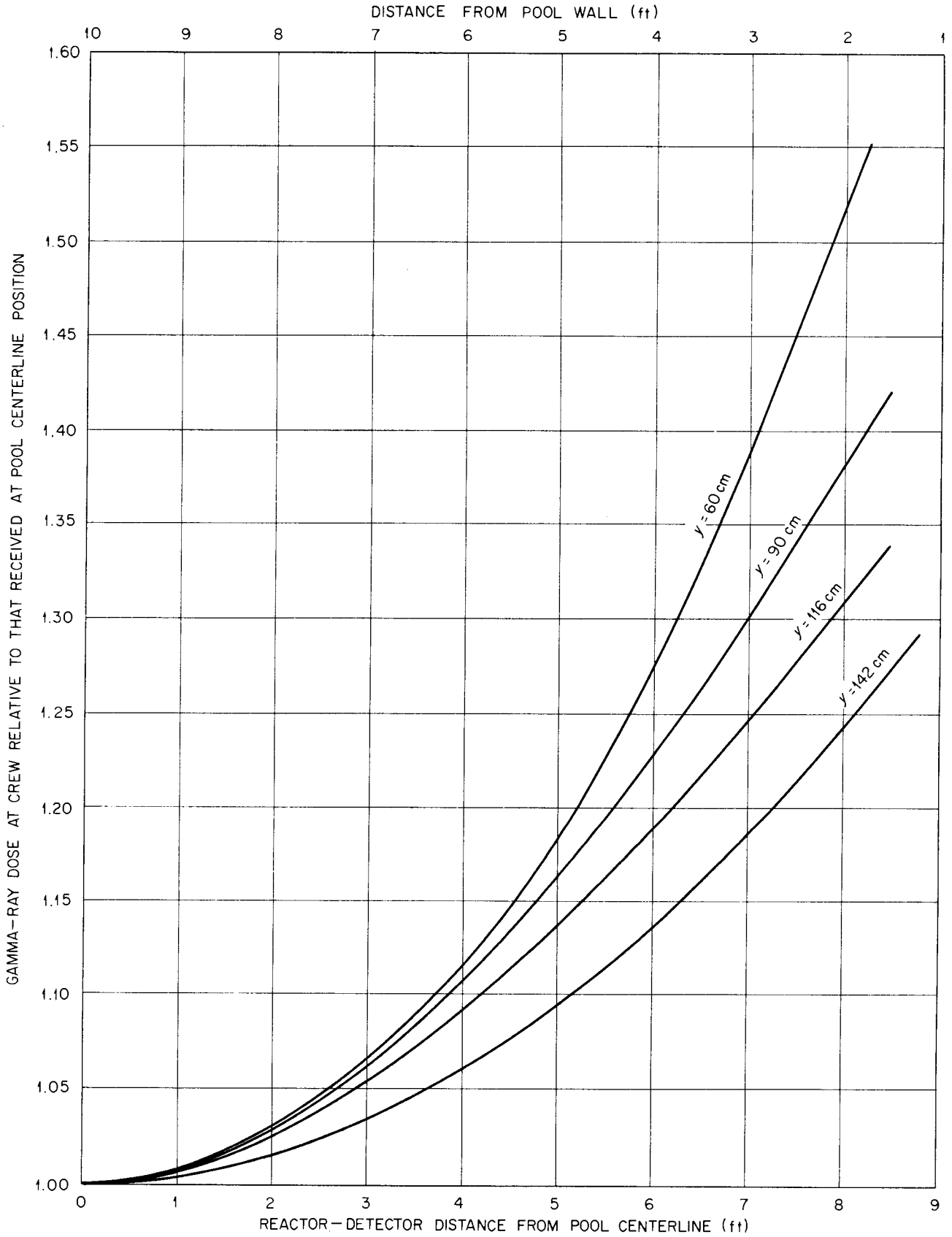

Fig. 30. Gamma-Ray Dose at Crew Position as a Function of Reactor-Detector Distance from Pool Centerline for Various Water Thicknesses (y) Above Reactor.

which show the dose at the surface of the crew position plotted against the distance from the pool centerline. For fast neutrons and gamma rays the wall effect is much greater at the lower water levels. This is understandable on the basis that at lower levels the radiation is less collimated and has greater opportunity to be scattered from the walls. For thermal neutrons the effect appears to be reversed. The measurements for these curves are given in Table A-27 through A-29.

In Appendix B, F. H. Murray shows that the presence of the walls contributes less than 40% of the gamma radiation received at the crew with reactor and crew located on the pool centerline. When the detector (or crew) position is swung toward the center of the pool from its position near the pool wall, leaving the reactor near the wall, very little effect (only about 3%) on the radiation received at crew is noted. This seems to indicate that wall scattering near the source is more important than wall scattering near the detector. Measurements of this effect are tabulated in Table A-30.

Shield Weight Calculations Based on New Data

With the data presented in Part II it is now possible to make a shield weight calculation based upon the following assumptions:

(1) For any given reactor-crew separation the attenuation factor between one side of the reactor shield and the crew side shield is the same both for the actual case and the mockup, and thus the doses between the two are directly comparable.

(2) The ratio of the dose at the crew to that at the reactor shield surface (water surface above reactor) does not change with the power level.

(3) For calculation purposes the outer surface of the aircraft reactor shield is considered to be a sphere with an average radius of 161 cm.

(4) The shape of the thermal neutron curve of Fig. 11 is typical of the attenuation for both fast and thermal neutrons through the outer portion of the aircraft shield.*

With the above assumptions in mind the allowed neutron dose $N_r(a)$ on the outside of the reactor shield is obtained as follows:

---

* This assumption is valid only at large distances from the reactor. At distances greater than 1 m the BSF water data shows that the thermal and fast neutron curves are parallel and have about the same attenuation at any given point. See for instance BSF Pure Water Data Work Sheet, CF 52-2-37. A small reproduction of the Work Sheet also appears in CF 51-10-70, Part II revised, p. 87.

$$N_r(a) = N_r(e) \frac{\phi_n(a)}{\phi_n(e)}$$

where

$N_r(e)$ = experimental neutron dose on outside of reactor shield (i.e. at water surface directly over reactor)

= dose reading on Fig. 11 at 161.3 cm from reactor center (or 130 cm from top of reactor)

= 6.3×10^{-1} nv_{th}/watt*,

$\phi_n(a)$ = allowed neutron dose at crew position (see p. 17)

= 1.02×10^{-7} mrep/hr/watt,

$\phi_n(e)$ = experimental neutron dose at crew position (see Fig. 3)

= 1.65×10^{-8} mrep/hr/watt.

Substituting,

$$N_r(a) = 0.63 \frac{1.02 \times 10^{-7}}{1.65 \times 10^{-8}}$$

$$= 3.89 \quad nv_{th}/\text{watt}^*,$$

---

* It matters little that these readings are thermal neutron flux readings, for reasons given in the previous footnote. The important thing here is the shield thickness difference given by the readings on the curve; i.e., the shape of the curve is the important consideration.

It is seen from Fig. 11 that:

Thickness of shield giving $N_r(e)$	=	116 cm
Thickness of shield giving $N_r(a)$	=	100 cm
Thickness to be saved		16 cm

Thus the weight saved will be:

$$W(g) = 4/3\ \pi(161^3 - 145^3)\ (\rho)g$$

$$= 4.65 \times 10^6 g$$

$$= 4.65 \text{ metric tons}$$

$$\cong 5.1 \text{ short tons}$$

$$\cong 10{,}200 \text{ lb water, or its equivalent in gasoline.}$$

Thus indications are that a much greater saving in weight can be accomplished by shaving neutron shielding from the reactor shield rather than from the crew shield. If this were done, the gamma dose at the crew would rise about 25% and could be compensated for at the crew compartment by the addition of 0.12 cm lead, resulting in 1800 lb additional weight. The final weight savings would be of the order of 8400 lb.

III. Summary and Conclusions

The most important result achieved from this set of experiments is undoubtedly that there now exists good experimental data which to a large extent confirms the predictions of dose received in the crew compartment of a divided shield configuration which were made by the 1950 ANP Shielding Board. Most of the experimental uncertainties of the earlier experiments were eliminated, including the largest single source of error, the extrapolation of the data necessary in the preliminary work.

Specifically, without extension of data beyond the normal scale-up factors necessary, it was shown in Part I that 9.5 cm of plastic neutron shielding could be removed from the crew shield, effecting a saving of 5100 lb of shield weight in the airplane. Calculations based on the data of Part II showed that a much greater shield weight saving may be had by shaving off 16 cm of water-equivalent thickness from the reactor shield, amounting to some 8400 lb.

The calculations based upon the present data indicate that the 1950 Shielding Board assumptions for their estimation of gamma-ray dose at the crew were about right, but that their assumptions for neutrons were conservative. The real importance of this experiment does not rest in the figures on the shield weight savings on a fictitious airplane but rather in the confidence in air-scattering calculations that has been established. Recently experimental verification of air-scattering calculations of gamma dose received at the crew has come from an entirely new direction. F. C. Maienschein has measured energy and angular distribution of gamma rays emerging from the reactor portion of the divided shield.(6) In a recent report(7) Bly and Maienschein calculated the dose that should be received at the crew by integration of Maienschein's data over energies and angles involved. Considering the difference in approach the

---

(6) F. C. Maienschein, Gamma-Ray Spectral Measurements with the Divided Shield Mockup, Part I, CF-52-3-1 (Mar. 3, 1952); Part II, CF-52-7-71 (July 8, 1952); Part III, CF-52-8-38 (Aug. 8, 1952); . . . and T. A. Love, Part IV, CF-52-11-124 (Nov. 17, 1952).

(7) F. Bly and F. C. Maienschein, A Calculation of the Gamma Radiation Reaching the ANP-53 Crew Shield, CF-53-5-117 (May 23, 1953).

agreement between their calculations and these is good.* Other important conclusions to be gained from a study of the data of Part II which are applicable to design of aircraft divided shields are

(1) The fast neutrons emerging from the pool above the reactor are highly collimated, but the gamma rays are not.

(2) The contributions to the dose received at the detector (in the center of the pool) by scattering from pool walls and instrument bridges is small.

(3) The small angle scattering of gamma rays contributes a greater part of the gamma dose received at crew.

(4) The 1/R attenuation law for scattered radiation was found to check well with experimental fast neutron data along the pool centerline.

---

* Bly and Maienschein calculated the dose received at the outside of the crew compartment. This value was compared to the measured gamma-ray dose at the surface of the water at the crew position of the present experiments corrected by an appropriate scale-up factor.

Appendix A

Tables of Data

All the tables for the body of this report are grouped together in this appendix to preserve continuity of the report. Following the tables is Fig. A-1, which is a chart giving the intercorrelation between tables and figures appearing in the report.

The tables, listed at the beginning of the report, are grouped under the following classifications for easy reference:

Classification	Table No(s).
Part I	
Repeat of preliminary experiments.....	1 - 7
Effect of shadow shield.....	8
Part II	
Vertical traverse measurements directly above reactor.....	9 - 12
Radiation patterns existing in the pool near water surface.....	13 - 17
Interpolation to find dose at water surface.....	18
Scattering effects from bridges.....	19 - 21
Effect of lead at crew.....	22
Effect of lead interposed between reactor and crew positions.....	23 - 25
Radiation pattern in air above crew position.....	26
Scattering effects from pool walls....	27 - 30

Table A-1. Neutron and Gamma-Ray Doses at Crew Position --

30-cm Water Thickness above Reactor

(Vertical Traverse Measurements)

Reactor-crew separation: 533 cm
(Exp. 9, Run 37)

Detector Distance above Water Surface (cm)	Gamma-Ray Dose (r/hr/watt) 50-cc Variable Resistance Ion Chamber	Fast Neutron Dose (mrep/hr/watt) Fast Neutron Dosimeter
23.0	2.13×10^{-4}	
16.8		1.20×10^{-2}
13.0	2.04×10^{-4}	
6.8		1.12×10^{-2}
3.0	1.79×10^{-4}	
-2.0	1.55×10^{-4}	
-3.2		5.81×10^{-3}
-7.0	8.47×10^{-5}	
-8.2		2.02×10^{-3}
-12.0	6.16×10^{-5}	
-13.2		6.78×10^{-4}
-17.0	3.48×10^{-5}	
-18.2		2.66×10^{-4}
-23.2		1.06×10^{-4}
-25.2		8.39×10^{-5}
-28.2		4.03×10^{-5}

Table A-2. Neutron and Gamma-Ray Doses at Crew Position --

60-cm Water Thickness above Reactor

(Vertical Traverse Measurements)

Reactor-crew separation: 533 cm
(Exp. 9, Run 38)

Detector Distance above Water Surface (cm)	Gamma-Ray Dose (r/hr/watt) 50-cc Standard Ion Chamber	Fast Neutron Dose (mrep/hr/watt) Fast Neutron Dosimeter
25.0	4.06×10^{-5}	
20.0		3.11×10^{-4}
15.0	3.60×10^{-5}	
10.0		2.62×10^{-4}
5.0	3.33×10^{-5}	
0.0	3.20×10^{-5}	1.65×10^{-4}
-5.0	1.87×10^{-5}	7.43×10^{-5}
-10.0	1.16×10^{-5}	2.50×10^{-5}
-15.0	6.80×10^{-6}	1.01×10^{-5}
-20.0	4.32×10^{-6}	3.66×10^{-6}
-25.0	2.72×10^{-6}	1.94×10^{-6}
-30.0	1.72×10^{-6}	1.10×10^{-6}
-35.0	1.10×10^{-6}	

Table A-3. Neutron and Gamma-Ray Doses at Crew Position --

90-cm Water Thickness above Reactor
(Vertical Traverse Measurements)

Reactor-crew separation: 533 cm
(Exp. 9, Run 39)

Detector Distance above Water Surface (cm)	Gamma-Ray Dose (r/hr/watt)	Fast Neutron Dose (mrep/hr/watt)		Thermal Neutron Flux (nv_{th}/watt)
	50-cc Standard Ion Chamber	Fast Neutron Dosimeter	12-in. BF_3 Ctr. Normalized	12-in BF_3 Ctr.
33.8	1.44×10^{-5}			
31.0			1.28×10^{-5}	1.19×10^{-2}
28.0		1.15×10^{-5}		
23.8	1.27×10^{-5}			
21.0			1.08×10^{-5}	1.05×10^{-2}
18.0		1.09×10^{-5}		
13.8	1.14×10^{-5}			
11.0			1.05×10^{-5}	9.79×10^{-3}
8.0		1.01×10^{-5}		
3.8	1.01×10^{-5}			
1.0			9.05×10^{-6}	8.85×10^{-3}
-1.2	8.97×10^{-6}			
-2.0		6.61×10^{-6}		
-4.0			5.76×10^{-6}	5.38×10^{-3}
-6.2	4.80×10^{-6}			
-7.0		2.62×10^{-6}		
-9.0			1.64×10^{-6}	1.53×10^{-3}
-11.2	3.05×10^{-6}			
-12.0		8.47×10^{-7}		
-14.0			5.66×10^{-7}	5.28×10^{-4}
-17.0		3.44×10^{-7}		
-21.2	1.15×10^{-6}			
-24.0			7.86×10^{-8}	7.33×10^{-5}
-31.2	4.52×10^{-7}			
-34.0			1.10×10^{-8}	1.03×10^{-5}

Table A-4. Neutron and Gamma-Ray Doses at Crew Position --

116-cm Water Thickness above Reactor

(Vertical Traverse Measurements)

Reactor-crew separation: 533 cm
(Exp. 9, Runs 40, 47, 53, 57)

Detector Distance above Water Surface (cm)	Gamma-Ray Dose (r/hr/watt)	Fast Neutron Dose (mrep/hr/watt)		Thermal Neutron Flux (nv_{th}/watt)
	50-cc Standard Ion Chamber	Fast Neutron Dosimeter	12-in. BF_3 Ctr. Normalized	12-in BF_3 Ctr.
29.5	4.62×10^{-6}			
28.0			9.48×10^{-7}	8.85×10^{-4}
22.5	3.86×10^{-6}			
22.0			9.90×10^{-7}	9.26×10^{-4}
21.3	4.32×10^{-6}			
20.0		1.04×10^{-6}		
19.0			8.13×10^{-7}	7.59×10^{-4}
11.3	3.78×10^{-6}			
9.0		8.6×10^{-7}	8.00×10^{-7}	7.47×10^{-4}
4.5	3.41×10^{-6}			
3.0			8.56×10^{-7}	7.97×10^{-4}
2.5	3.38×10^{-6}			
2.0			8.14×10^{-7}	7.61×10^{-4}
1.3	3.36×10^{-6}			
-1.0			5.95×10^{-7}	5.55×10^{-4}
-3.7	2.30×10^{-6}			
-5.5	1.84×10^{-6}			
-6.0		2.1×10^{-7}	2.27×10^{-7}	2.13×10^{-4}
-7.0			1.80×10^{-7}	1.68×10^{-4}
-7.5	1.55×10^{-6}			
-8.0			1.43×10^{-7}	1.34×10^{-4}
-8.7	1.29×10^{-6}			
-11.0			7.24×10^{-8}	6.77×10^{-5}
-12.5	9.48×10^{-7}			
-13.0			4.79×10^{-8}	4.56×10^{-5}
-13.7	8.15×10^{-7}			
-15.5	6.69×10^{-7}			
-16.0			2.35×10^{-8}	2.20×10^{-5}
-17.0			1.86×10^{-8}	1.73×10^{-5}
-17.5	5.86×10^{-7}			
-18.0			1.63×10^{-8}	1.52×10^{-5}
-18.7	5.27×10^{-7}			
-21.0			8.23×10^{-9}	7.68×10^{-6}
-25.5	2.58×10^{-7}			
-26.0			3.23×10^{-9}	3.09×10^{-6}
-27.0			3.58×10^{-9}	3.34×10^{-6}
-31.0			1.49×10^{-9}	1.39×10^{-6}
-35.5	9.73×10^{-8}			

Table A-5. Neutron and Gamma-Ray Doses at Crew Position --

142-cm Water Thickness above Reactor

(Vertical Traverse Measurements)

Reactor-crew separation: 533 cm
(Exp. 9, Runs 41, 45, 54)

Detector Distance above Water Surface (cm)	Gamma-Ray Dose (r/hr/watt) 50-cc Standard Ion Chamber	Fast Neutron Dose (mrep/hr/watt) 12-in. BF_3 Ctr. Normalized	Thermal Neutron Flux (nv_{th}/watt) 12-in. BF_3 Ctr.
29.0	1.98×10^{-6}	5.86×10^{-8}	5.46×10^{-5}
25.6		6.08×10^{-8}	5.60×10^{-5}
24.0	1.64×10^{-6}		
22.0		5.86×10^{-8}	5.47×10^{-5}
12.0		5.77×10^{-8}	5.38×10^{-5}
5.6		5.15×10^{-8}	4.80×10^{-5}
4.0	1.27×10^{-6}		
3.0	1.30×10^{-6}	5.19×10^{-8}	4.84×10^{-5}
2.0		5.25×10^{-8}	4.90×10^{-5}
-3.0		3.06×10^{-8}	2.85×10^{-5}
-4.4		2.13×10^{-8}	1.98×10^{-5}
-6.0	6.53×10^{-7}	1.50×10^{-8}	1.40×10^{-5}
-6.0	6.76×10^{-7}		
-7.0		1.30×10^{-8}	1.21×10^{-5}
-8.0		1.20×10^{-8}	1.12×10^{-5}
-9.4		7.87×10^{-9}	7.35×10^{-6}
-11.0	3.95×10^{-7}		
-13.0		4.07×10^{-9}	3.80×10^{-6}
-16.0	2.77×10^{-7}	2.79×10^{-9}	1.67×10^{-6}
-17.0	2.10×10^{-7}		
-18.0		1.43×10^{-9}	1.34×10^{-6}
-23.0		6.55×10^{-10}	6.11×10^{-7}
-26.0	1.19×10^{-7}	4.21×10^{-10}	3.93×10^{-7}

Table A-6. Neutron and Gamma-Ray Doses at Surface of Crew Position as a Function of Reactor Shield Thickness

Reactor Shield Thickness[a] (cm)	Gamma-Ray Dose (r/hr/watt)	Fast Neutron Dose (mrep/hr/watt)
30	1.83×10^{-4}	1.12×10^{-2}
60	3.25×10^{-5}	2.25×10^{-4}
90	9.70×10^{-6}	1.00×10^{-5}
116	3.35×10^{-6}	8.20×10^{-7}
142	1.23×10^{-6}	5.5×10^{-8}

(a) Water thickness above reactor.

Table A-7. Attenuation of Gamma Rays by Lead Crew Shield

Water thickness above reactor: 142 cm
Plastic crew shield thickness: 17.8 cm
Detector at crew position
(Exp. 9)

Lead Crew Shield Thickness (cm)	Gamma-Ray Dose (r/hr/watt)		
	Scintillation Counter		Ion Chamber,
	Run 81	Run 82	Run 82
0.00	2.05×10^{-7} [a]	2.05×10^{-7} [a]	2.05×10^{-7}
0.20	4.31×10^{-8}	4.17×10^{-8}	4.17×10^{-8}
0.35	2.41×10^{-8}		
0.37		2.21×10^{-8}	2.00×10^{-8}
0.70	1.10×10^{-8}		
0.73		9.34×10^{-9}	8.61×10^{-9}
1.42	3.19×10^{-9}	3.08×10^{-9}	2.71×10^{-9}
2.11		9.72×10^{-10}	
2.77	3.94×10^{-10}		
2.83		3.17×10^{-10}	

[a] This reading normalized to ion chamber value.

Table A-8. Comparison of Gamma-Ray Doses at Crew Position -- With and Without Lead Shadow Shields in Place

(From preliminary experiments)

Reactor-crew separation: 510 cm
Water thickness above reactor: 90 cm
(Exp. 9)

Detector Distance above Water Surface (cm)	Gamma-Ray Dose[a] (r/hr/watt)	
	Lead Shadow Shield,[b] Run 2	No Lead Shadow Shield,[c] Run 7
24.0	1.38×10^{-5}	
21.3		6.76×10^{-6}
14.0	1.29×10^{-5}	
11.3		6.76×10^{-6}
4.0	1.26×10^{-5}	
1.3		6.38×10^{-6}
0[d]	(1.21×10^{-5})	(6.3×10^{-6})
-1.0	1.05×10^{-5}	
-3.7		4.46×10^{-6}
-6.0	6.20×10^{-6}	
-8.7		2.64×10^{-6}
-11.0	4.32×10^{-6}	
-13.7		1.65×10^{-6}
-16.0	2.32×10^{-6}	
-18.7		1.02×10^{-6}
-21.0	1.41×10^{-6}	
-23.7		6.62×10^{-7}
-26.0	8.57×10^{-7}	
-28.7		3.36×10^{-7}

(a) Power correction of 0.8306 should be applied to this data to compare it with data of present experiments.

(b) Published data; see CF-52-7-37, op. cit., p. 22.

(c) Not previously published.

(d) These values were read from curves in Fig. 9; ratio of radiation with lead shadow shields in position to radiation without shadow shields is 0.52.

Table A-9. Thermal Neutron Flux Measurements on a Vertical Line Directly above BSR

Traverse on (0,y,7.5)[a]
Pool Filled

Detector Distance above Top of Reactor (cm)	Thermal Neutron Flux (nv_{th}/watt)	
	Exp. 6, Run 46C[b]	Exp. 9, Run 15
30.0		3.80×10^{4}
48.7	1.98×10^{3}	
58.7	4.38×10^{2}	
60.0		4.00×10^{2}
68.7	1.06×10^{2}	
78.7	2.83×10^{1}	
88.7	7.55×10^{0}	
90.0		6.68×10^{0}
98.7	2.47×10^{0}	
108.7	7.39×10^{-1}	
116.0		3.52×10^{-1}
118.7	2.42×10^{-1}	
128.7	8.24×10^{-2}	
138.7	2.90×10^{-2}	

(a) For position of traverse see Fig. 10. The measurements were taken along a vertical line above reactor which was located on x-centerline and at a z distance of 15.5 cm from north face and 7.5 cm from reactor center. This was as near to the vertical centerline of the reactor as it was physically possible to place the detectors.

(b) Measurements taken in connection with Divided Shield Reactor; not previously published.

Table A-10. Thermal Neutron Flux Measurements near Water Surface Directly above BSR

Vertical traverses on (0,y,7.5)[a] for various water thicknesses above reactor (Exp. 9)

Run No.	Water Thickness above reactor (cm)	Detector Distance above Water Surface (cm)	Thermal Neutron Flux (nv_{th}/watt)
17	30	7	4.16×10^{3}
		0	2.16×10^{4}
		-10	2.74×10^{5}
21	60	12	4.72×10^{1}
		10	4.88×10^{1}
		5	6.84×10^{1}
		0	2.09×10^{2}
		-10	1.83×10^{3}
22	90	18	1.12×10^{0}
		15	1.13×10^{0}
		10	1.15×10^{0}
		5	1.54×10^{0}
		0	3.46×10^{0}
	116	18	5.84×10^{-2}
		10	5.82×10^{-2}
		6	6.65×10^{-2}
		0	1.67×10^{-1}

(a) For position of traverse see Fig. 10. The measurements were taken along a vertical line above reactor which was located on x-centerline and at a z distance of 15.5 cm from north face and 7.5 cm from reactor center. This was as near to the vertical centerline of the reactor as it was physically possible to place the detectors.

Table A-11. Gamma-Ray Dose Measurements on a Vertical Line Directly above BSR

Traverse on (0,y,7.5)[a]
Pool filled

Detector Distance above Top of Reactor (cm)	Gamma-Ray Dose (r/hr/watt)	
	Exp. 6, Run 45[b]	Exp. 9, Run 16
23.7	4.17×10^{0}	
30.0		2.63×10^{0}
43.7	1.00×10^{0}	
60.0		3.49×10^{-1}
63.7	2.82×10^{-1}	
83.7	9.43×10^{-2}	
90.0		6.42×10^{-2}
103.7	3.3×10^{-2}	
116.0		1.79×10^{-2}
123.7	1.23×10^{-2}	
142.0		5.71×10^{-3}
143.7	5.06×10^{-3}	
163.7	2.21×10^{-3}	
183.7	1.03×10^{-3}	
203.7	5.10×10^{-4}	
223.7	2.42×10^{-4}	
243.7	1.19×10^{-4}	
263.7	6.42×10^{-5}	
283.7	3.83×10^{-5}	

(a) For position of traverse see Fig. 10. The measurements were taken along a vertical line above reactor which was located on x-centerline and at a z distance of 15.5 cm from north face and 7.5 cm from reactor center. This was as near to the vertical centerline of the reactor as it was physically possible to place the detectors.

(b) Measurements taken in connection with Divided Shield Reactor; not previously published.

Table A-12. Gamma-Ray Dose Measurements near Water Surface Directly above BSR

Vertical traverses on (0,y,7.5)[a] for various water thicknesses above reactor

(Exp. 9)

Water Thickness above Reactor (cm)	Detector Distance above Water Surface (cm)	Run No.	Gamma-Ray Dose (r/hr/watt)
30	20	30	8.02×10^{-1}
	5		1.30×10^{0}
	0		1.56×10^{0}
	-10		3.38×10^{0}
60	20		1.29×10^{-1}
	0		2.03×10^{-1}
	-20		7.24×10^{-1}
90	20		2.84×10^{-2}
	5		3.85×10^{-2}
	0		5.04×10^{-2}
	-20		1.60×10^{-1}
116	20		8.77×10^{-3}
	5		1.08×10^{-2}
	0		1.39×10^{-2}
	-20		3.94×10^{-2}
142	20	26	3.12×10^{-3}
	10		3.49×10^{-3}
	5		3.67×10^{-3}
	0		4.45×10^{-3}
	-5		5.68×10^{-3}
	-10		7.19×10^{-3}
	-20		1.14×10^{-2}

(a) For position of traverse see Fig. 10. The measurements were taken along a vertical line above reactor which was located on x-centerline and at a z distance of 15.5 cm from north face and 7.5 cm from reactor center. This was as near to the vertical centerline of the reactor as it was physically possible to place the detectors.

Table A-13. Thermal Neutron Flux Measurements near Water Surface over 1 m^2 Quadrant above BSR

Water thickness above reactor: 116 cm
(Exp. 9)

Point of Measurement[a]	Detector Distance above Water Surface (cm)	Thermal Neutron Flux (nv_{th}/watt)		
		Run 22	Run 24	Run 25
A	11	5.84×10^{-2}		
	3	5.82×10^{-2}		
	-1	6.65×10^{-2}		
	-7	1.67×10^{-1}		
B	20		6.18×10^{-3}	
	13	5.89×10^{-3}		
	10		5.74×10^{-3}	
	5	5.33×10^{-3}	5.28×10^{-3}	
	0	5.03×10^{-3}	5.03×10^{-3}	5.05×10^{-3}
	-2.5			5.89×10^{-3}
	-5			9.21×10^{-3}
	-7.5			1.21×10^{-2}
	-10			1.47×10^{-2}
C	10			3.67×10^{-3}
	0			2.87×10^{-3}
	-10			2.37×10^{-3}
	-20			2.61×10^{-3}
D	10			8.70×10^{-3}
	0			9.02×10^{-3}
	-10			4.08×10^{-2}

(a) See Fig. 13.

Table A-14. Gamma-Ray Dose Measurements at Water Surface over 1 m^2 Quadrant above BSR

Water thickness above reactor: 142 cm
(Exp. 9, Runs 26, 27)

Point of Measurement [a]	Gamma-Ray Dose (r/hr/watt)
A	3.67×10^{-3}
B	1.25×10^{-3} [b]
C	(5.2×10^{-4}) [c]
D	(1.13×10^{-3}) [c]
E	4.06×10^{-3} [b]
F	3.48×10^{-3} [b]
G	3.67×10^{-3} [b]
H	3.12×10^{-3} [b]
I	2.10×10^{-3} [b]

(a) See Fig. 15.
(b) Corrected to water surface.
(c) Interpolated point.

Table A-15. Thermal Neutron Flux Measurements at Water Surface along Pool Centerline

Water thickness above reactor: 116 cm

(Exp. 9)

Run No.	Detector Distance from Vertical Axis of Reactor[a]	Thermal Neutron Flux (nv_{th}/watt)	1/R Attenuation Law (Arbitrary Scale)
22	7	5.82×10^{-2}	
25	107	5.05×10^{-3}	4.67×10^{-3}
	152	2.65×10^{-3}	3.29×10^{-3}
33	227	1.97×10^{-3}[b]	2.20×10^{-3}
34	310	1.29×10^{-3}[b]	1.61×10^{-3}
67	423	1.10×10^{-3}	1.18×10^{-3}
40	533	7.46×10^{-4}	9.38×10^{-4}

(a) The reactor vertical centerline is taken to be 23 cm south of the north face, as shown in Fig. 10.
(b) Corrected for water level.

Table A-16. Gamma-Ray Vertical Traverse Measurements near Water Surface at Various Points along Pool Centerline

Water thickness above reactor: 142 cm

(Exp. 9)

Run No.	Detector Distance from Vertical Axis of Reactor[a] (cm)	Detector Distance above Water Surface (cm)	Gamma-Ray Dose (r/hr/watt)
26	7	16	3.12×10^{-3}
		6	3.49×10^{-3}
		1	3.67×10^{-3}
		0	(3.70×10^{-3})[b]
		-4	4.45×10^{-3}
		-9	5.68×10^{-3}
		-14	7.19×10^{-3}
		-24	1.14×10^{-2}
27	32	0	4.06×10^{-3}[c]
		-3	4.58×10^{-3}
27	57	0	3.12×10^{-3}[c]
		-3	3.52×10^{-3}
27	82	0	2.10×10^{-3}[c]
		-3	2.37×10^{-3}
27	107	17	1.32×10^{-3}
		2	1.32×10^{-3}
		0	(1.33×10^{-3})[b]
		-3	1.49×10^{-3}
		-23	3.06×10^{-3}
28	157	17	5.05×10^{-4}
		7	4.59×10^{-4}
		2	4.44×10^{-4}
		0	(4.36×10^{-4})[b]
		-3	4.76×10^{-4}
		-23	8.87×10^{-4}
28	207	18	1.77×10^{-4}
		3	1.35×10^{-4}
		0	(1.30×10^{-4})[b]
		-2	1.37×10^{-4}
		-22	2.19×10^{-4}

Table A-16 (continued)

Run No.	Detector Distance from Vertical Axis of Reactor[a] (cm)	Detector Distance above Water Surface (cm)	Gamma-Ray Dose (r/hr/watt)
28	257	18	6.13×10^{-5}
		3	4.12×10^{-5}
		0	(3.80×10^{-5})[b]
		-2	3.86×10^{-5}
		-22	5.42×10^{-5}
29	307	17	1.95×10^{-5}
		7	1.50×10^{-5}
		2	1.28×10^{-5}
		0	(1.20×10^{-5})[b]
		-3	1.21×10^{-5}
		-23	1.26×10^{-5}
28	357	15	7.72×10^{-6}
		0	5.12×10^{-6}
		-5	4.66×10^{-6}
		-25	3.45×10^{-6}
66	423	34.5	1.92×10^{-6}
		9.5	1.57×10^{-6}
		0	(1.50×10^{-6})[b]
		-0.5	1.41×10^{-6}
		-9.5	5.64×10^{-7}
		-10.5	4.82×10^{-7}
		-20.5	1.82×10^{-7}
54	533	29	1.98×10^{-6}
		3	1.30×10^{-6}
		0	(1.25×10^{-6})[b]
		-6	6.76×10^{-7}
		-16	2.77×10^{-7}
		-26	1.19×10^{-7}

(a) The reactor vertical centerline is taken to be 23 cm south of the north face, as shown in Fig. 10.
(b) Water surface reading of curve.
(c) Corrected to water surface by interpolation.

Table A-17. Gamma-Ray Measurements near Water Surface along Pool Centerline

Water thickness above reactor: 142 cm

(From experimental data, see Fig. 17)

Detector Distance from Vertical Axis of Reactor (cm)	Gamma-Ray Dose (r/hr/watt)			1/R Attenuation Law (Arbitrary Scale)
	At Water Surface	20 cm above Water Surface	20 cm below Water Surface	
7	3.67×10^{-3}	2.87×10^{-3}	8.97×10^{-3}	
32	4.06×10^{-3}			
57	3.12×10^{-3}			
82	2.10×10^{-3}			
107	1.33×10^{-3}	1.33×10^{-3}	2.70×10^{-3}	6.23×10^{-6}
157	4.36×10^{-4}	5.13×10^{-4}	7.97×10^{-4}	4.25×10^{-6}
207	1.30×10^{-4}	1.86×10^{-4}	2.09×10^{-4}	3.22×10^{-6}
257	3.80×10^{-5}	6.44×10^{-5}	5.23×10^{-5}	2.59×10^{-6}
307	1.18×10^{-5}	2.20×10^{-5}	1.28×10^{-5}	2.17×10^{-6}
357	5.15×10^{-6}	8.80×10^{-6}	3.65×10^{-6}	1.87×10^{-6}
423	1.50×10^{-6}	1.73×10^{-6}	1.94×10^{-7}	1.57×10^{-6}
533	1.25×10^{-6}	1.73×10^{-6}	1.91×10^{-7}	1.25×10^{-6}

Table A-18. Comparison of Experimental Gamma-Ray Dose D_L at Point Q with Interpolated Dose D_L' at Point Q'

Q = point on water surface at a distance z from vertical axis of reactor and a distance L from center of reactor

Q' = point directly above reactor at a distance L from center of reactor and at a distance L' from top of reactor core (L' = L - 31.3 cm)

z(cm)	L (cm)	L' (cm)	Gamma-Ray Dose (r/hr/watt)	
			D_L (a) (Experimental)	D_L' (b) (Interpolated)
0	173.3	142.0	3.65×10^{-3}	3.65×10^{-3}
50	180.8	149.5	3.5×10^{-3}	3.5×10^{-3}
100	199.6	168.3	1.6×10^{-3}	1.45×10^{-3}
150	228.1	196.8	5.0×10^{-4}	5.1×10^{-4}
200	265.0	233.7	1.5×10^{-4}	1.5×10^{-4}
250	304.0	272.7	4.5×10^{-5}	4.6×10^{-5}
300	347.3	316.0	1.5×10^{-5}	1.5×10^{-5}

(a) Read from Fig. 17.

(b) Interpolated from apparent water surface curve in Fig. 12.

Table A-19. Effect of Moving Instrument Bridge to Various Positions over Pool on Radiation Received at Crew Position

Water thickness above reactor: 130 cm
Reactor-crew separation: 533
(Exp. 9, Runs 43, 45)

Distance of Center of Bridge from Reactor Vertical Centerline	Gamma-Ray Dose (r/hr/watt)	Fast Neutron Dose (mrep/hr/watt)	Thermal Neutron Flux (nv_{th}/watt)
163[a]	3.613×10^{-6}	3.29×10^{-7}	2.81×10^{-4}
353	3.472×10^{-6}	3.52×10^{-7}	2.721×10^{-4}
576	3.316×10^{-6}	3.16×10^{-7}	2.602×10^{-4}
796	3.199×10^{-6}	3.06×10^{-7}	2.482×10^{-4}
927[b]	3.214×10^{-6}	1.98×10^{-7}	2.411×10^{-4}
927[b,c]	3.11×10^{-6}		2.23×10^{-4}

(a) Instrument bridge located next to reactor bridge.

(b) Instrument bridge rolled completely off pool.

(c) For this measurement only the reactor bridge was removed and the reactor was suspended from an H-beam; data is interpolated to this water thickness (Run 45).

Table A-20. Gamma-Ray Vertical Traverse Measurements under Reactor Bridge and under H-Beam

Water thickness above reactor: 142 cm[a]
Traverse at (150, y, 0)

(Exp. 9)

Detector Distance above Water Surface (cm)	Gamma-Ray Dose (r/hr/watt)	
	Under Bridge, Run 42	Under H-Beam, Run 58
0	5.54×10^{-4}	5.57×10^{-4}
42		6.66×10^{-4}
50	6.04×10^{-4}	
92		6.73×10^{-4}
100	5.74×10^{-4}	
142		6.10×10^{-4}
150	5.10×10^{-4}	
192		5.17×10^{-4}
200	4.37×10^{-4}	
367		2.91×10^{-4}
376.5	2.44×10^{-4}	
367[b]		2.80×10^{-4}

(a) Although portions of both the reactor bridge and the H-beam are directly above the reactor, their east-west axes do not coincide with each other or with the east-west axis of the reactor. Their relative widths are indicated in Fig. 20. The position (150,y,0) indicates a vertical traverse 150 cm west of the vertical axis of the reactor as shown in Fig. 19; y = 0 at the water surface.

(b) This reading was taken directly under the east-west axis of the H-beam, i.e. at (150, 367,-50).

Table A-21. Gamma-Ray Horizontal Traverse Measurements on Water Surface under Reactor Bridge and under H-Beam

Water thickness above reactor: 142 cm
Traverse at (150,0,z)[a]
(Exp. 9)

Detector Distance from East-West Axis of Reactor (cm)	Gamma-Ray Dose (r/hr/watt)	
	Under Bridge, Run 42	Under H-Beam, Run 58
245	1.26×10^{-5}	
205	2.82×10^{-5}	
150	8.02×10^{-5}	
120		(1.77×10^{-4})[b]
100		(2.49×10^{-4})[b]
75	2.68×10^{-4}	
50		(4.36×10^{-4})[b]
0	5.54×10^{-4}	5.57×10^{-4}
- 50		(4.53×10^{-4})[b]
- 75	3.16×10^{-4}	
-100		(2.56×10^{-4})[b]
-147		(1.25×10^{-4})[b]
-150	8.06×10^{-5}	
-200	2.86×10^{-5}	4.15×10^{-5}
-245	1.12×10^{-5}	

(a) As explained in footnote (a) of Table A-20, the east-west axes of the reactor, reactor bridge, and H-beam do not coincide (see Fig. 20). The position (150,0,z) indicates a water surface horizontal traverse 150 cm west of the pool north-south centerline.

(b) Interpolated points from a similar run made with detector 8 cm below water surface.

Table A-22. Effect of Lead at the Crew Position on the Gamma-Ray Dose Received

Water thickness above reactor: 142 cm
Scintillation counter in lead-lined container shown in Fig. 7
(Exp. 9, Run 61)

Detector Height above Water Surface (cm)	Gamma-Ray Dose (r/hr/watt)	
	No Lead on Container Cover	5/64 in. Lead on Container Cover
28	1.19×10^{-6}	2.50×10^{-7}
3	1.12×10^{-6}(a)	2.35×10^{-7}
- 7	5.36×10^{-7}	1.16×10^{-7}
-17	1.92×10^{-7}	4.00×10^{-8}
-28	6.80×10^{-8}	1.62×10^{-8}
-37	3.49×10^{-8}	1.01×10^{-8}

(a) Lead lining reduces water surface gamma reading by about 10%; compare with 142-cm curve in Fig. 4.

Table A-23. Vertical Traverse Lines of Lead Slab Interposed Between Reactor and Detector (see Fig. 22)

Vertical Traverse Line	Slab Distance from Reactor Vertical Centerline (cm)
A	123
B	243
C	383

Table A-24. Positions of Lead Slab Along Vertical Traverse Lines (see Fig. 22)

Slab Position No.	Slab Distance above Water Surface (ft)		
	Top Edge	Midpoint	Bottom Edge
1	0	-2.5	-5.0
2	2.5	0	-2.5
3	5	2.5	0
4	10	7.5	5
5	15	12.5	10
6	~ 19.5	~ 17	~ 14.5

Table A-25. Effect on Radiation of Interposing Lead Slab Between BSR and Detector at Crew Position[a]

Water thickness above reactor: 142 cm
Reactor-crew separation: 463 cm

(Exp. 9, Run 55)

Slab Position No.	Gamma-Ray Dose (r/hr/watt)			Thermal Neutron Flux (nv_{th}/watt)		
	Vertical Traverse Line			Vertical Traverse Line		
	A	B	C	A	B	C
1	1.42×10^{-6}		1.42×10^{-6}	6.12×10^{-5}		5.22×10^{-5}
2		1.38×10^{-6}	6.99×10^{-7}		6.60×10^{-5}	5.01×10^{-5}
3	1.51×10^{-6}	1.34×10^{-6}	6.84×10^{-7}	1.39×10^{-4}	8.69×10^{-5}	6.22×10^{-5}
4	1.59×10^{-6}	1.60×10^{-6}	1.59×10^{-6}	9.37×10^{-5}	9.58×10^{-5}	7.59×10^{-5}
5	1.68×10^{-6}	1.62×10^{-6}	1.61×10^{-6}	6.89×10^{-5}	7.20×10^{-5}	6.86×10^{-5}
6	1.62×10^{-6}		1.63×10^{-6}	6.01×10^{-5}		6.32×10^{-5}

(a) For description of slab positions see Tables A-23 and A-24.

Table A-26. Radiation Distribution in Air above Crew Position

Reactor-detector separation: 423 cm
Water thickness above reactor: 60 cm

(Exp. 9, Run 75)

Detector Distance above Water Surface (cm)	Gamma-Ray Dose (r/hr/watt)	Fast Neutron Dose (mrep/hr/watt)	Thermal Neutron Flux (nv_{th}/watt)
3.5		3.37×10^{-4}	
6.5			3.25×10^{-1}
9.0	3.28×10^{-5}		
28.5		4.03×10^{-4}	
31.5			3.27×10^{-1}
34.0	3.65×10^{-5}		
48.5		4.34×10^{-4}	
51.5			3.30×10^{-1}
54.0	4.06×10^{-5}		
98.5		5.08×10^{-4}	
101.5			3.35×10^{-1}
104.0	5.21×10^{-5}		
148.5		6.59×10^{-4}	
151.5			3.47×10^{-1}
154.0	5.28×10^{-5}		
198.5		8.43×10^{-4}	
201.5			3.67×10^{-1}
204.0	6.85×10^{-5}		
248.5		1.02×10^{-3}	
251.5			3.67×10^{-1}
254.0	1.05×10^{-4}		
298.5		1.24×10^{-3}	
301.5			3.65×10^{-1}
304.0	1.47×10^{-4}		
348.5		1.44×10^{-3}	
351.5			3.57×10^{-1}
354.0	1.39×10^{-4}		

Table A-27. Effect of Wall Scattering on Fast Neutron Dose Received at Crew Position for Various Water Thicknesses above Reactor

Reactor-crew separation: 423 cm
(Vertical traverse measurements)
(Exp. 9)

Water Thickness above Reactor (cm)	Detector Height above Water Surface (cm)	Fast Neutron Dose (mrep/hr/watt)			
		Reactor-Detector on Pool Centerline		Reactor-Detector 7.5 ft from Pool Centerline	
		Fast Neutron Dosimeter	12-in. BF_3 Ctr. Normalized	Fast Neutron Dostimeter	12-in. BF_3 Ctr. Normalized
		Runs 69, 75	Run 75	Run 80	Run 80
60	32.0		3.50×10^{-4}		
	30.0				4.92×10^{-4}
	29.0	4.03×10^{-4}			
	26.5			6.03×10^{-4}	
	7.0		3.49×10^{-4}		
	7.5	3.51×10^{-4}			
	5.0				4.90×10^{-4}
	4.0	3.37×10^{-4}			
	1.5			4.91×10^{-4}	
	-3.0		1.60×10^{-4}		
	-5.0				1.62×10^{-4}
	-6.0	8.31×10^{-5}			
	-8.5			7.90×10^{-5}	
	-13.0		1.77×10^{-5}		
	-15.0				1.76×10^{-5}
	-16.0	1.14×10^{-5}			
	-18.5			1.13×10^{-5}	
	-23.0		1.84×10^{-6}		

Table A-27. (continued)

Water Thickness above Reactor (cm)	Detector Height above Water Surface (cm)	Fast Neutron Dose (mrep/hr/watt)			
		Reactor-Detector on Pool Centerline		Reactor-Detector 7.5 ft from Pool Centerline	
		Fast Neutron Dosimeter	12-in. BF_3 Ctr. Normalized	Fast Neutron Dosimeter	12-in. BF_3 Ctr. Normalized
		Runs 69, 75	Run 75	Run 80	Run 80
60	-25.0				2.20×10^{-6}
	-28.5			1.19×10^{-6}	
		Runs 68, 74	Run 74	Run 79	Run 79
90	31.5		1.38×10^{-5}		
	30.5	1.62×10^{-5}			
	29.0				1.98×10^{-5}
	26.0			2.61×10^{-5}	
	7.5	1.39×10^{-5}			
	6.5		1.34×10^{-5}		
	5.5	1.31×10^{-5}			
	4.0				1.92×10^{-5}
	1.0			1.94×10^{-5}	
	- 3.5		5.91×10^{-6}		
	- 4.5	4.52×10^{-6}			
	- 6.0				5.32×10^{-6}
	- 9.0			2.86×10^{-6}	
	-13.5		6.52×10^{-7}		
	-14.5	4.36×10^{-7}			

Continued next page

Table A-27. (continued)

Water Thickness above Reactor (cm)	Detector Height above Water Surface (cm)	Fast Neutron Dose (mrep/hr/watt)			
		Reactor-Detector on Pool Centerline		Reactor-Detector 7.5 ft from Pool Centerline	
		Fast Neutron Dosimeter	12-in. BF_3 Ctr. Normalized	Fast Neutron Dosimeter	12-in. BF_3 Ctr. Normalized
		Runs 68, 74	Run 74	Run 79	Run 79
90	-16.0				5.85×10^{-7}
	-19.0			3.94×10^{-7}	
	-23.5		7.53×10^{-8}		
	-24.5	1.25×10^{-7}			
	-26.0				7.75×10^{-8}
	-29.0			8.97×10^{-8}	
		Runs 63, 64, 67	Runs 63, 67	No data	No data
116	33.0		9.90×10^{-7}		
	32.5		9.97×10^{-7}		
	31.5	1.52×10^{-6}			
	30.0	1.07×10^{-6}			
	8.0		9.71×10^{-7}		
	7.5		9.70×10^{-7}		
	6.5	8.97×10^{-7}			
	5.0	9.90×10^{-7}, 1.06×10^{-6}			
	-2.0		5.72×10^{-7}		
	-2.5		5.29×10^{-7}		

Continued next page

Table A-27. (continued)

Water Thickness above Reactor (cm)	Detector Height above Water Surface (cm)	Fast Neutron Dose (mrep/hr/watt)			
		Reactor-Detector on Pool Centerline		Reactor-Detector 7.5 ft. from Pool Centerline	
		Fast Neutron Dosimeter	12-in BF_3 Ctr. Normalized	Fast Neutron Dosimeter	12-in BF_3 Ctr. Normalized
		Runs 63, 64, 67	Runs 63, 67	No data	No data
116	- 3.5	4.37×10^{-7}			
	-8.5	1.48×10^{-7}			
	-12.0		6.88×10^{-8}		
	-12.5		5.52×10^{-8}		
	-22.0		7.80×10^{-9}		
	-22.5		7.32×10^{-9}		
		Run 64	Run 66	No data	
142	34.0		7.77×10^{-8}		
	30.0	1.15×10^{-7}			
	9.0		7.79×10^{-8}		
	-1.0		5.62×10^{-8}		
	-9.0		1.10×10^{-8}		
	-10.0		8.22×10^{-9}		
	-20.0		2.01×10^{-9}		

Table A-28. Effect of Wall Scattering on Thermal Neutron Flux Received at Crew Position for Various Water Thicknesses above Reactor

Reactor-crew separation: 423 cm
(Vertical traverse measurements)
(Exp. 9)

Water Thickness above Reactor (cm)	Detector Height above Water Surface (cm)	Thermal Neutron Flux (nv_{th}/watt)		
		Reactor-Detector on Pool Centerline	Reactor-Detector 5 ft from Pool Centerline	Reactor-Detector 7.5 ft from Pool Centerline
		Run 75	Run 73	Run 80
60	32.0	3.00×10^{-1}		
	30.0		3.29×10^{-1}	4.14×10^{-1}
	7.0	2.98×10^{-1}		
	5.0		3.29×10^{-1}	4.13×10^{-1}
	- 3.0	1.37×10^{-1}		
	-5.0		1.11×10^{-1}	1.37×10^{-1}
	-13.0	1.51×10^{-2}		
	-15.0		1.17×10^{-2}	1.48×10^{-2}
	-23.0	1.57×10^{-3}		
	-25.0		1.36×10^{-3}	1.85×10^{-3}
		Run 74	Run 72	Run 79
90	31.5	1.37×10^{-2}		
	30.0		1.53×10^{-2}	
	29.0			1.78×10^{-2}
	6.5	1.33×10^{-2}		

Continued next page

Table A-28. (continued)

Water Thickness above Reactor (cm)	Detector Height above Water Surface (cm)	Thermal Neutron Flux (nv_{th}/watt)		
		Reactor-Detector on Pool Centerline	Reactor-Detector 5 ft from Pool Centerline	Reactor-Detector 7.5 ft from Pool Centerline
		Run 74	Run 72	Run 79
90	5.0		1.51×10^{-2}	
	4.0			1.77×10^{-2}
	-3.5	5.86×10^{-3}		
	-5.0		5.03×10^{-3}	
	-6.0			4.88×10^{-3}
	-13.5	6.46×10^{-4}		
	-15.0		5.60×10^{-4}	
	-16.0			5.28×10^{-4}
	-23.5	7.45×10^{-5}		
	-25.0		6.90×10^{-5}	
	-26.0			7.00×10^{-5}
		Runs 63, 67	Run 71	Run 77
116	33.0	1.03×10^{-3}		
	32.5	1.03×10^{-3}		
	30.0		1.21×10^{-3}	1.36×10^{-3}
	8.0	1.01×10^{-3}		
	7.5	1.01×10^{-3}		
	5.0		1.20×10^{-3}	

Continued next page

Table A-28. (continued)

Water Thickness above Reactor (cm)	Detector Height above Water Surface (cm)	Thermal Neutron Flux (nv_{th}/watt)		
		Reactor-Detector on Pool Centerline	Reactor-Detector 5 ft from Pool Centerline	Reactor-Detector 7.5 ft from Pool Centerline
		Runs 63, 67	Run 71	Run 77
116	4.0			1.35×10^{-3}
	-2.0	5.93×10^{-4}		
	-2.5	4.91×10^{-4}		
	-5.0		4.19×10^{-4}	
	-6.0			3.88×10^{-4}
	-12.0	7.13×10^{-5}		
	-12.5	5.71×10^{-5}		
	-15.0		4.89×10^{-5}	
	-16.0			4.57×10^{-5}
	-22.0	8.22×10^{-6}		
	-22.5	7.57×10^{-6}		
	-25.0		6.53×10^{-6}	
	-26.0			7.20×10^{-6}
		Run 66	Run 70	Runs 76, 78
142	34.0	5.53×10^{-5}		
	33.0			9.00×10^{-5}
	30.5		6.25×10^{-5}	
	9.0	5.54×10^{-5}		

Continued next page

Table A-28. (continued)

Water Thickness above Reactor (cm)	Detector Height above Water Surface (cm)	Thermal Neutron Flux (nv_{th}/watt)		
		Reactor-Detector on Pool Centerline	Reactor-Detector 5 ft from Pool Centerline	Reactor-Detector 7.5 ft from Pool Centerline
		Run 66	Run 70	Runs 76, 78
142	8.0			9.15×10^{-5}
	5.5		6.33×10^{-5}	
	4.0			9.15×10^{-5}
	-1.0	4.00×10^{-5}		
	-2.0			6.13×10^{-5}
	-4.5		2.27×10^{-5}	
	-9.0	7.81×10^{-6}		
	-10.0	5.84×10^{-6}		
	-12.0			8.18×10^{-6}
	-14.5		2.38×10^{-6}	
	-17.0			2.82×10^{-6}
	-22.0			1.49×10^{-6}

Table A-29. Effect of Wall Scattering on Gamma-Ray Dose Received at Crew Position for Various Water Thicknesses above Reactor

Reactor-crew separation: 423 cm
(Vertical traverse measurements)
(Exp. 9)

Water Thickness above Reactor (cm)	Detector Height above Water Surface (cm)	Gamma-Ray Dose (r/hr/watt)		
		Reactor-Detector on Pool Centerline	Reactor-Detector 5 ft from Pool Centerline	Reactor-Detector 7.5 ft from Pool Centerline
		Runs 69, 75	Run 73	Run 80
60	34	3.65×10^{-5}		
	32		3.95×10^{-5}	
	30			4.77×10^{-5}
	9.5	3.27×10^{-5}		
	9	3.28×10^{-5}		
	7		3.69×10^{-5}	
	5			4.72×10^{-5}
	-1	2.80×10^{-5}		
	-3		2.67×10^{-5}	
	-5			2.87×10^{-5}
	-11	9.55×10^{-6}		
	-13		8.64×10^{-6}	
	-15			9.05×10^{-6}
	-21	3.42×10^{-6}		
	-23		3.23×10^{-6}	
	-25			3.43×10^{-6}

Continued next page

Table A-29. (continued)

Water Thickness above Reactor (cm)	Detector Height above Water Surface (cm)	Gamma-Ray Dose (r/hr/watt)		
		Reactor-Detector on Pool Centerline	Reactor-Detector 5 ft from Pool Centerline	Reactor-Detector 7.5 ft from Pool Centerline
		Runs 68, 74	Run 72	Run 79
90	33	1.50×10^{-5}		
	32		1.59×10^{-5}	
	30			1.67×10^{-5}
	9.5	1.15×10^{-5}		
	8	1.14×10^{-5}		
	7		1.30×10^{-5}	
	5			1.48×10^{-5}
	-2	8.64×10^{-6}		
	-3		9.39×10^{-6}	
	-5			8.31×10^{-6}
	-12	2.78×10^{-6}		
	-13		2.99×10^{-6}	
	-15			2.72×10^{-6}
	-22	1.01×10^{-6}		
	-23		1.10×10^{-6}	
	-25			1.01×10^{-6}

Continued next page

Table A-29. (continued)

Water Thickness above Reactor (cm)	Detector Height above Water Surface (cm)	Gamma-Ray Dose (r/hr/watt)		
		Reactor-Detector on Pool Centerline	Reactor-Detector 5 ft from Pool Centerline	Reactor-Detector 7.5 ft from Pool Centerline
		Run 67	Run 71	Run 77
116	34.5	5.25×10^{-6}		
	32		5.96×10^{-6}	
	30			5.96×10^{-6}
	9.5	4.12×10^{-6}		
	7.0		4.75×10^{-6}	
	5.0			4.98×10^{-6}
	-0.5	3.65×10^{-6}		
	-3.0		3.33×10^{-6}	
	-5.0			2.81×10^{-6}
	-10.5	1.30×10^{-6}		
	-13.0		1.10×10^{-6}	
	-15.0			9.97×10^{-7}
	-20.5	4.87×10^{-7}		
	-23.0		4.10×10^{-7}	
	-25.0			3.58×10^{-7}

Continued next page

Table A-29. (continued)

Water Thickness above Reactor (cm)	Detector Height above Water Surface (cm)	Gamma-Ray Dose (r/hr/watt)		
		Reactor-Detector on Pool Centerline	Reactor-Detector 5 ft from Pool Centerline	Reactor-Detector 7.5 ft from Pool Centerline
		Run 66	Run 70	Run 76
142	34.5	1.92×10^{-6}		2.33×10^{-6}
	32		2.05×10^{-6}	
	9.5	1.57×10^{-6}		1.91×10^{-6}
	7.0		1.72×10^{-6}	
	-0.5	1.41×10^{-6}		1.66×10^{-6}
	-3.0		1.23×10^{-6}	
	-9.5	5.64×10^{-7}		
	-10.5	4.82×10^{-7}		5.70×10^{-7}
	-13.0		4.11×10^{-7}	
	-15.5			3.87×10^{-7}
	-20.5	1.82×10^{-7}		2.28×10^{-7}
	-23.0		1.64×10^{-7}	

Table A-30. Effect of Rotating Crew Position Around Reactor Toward Pool Centerline from Original Reactor-Detector Position 5 ft from Pool Walls

Constant reactor-crew separation: 423 cm
Water thickness above reactor: 142 cm

(Exp. 9, Run 70)

Detector Angle with Original Axis	Gamma-Ray Dose (r/hr/watt)	Fast Neutron Dose[a] (mrep/hr/watt)	Thermal Neutron Flux (nv_{th}/watt)
0°	1.72×10^{-6}	8.90×10^{-8}	6.75×10^{-5}
6° 48'	1.70×10^{-6}	8.71×10^{-8}	6.61×10^{-5}
13° 36'	1.75×10^{-6}	8.69×10^{-8}	6.59×10^{-5}
20° 52'	1.70×10^{-6}	8.54×10^{-8}	6.48×10^{-5}
Detector Height above Water Surface (cm)	7.0	5.5	5.5

(a) Thermal neutron data normalized.

[redacted]

DWG 22390

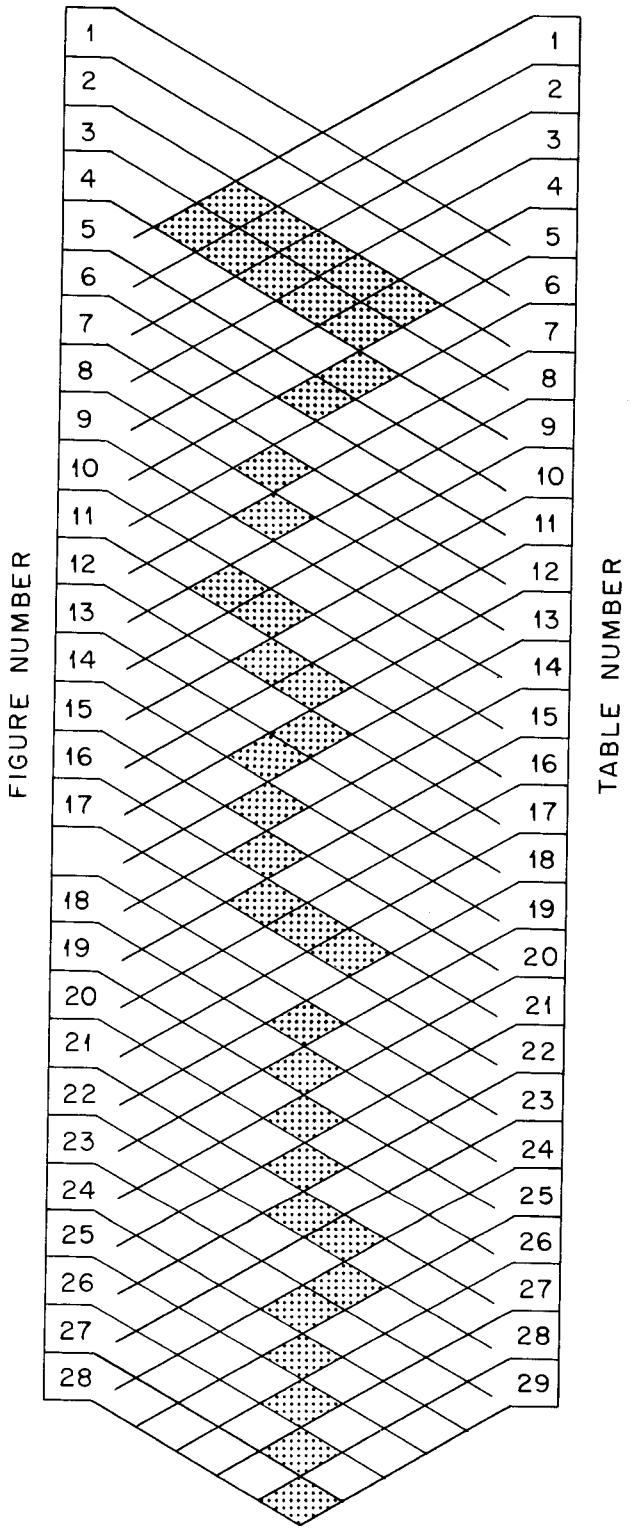

DARKENED INTERSECTIONS INDICATE THE TABLE(S) CORRESPONDING TO A GIVEN FIGURE, ETC.

IF THERE IS NO DARKENED INTERSECTION FOR A GIVEN FIGURE OR TABLE, THERE IS NO CORRELATION EXISTING.

Fig. A-1. Correlation Chart of Figures and Tables.

Appendix B

Predictions of Scattering Effects by Pool Walls

F. H. Murray

If the reactor-detector distance is small compared to the ray distance from the reactor to a point on the wall, and if the water surface within a small circle above the reactor is considered as a source of gammas, then the flux scattered back from a wall is nearly of the form $F = C/d^2$, d being the distance of the wall which is assumed to extend indefinitely upward and outward.

Let A be the total flux into the detector from air scattering if the reactor and detector lie on a line along the pool center, while aA is the flux when d_o (center to wall distance) is replaced by $d_o/2$ (distance to nearer wall), or $3d_o/2$ (distance to farther wall). The total flux at the center is $A + 2C/d_o^2$, while the flux at the distance $d_o/2$ from a wall becomes

$$aA + C\Big/\left(\frac{3d_o}{2}\right)^2 + C\Big/\left(\frac{d_o}{2}\right)^2 = aA + \frac{40}{9}\cdot\frac{C}{d_o^2}$$

Let R be the ratio of the total flux at any distance from the center to the flux at the center. Then

$$R = 1 + x = \left[Aa + \frac{4C}{d_o^2}(1.1111)\right] \Big/ \left[A + \frac{2C}{d_o^2}\right]$$

[redacted]

$$\frac{2C}{d_o^2}\Big/A = \frac{1 + x - a}{1.222 - x}$$

The experimental curves for R* show that $x \ll 1$; a lies between 1/2 and 1, and the ratio on the left depends strongly on the value assumed for a. For x between 0.1 and 0.25, a about 0.75, it appears that the ratio $2C/Ad_o^2$ is about 0.4. If the assumption $a \doteq 1$ may be justified, the ratio is very much smaller. The experimental values of x are $\alpha = 0.09$, 0.15, 0.18, 0.23, corresponding to depths of 142, 116, 90, and 60 cm for the reactor below the surface.

---

* Fig. 30.

[redacted]